Stony Brook University

Manipulation of DNA at Polymer Surfaces: Electric-Field Controlled Adsorption, Patterned Cutting and Stretching

A Dissertation Presented

by

Ke Zhu

to

The Graduate School

in Partial Fulfillment of the

Requirements

for the Degree of

Doctor of Philosophy

in

Materials Science and Engineering

Stony Brook University

August 2016

Stony Brook University

The Graduate School

Ke Zhu

We, the dissertation committee for the above candidate for the

Doctor of Philosophy degree, hereby recommend

acceptance of this dissertation.

Dr. Jonathan Sokolov– Dissertation Advisor
Professor, Department of Materials Science and Engineering
Stony Brook University

Dr. Miriam H. Rafailovich - Chairperson of Defense
Distinguished Professor, Department of Materials Science and Engineering
Stony Brook University

Dr. Gary Halada
Associate Professor, Department of Materials Science and Engineering
Stony Brook University

Dr. Ming Lu
Staff Scientist, Center for Functional Nanomaterials, Brookhaven National Laboratory

This dissertation is accepted by the Graduate School

Nancy Goroff

Interim Dean of the Graduate School

Abstract of the Dissertation

Manipulation of DNA at Polymer Surfaces: Eletric-Field Controlled Adsorption, Patterned Cutting and Stretching

by

Ke Zhu

Doctor of Philosophy

in

Materials Science and Engineering

Stony Brook University

2016

Recent developments in next generation DNA sequencing and optical restriction mapping involve manipulation of DNA molecules on surfaces. Here we propose a novel method that can control the adsorbed DNA density on polymer surfaces by applying an electric field. The efficiency of deposition was optimized with respect to DNA concentration in solution, electric field type and electric field strength. Enhancement of adsorption density of greater than twenty-fold was found. In addition, DNA molecules are fragmented on a polymer surface by soft lithography. Several experimental conditions have been tested to optimize the polydimethylsiloxane (PDMS) stamp fabrication and DNA cutting method. Fragmented DNA strands of 3.5μm in length can be fabricated over a large area (2cm by 5cm) in one single cutting. The mechanism of DNA cutting behind this method has been discussed as well. This method can potentially improve current sequencing techniques in both efficiency and sensitivity. Finally, DNA molecules were then deposited and stretched on a flexible PDMS substrate. Incident light polarization was varied and fluorescence emission intensity was measured as a function of polarization angle and degree of stretching of the DNA. The stretching and breakage

properties of lambda DNA on the PDMS substrate were determined. The amount of stretching before breakage occurred was found to be up to 50% relative to the as-deposited length.

Table of Contents

List of Figures

List of Tables

Acknowledgments

I would like to express my sincere gratitude to my advisor Prof. Jonathan Sokolov. It has been an honor to be his Ph.D. student. I truly appreciate all his contributions of time, ideas and funding throughout the years to help me pursue my Ph.D. degree. The passion and commitment he has for his research was motivational for me even during the tough times. I sincerely thank Prof. Miriam H. Rafailovich, she has been actively interested in my work and has always been available to help me. I am also very grateful to Dr. Ming Lu for his help in the field of photolithography. The knowledge and technical support that he provided was extremely helpful to our research. I greatly thank Prof. Gary Halada for serving as my dissertation committee and his insightful comments.

Special thanks to all the members of DNA group including Dr. Nahyun Cho and graduate student Julia Budassi, the generous assistance and invaluable ideas that they provided have inspired me a lot and I am truly appreciated.

I want to thank the present and past members of the Garcia MRSEC members for the stimulating discussions, for the busy summer we were working together and all the fun we have had in the past 6 years.

I would also like to thank the faculty and staff members of the Department of Materials Science and Engineering.

I particularly want to thank Pan Xu, Ning Sun and Jue Liu for living in the same house for last 4 years as a family and for being great support for me all the time.

Last but not least, I would like to thank my family: my parents and my wife for their unconditional love and support through my life.

Chapter 1: Electric-Field Controlled Adsorption of DNA molecules on a Polymer Surface Using Dynamic Molecular Combing

1.1 Introduction

Over the past 20 years, the DNA research has been brought down to the single molecule level. However, single molecule analysis is difficult when DNA molecules are free in solution. Thus, techniques that permit stretching and immobilization of DNA molecules on a solid surface hold great value. To achieve this aim, several methods have been developed, such as optical tweezers[1-3], magnetic tweezers[3-6], microfibers[7,8] and molecular combing[9,10]. These techniques, combined with optical imaging[11], have helped researchers to made great progress in both biophysics[12,13] and nanotechnologies[14,15].

Molecular combing

Molecular combing is a technique in which single DNA molecules are attached by one or both of their extremities to a hydrophobic surface and are then uniformly stretched by a receding meniscus. Compared with other DNA stretching and immobilization methods, the advantages of molecular combing are: 1) attachment of the extremities of DNA molecules to the solid surface without end modification, 2) stretching of a large amount of DNA simultaneously and uniformly, 3) capability of stretching very long DNA molecules, 4) the procedure of this technique is straightforward and convenient to be performed in a standard lab environment.

The Mechanism of Molecular Combing

The combing process has three steps: the extremities of random coiled DNA in solution get adsorbed onto a hydrophobic substrate, then the DNA molecules are stretched and extended by a receding meniscus and finally, once out of the solution, the DNA sticks to the surface and is fixed in the stretched state. The key point of this method is the end specific binding of DNA molecules. Although this process is not well understood, it is believed that under certain pH conditions, usually pH 5-7, the double helix has a higher possibility to denature of its extremities rather than along its mid-segments[16]. This pH-induced end specific denaturation exposes the hydrophobic domains

of the bases, and/or leads to higher negative charge at the ends, so the end specific binding is due to: 1) the strong interaction between the hydrophobic domain of bases and the hydrophobic surface, 2) electrostatic interaction between the more negatively charged DNA ends and the positively charged surface[17]. At very low pH conditions, DNA prefers to denature along its mid-segments which results in non-specific binding. When the pH is too high, unwinding at DNA extremities is inhibited and then the attachment is less efficient. It is important to point out that the pH range depends on the solid surface[16,18]. For example, to deposit DNA molecules on a polystyrene coated surface, the optimum pH is 5.5 while for a ploy(melthy methacylate) (PMMA)coated surface, the best pH is in the range of 6.5 to 7.5.

The extension and stretching process of DNA molecules occurs at the air/water interface. The extension force is proportional to the surface tension g at the air water interface and the diameter of the DNA molecule[18,19]:

$$F = \gamma \pi d$$

where $\gamma = 7 \times 10^{-2}$ N/m for air/water interface, d=0.2nm for B-form DNA. Here we assume that the DNA molecule is normal to the interface. Thus, the extension force of the receding meniscus is in the range of 400pN. This force is large enough to transform DNA molecules from their natural random coiled state, B-DNA, into overstretched S-DNA[20], yet is not enough to break the DNA strands (which requires about 800pN[21]), nor to beak the bond between the ends of the DNA molecules and the substrate. This structural transition of DNA molecules comes with an extension of up to 1.7 fold compared with unstretched contour length. Such extension has been reported from different combing experiments[10,22]. The degree of extension of combed DNA strongly depends on the surface character[16,23]: hydrophobic surfaces usually yield a greater degree of stretching compared to hydrophilic surfaces. The degree of extension is also dependent on the pH[16,18] of the DNA solution and the speed of the receding meniscus. However, once the molecules are left dry behind the meniscus, the adhesion to the surface is strong enough that rehydration will not result in significant desorption.

Different Molecular Combing Methods

After the development of the molecular combing technique in 1994, significant efforts have been made to optimize combing methods. Most of them are focused on controlling the movement of the receding meniscus. This includes: 1) DNA droplet evaporation[9], 2) air-blowing of droplet[24], 3) spin-stretching[22,25], 4) moving surface on a droplet of DNA solution that placing on another substrate[26], 5) filter paper adsorption[27] and 6) dipping a substrate into a solution and pulling it out which also is referred to as dynamic molecular combing[28-30]. Some other modified methods vary the binding of DNA molecules to the solid surface in a controlled fashion, such as combing on e-beam patterned polystyrene templates[31], combing on Dip Pen Lithography templates[32] and combing with transfer printing[27,33,34].

DNA droplet evaporation method

The DNA droplet evaporation method is the simplest among all the methods[9]. A droplet of strained DNA, usually 1-2μL, with an appropriate value of pH and ionic strength, is deposited onto a hydrophobic surface. At first, the ends of DNA molecules attach to the surface but the interface does not move at all. After about 5 minutes, the air/water interface starts to shrink due to evaporation and the attached DNAs are stretched and immobilized on the solid surface. After the droplet is totally dry, most of the combed DNA are to be found near the droplets round periphery, forming a ring pattern. The main disadvantage of this method is that the combed DNA area is small since one droplet can only cover a small area on the surface (typically 5 to 20 mm^2). Also, the combed DNA molecules are not parallel, but rather, radically directed, which can be inconvenient for some applications.

The Moving Droplet Method

In this type of approach, the movement of the air/water interface is created by moving the droplet of the DNA solution. The simplest way to do this is by using the force of gravity[18]. Firstly, the DNA sample is placed on to the edge of a solid substrate, then this edge would be inclined to approximately 45°, causing the DNA droplet to roll down

due to gravity. After sliding down the inclined surface, DNA molecules are adsorbed and combed on the surface.

Another way to create this droplet movement is by using gas flow[22]. By carefully adjusting the angle and strength of the gas flow that is blown onto the droplet, DNA molecules are effectively combed onto the surface. The main drawback of this approach is the lack of precise control of the force that is applied to the droplet.

Dynamic Molecular Combing

After its introduction in 1997[28], the dynamic molecular combing method has become the most widely used molecular combing technique. In this method, a surface modified substrate is dipped into a DNA solution, usually several milliliters in volume, for a certain period of time, and then is withdrawn at a constant speed. The DNA molecules are stretched due to the surface tension and aligned parallel to each other. Because this technique uses a relatively large volume of DNA solution which does not significantly evaporate during the experiment, it gives better control of pH and ionic strength which is essential to successful molecular combing. Also, the retraction speed can be easily controlled by a stepping motor so that the force from the receding meniscus can be well controlled and repeatable in a set of experiments. What's more, this technique gives more control of the orientation and density of the combed DNA molecules. Details of dynamic molecular combing will be discussed later in this chapter.

Combing DNA between Microfabricated Polystyrene Lines[31]

The aim of this approach is to control the binding regions on the substrate. Firstly, a PS coated substrate is exposed under e-beam radiation and patterned with lines. Then, the substrate is soaked into an organic solvent. Since PS is crossed linked under the e-beam radiation, the exposed line patterns are less soluble compared with the unexposed part of the PS film. The result is a pattern of PS lines on the substrate.

Then this patterned surface is dipped in a DNA solution, DNA molecules is bound to those PS lines in the same way as they bind to normal PS films. Finally, the substrate is pulled out from the solution, ending up with stretched DNA between the PS lines.

Because it is possible to control the positioning of DNA arrays on the surface, this technique has a great potential in fabricating DNA-based nanoscale devices.

Recently, molecular combing has been combined with photolithography[35] and microcontact printing[33,36] to lead to some new and complex combing methods. Those approaches and their applications will be discussed in the following chapter.

The application of molecular combing

The molecular combing method has the advantages that it can be used to stretch large amount of DNA uniformly and reproducibly onto surfaces without end modification of DNA molecules. When combined with imaging techniques such as Fluorescence In-Situ Hybridization (FISH), it is a powerful tool in the field of genomics and has been used widely[11,17,37-39]. With molecular combing, precise gene positions can be located and high resolution physical mapping can be obtained. Thus, it is possible to measure the micro-deletions of a gene such as the TSC2 gene responsible for the disease tuberous sclerosis[28,40]. The procedure is as follows: DNA was prepared from a normal subject and three patients. Each sample was then combed separately using dynamic molecular combing. After that, FISH analysis was performed on the sample and deletions of 69kbps, 38kps and 136kbps in the TSC2 gene from patients were detected. Later, using a combination of molecular combing and a four-color bar coding system, microdeletions and amplifications were both found in a complex rearrangement of BRCAI gene, which is responsible for majority of breast cancer cases[41]. Molecular combing technology has also been used in studying DNA replication[17,37,39], transcription[42] and the interaction between enzymes[43] and histones[44].

In the field of nanotechnology, DNA is an ideal choice for nanowire assembling because of its size, structure, self-assembly and base pairing. In order to serve as templates for nanowire fabrication, DNA molecules must be individually separated and stretched from its random coil state. To control the nanostructure and positioning of the DNA-templated nanowires, DNA molecules must be manipulated on a hard surface before further processing. This is where molecular combing technique is useful. For example, with the help of molecular combing, poly aniline nanowires were synthesized[45].

Combined with dip pen lithography, pre-templated DNA with Fe_3O_4 magnetic nanoparticles was deposited in a site specific manner[46]. Utilizing a lithography technique which masks desired sites on DNA with protein and the remaining sites with gold nanoparticles, sequence specific DNA-templated junctions were produced[47].

The Efficiency of Molecular Combing

The efficiency of molecular combing is based on a combination of surface properties, the pH and ionic strength of the buffer solution, the retraction speed of the receding meniscus and so on. As discussed above, the pH of DNA solution has a great impact on the number of combed DNA molecules. Most of the results, with some exceptions[22], reported that 5 to 7 is the optimum pH range[16,18] for DNA end-specific binding, depending on the surface hydrophobicity. When the pH is too low, the non-specific binding of DNA to surface results. On the other hand, if the pH is too high, the binding efficiency decreases dramatically.

Another important factor for molecular combing is the ionic strength of the buffer solution[48]. The ionic strength can affect the charges of the DNA molecules in solution, the melting points of the DNA double strands and the radius of gyration, which all have a large impact on the combing results. It has been reported that for combing DNA molecules on a PDMS surface, the addition of Na+ causes an increase of adsorbed DNA molecules, decreasing at higher and lower concentrations over the range sampled of 10mM to 100mM, with a maximum at 100mM.

Previous research has also suggested that the retraction speed of the receding meniscus can affect the efficiency of molecular combing. For most of the reported results, the meniscus moving speed was found to be best in the range of 300 to 500μm/s[28,42,49]. However, some other reports claimed that the best speed could be as high as 5mm/s[26]. In our lab, we had a dynamic molecular combing set up and according to our results, no regular trend was observed ranging from 0.005mm/s to 5mm/s, but a significant decrease was observed at the speed of 8mm/s.

For high DNA concentrations, it is believed that the number of combed DNA molecules on the surface is not primarily dependent on the DNA concentration of the

solution but rather is related to the radius of gyration (R_g) of the DNA molecules in the buffer solution[31]. R_g basically determines how close together two DNA molecules can be in the solution. When the DNA concentration is very low so that all DNA molecules are well separated from each other, then the density of DNA molecules on surface does depend strongly on the DNA concentration. Previous research in our group has confirmed that a clear trend of increasing DNA density on surface can be found with increasing DNA concentration in solution over the range 0.5 to 12.5μg/ml (those experiments were conducted with lambda DNA).

Improving the efficiency of molecular combing at very low DNA concentration can be very important to some emerging techniques such as single-cell mapping[50,51] where the DNA concentration can be as low as picograms per microliter. Furthermore, for applications like characterization of circulating tumor cells[52] and prenatal diagnosis of inherited diseases[53], the starting materials are extremely rare. For example, is estimated that there are approximately one CTC per billion normal blood cells in the circulation of patients with advanced cancer[52]. Some groups have tried to address these issues by stretching DNA onto a microfluid chip[51] or combing DNA by dragging a DNA droplet across a special polymer (Zeonex) surface[54]. Here, we propose a new method to increase the combing efficiency that combines the use of an applied electric field with dynamic molecular combing. The fact that DNA is negatively charged in solution has been widely used in electrophoresis and other techniques. In addition, with the application of an electric field, DNA immobilization and hybridization have been achieved on thin film microchips or used to stretch in an agarose gel. However, the use of an electric field used in DNA solution to assist molecular combing has not been reported.

Unlike the previous work that mostly focused on the pH of buffer, the wettability of the surface or the ionic strength of the buffer, our study concentrates on the impact of electric field. We have found that varying the intensity and type (DC/AC) of the electric field has a large impact on the absorbed density of combed DNA. By testing different electric field parameters, we would like to determine the optimized conditions that will produce good combing in which individual DNA molecules are well separated and linearized but the overall combed DNA density is high. The goal of this work is to

develop a robust and repeatable method of molecular combing that enables us to control the combing efficiency even if the DNA concentration in solution is very low.

1.2 Materials and Methods

1.2.1 Preparation of DNA solution

Lambda DNA (New England Biolabs) was stained with YOYO-1 (Molecular Probes, Invitrogen) for visualizing the DNA by fluorescence microscopy. Typically, 7% (by volume) YOYO-1 (0.1mM stock solution), 10% lambda DNA stock solution (500ug/ml) and 83% buffer solution were mixed and then incubated in a 45°C oven for 120 minutes to assist dye binding before further dilution. The buffer solution used in the experiment is a mixture of 6:50 (by volume) 0.1M NaOH: 0.02M 2-(N-morpholino)ethanesulfonic acid (MES) and the pH is 6.45, found previously to be effective for combing onto PMMA. After incubation, different concentrations of DNA were tested by diluting the 10% DNA solution with the 6:50 NaOH:MES buffer solution.

1.2.2 Preparation of substrate

Polished silicon wafers (100) were cut into approximately 10mm by 10mm squares using a scribe-and-break setup. Before spin-casting, these silicon surfaces were cleaned with following steps: 1) sonication in ethanol for 10 minutes, 2) boiling in 1:1:4 solution of ammonium hydroxide: hydrogen peroxide: DI water for 10 minutes followed by rinsing with deionized water (DI), 3) soaking at room temperature for 15 minutes in 1:1:3 solution of sulfuric acid: hydrogen peroxide: DI water, 4) DI water rinse. After cleaning, polymethylmethacrylate (PMMA) of molecular weight 225kg/mole (Sigma) that was dissolved in toluene at the concentration of 15mg/ml was spun-cast for 30 seconds (Headway Research Inc.) at 2500rpm onto the silicon samples. PMMA surfaces have been reported to permit successful binding of DNA molecules over a broad band of pH conditions. Ellipsomerty (Rudolf Auto EL) was used to measure the PMMA thickness. Typical thicknesses were 600-800A. Before adsorbing DNA molecules onto the PMMA, all the surfaces were annealed at 130 degree Celsius for at least 1 hour in an ion pumped vacuum oven with a pressure $\leq 1\times10^{-7}$ torr.

1.2.3 Preparation of dipping well and application of electric field

A custom made Teflon well with dimensions 36mm by 11mm by 10mm is used for containing the DNA solution. For DC fields, Pt wires (Goodfellow metals) were used as anode and gold-coated silicon wafers that were cut into 6mm by 25mm pieces were used as cathode. For AC fields, both electrodes were Pt wires for the reason that an electrochemical reaction occurred when using a gold surface as cathode, which caused delamination from the silicon substrate. All samples were cleaned by 15 minutes sonication in methanol and then DI water rinse for 15 minutes before each experiment. When conducting experiments, the electrodes were set up 27.9 ± 0.5 mm apart at either end of the Teflon well and held in place with an adjustable holder. Also, both electrodes were fixed symmetrically with respect to the sample (at the center of the well), resulting in an electric field normal to the sample.

A power supply (Hewlett Packard, 6216A) was used to create DC fields by applying 0-30V across the electrodes. Higher voltages and pulsed fields were generated by another power source (Keithley, 228A Voltage/Current Source). The electric fields were examined at different positions within the cell using a digital voltmeter (BK, 2703A).

1.2.4 Adsorption of DNA molecules onto polymer surfaces

DNA molecules were deposited on the PMMA surfaces with dynamic molecular combing methods. Teflon tweezers that hold the sample while dipping are controlled by a linear stage connected to a stepper motor system (Arrick MD-2). A computer program is used to control the system, varying parameters such as soak time, retraction speed and travel distance. For dipping, 3mL of DNA buffer solution was first pipetted into the Teflon well and a PMMA coated silicon sample was placed facing the cathode and submerged into the solution. After a certain period of soaking time, the samples were retraced from the solution at different speeds and with various applied electric fields.

Imaging of DNA molecules on the surfaces was performed with a Leica Laser Scanning Confocal Microscope (TCS SP2), equipped with an Hg lamp source for fluorescence microscopy and a CCD camera (Leica DC350F). A blue filter cube was used to achieve the excitation of the YOYO-1 dye and to select the emission (YOYO-1's emission maximum is 509nm). All images in the figures were taken with a 40X magnification oil lens using a typical exposure time of 3 to 5 seconds. Image analysis was done with ImageJ software (NIH).

1.3 Results and discussion

This work was focused on testing different conditions to control the DNA density on polymer surfaces using an electric field. In order to find the optimal parameters for DNA adsorption on PMMA surfaces, variables such as filed strength, direct and alternating currents, DNA concentration and soak time were changed. Other parameters were considered, but not every combination was tested. From a previous study: the 6:50 buffer (pH 6.5) produced the best combing on PMMA surface and this remained fixed. The retracting speed, accelerating from 0.5mm/s to 2mm/s, over 2 seconds, was also fixed. The incubation time was set at 60 seconds, except for the incubation time tests, as noted below.

1.3.1 DC fields

The electric potential showed a linear relation with distance between the two electrodes, implying that the electric field (voltage over distance) was rather uniform throughout the entire cell (Figure 1.1).

1.3.2 DC field-assisted molecular combing

The electric field was changed by varying the voltage in each experiment and as expected, with the increase in the electric field strength, more DNA molecules were adsorbed on the surface. Experiments were conducted with DNA concentration of 500 ng/mL at electric field strength of 0, 3.54V/cm, 7.09V/cm, and 10.64V/cm. The electric field strength was found by dividing the applied voltage by the distance between the two

electrodes (27.94mm). To calculate the density of combed DNA molecules, for field strengths of 0 and 3.54V/cm, 5 images from different random areas of the same sample were taken and the average number of molecules was found for the selected areas. For the 7.09V/cm and 10.64V/cm data, with significantly higher densities, the density of the DNA was found by dividing the number of molecules by the area of a selected region-of-interest (ROI) and an over 5 ROIs was calculated. Figure 1.2 shows microscopy images of the results of DNA adsorption and Figure 1.3 shows their corresponding number of DNA molecules with varying length, the different electric fields.

Figure 1.4 shows the dramatic increase of DNA adsorption efficiency with increasing electric fields strength: without the presence of the electric field, the adsorbed DNA density on PMMA surface is about $120/\mathrm{mm}^2$. However, with the application of a 10.64V/cm electric field, the density increased to about $15000/\mathrm{mm}^2$, more than 100 times higher.

The distribution of DNA molecule length seems broader than other reports and more breakage appears when the DNA density on the surface is very low. However, as the electric field strength increased, more molecules were adsorbed onto the surface and the average length of adsorbed molecules got closer to 16.2μm, which is very close to earlier reports. Another thing to notice is that the distribution did not change much during the process of changing the electric field strength. All the absorbed DNA densities from different length groups increased with increasing the electric field strength as shown in Figure 1.3, which means this technique can be used for combing various length of DNA molecules. The short fragments of DNA molecules might due to the vortex when we mixed the DNA solution or from the Na+ irons in the buffer solution. Reports have shown that more DNA fragments will appear if the concentration of Na+ irons is <100mM[48].

1.3.3 Very low DNA concentration condition

As we showed that with the electric field, the adsorption efficiency can be significantly improved, then it is possible for us to accomplish DNA combing with very

low DNA concentration. Figure 1.5 is the histograms of lengths of adsorbed DNA density under different electric field strength for DNA concentrations of 125ng/mL and 250ng/mL. Figure 1.6 shows their adsorbed DNA density at different electric field strengths. Because of the extremely low DNA concentration in solution, without the help of electric field, it is almost impossible to see any DNA molecules under the microscope, so the adsorbed DNA density at 0V/cm is an estimation based on previous results.

Again, with the application of electric field, the adsorption efficiency improved dramaticaly. For the DNA concentration of 125ng/mL, the adsorped DNA density is about $540\,mm^2$ at an electric field strength of 10.64V/cm, which is about 80 times higher then at 3.54V/cm, and 180 times higher then without an applied electric field.

1.3.4 Moderate DNA concentration conditions

As the DNA concentraion goes higher in solution, more combed DNA can be seen for the condition of no electric field. However, counting of DNA molecules was challenging for an electric field strength of 10.64v/cm since there are overlaps of molecules (due to the very high densities) and thus some inaccuracies in the measurement process. However, judging by the small number of molecules with the lengths above 20μm (shown in Figure 1.7), the error appears small.

Compared with the absorbed DNA density at 0V/cm, for 10.64V/cm, the improvement is about 7 times (Figure 1.8), which is lower than for the low DNA concentration condition seen above. Two reasons might account for this phenomenon: first, as so many molecules gather near the PMMA surface in the solution, it is unlikely to have more free space for extra DNA molecules to be pushed onto the surface. Second, as the local concentration goes higher, the internal field created by the charged DNA molecules becomes stronger and may cancel out part of the external electric field.

The primary goal for this work is to improve the efficiency of DNA adsorption with the help of electric field so that dynamic molecular combing can be used even if the DNA concentration is very low and the result is positive: using 125ng/mL DNA solution with an electric field of 10.64 V/cm for deposition yielded similar density of DNA

molecules on the PMMA surface as using 2.5μg /ml DNA solution with no electric field, raising the efficiency of DNA deposition by about 20 fold in concentration.

1.3.5 Modified DNA adsorption efficiency

To compare the DNA adsorption efficiency of different DNA solution concentrations in the presence of an electric field, we define the modified DNA adsorption efficiency as follows:

$$N = \frac{Number\ of\ DNA\ molecules}{[area][DNA\ concentration\ in\ solution]}$$

$$= [DNA\ Density\ on\ PMMA\ surface]\frac{1}{[DNA\ concentration\ in\ solution]}$$

As can be seen from Table 1.1, the highest modified adsorption efficiency occurs at 10.64V/cm with lowest DNA concentration of 0.125ng/ mm^3, and deceases as the DNA concentration increases. This indicates that the electric field effect is more pronounced when the DNA concentration is low. This result is consistent with our previous explanation.

1.3.6 Soaking Time

Without the assistance of electric field, the DNA molecules motion toward the PMMA surface would be a random diffusion process. Previous tests showed that without the electric field, increasing the soaking time (which is the time that PMMA surface is in the DNA solution while the electric field is on) did not have any significant impact on the adsorbed DNA density. However, once the electric field is applied, the process of drift in the field becomes dominant. Therefore, more DNA molecules might be 'pushed' onto the PMMA surface with increasing soaking time, so that the density of adsorbed DNA molecules may also be increased. For this set of experiments, the concentration of DNA in solution was 500ng/mL or 1.25μg/mL. The electric field strength was fixed at 7.09V/cm. The results are shown in Figure 1.9: the adsorbed DNA density increases rather linearly at the beginning, but after 60 seconds the rate of increase slows down,

reaches a maxima at 90 seconds and no significant change could be observed after that. The plateau on the adsorbed DNA density curve suggests that the internal electric field created by the accumulation of ether the DNA molecules or the ions from the buffer near or on the PMMA surface is large enough to partially or completely cancel out the external field. So instead of extending the soaking time over 90 seconds, applying a stronger electric field is a better way to further increase the adsorbed DNA density.

1.3.7 Pulsing/Alternating Current (AC)

The idea of applying a pulsed or alternating current is to avoid significant charge build up of the negatively charged DNA molecules or the ions near the PMMA surface and also to enable attempt higher voltage to be applied without corroding the electrodes excessively. As previously described, when the gold-coated silicon wafer acted as the anode, it would undergo a corrosion reaction which weakened the gold-silicon adhesion. For this reason, this electrode was substituted with a platinum wire. While the reduced surface area and the shape of the wires may create a less uniform field, due to the cost of the platinum and available resources, a rectangular shaped platinum wire or plate could not be used for the experiments. However, measurements of the field indicated that the field was fairly uniform near the middle of the cell, where the sample was located.

In this experiment, the pulsed electric field used a 3:1 ratio for the forward to backward electric fields (the forward direction being that which directed DNA towards the PMMA surface). The alternating current field was not a sinusoidal wave, but a saw tooth wave, with field of a constant peak voltage applied in the positive direction and then the negative direction in a 3:1 time ratio. For electric field “pulsing”, a voltage was applied for 1.5 seconds and then turned off for 0.5 seconds. The saw tooth “alternating currents” were made by applying a ramped voltage in the positive direction for 1.5 seconds and in the negative direction for 0.5 seconds. Higher voltages were attempted with puled and AC fields, but above 30V (corresponding to an electric field of 10.64V/cm) the PMMA coating came off the silicon wafer and made the experiment impossible. In order to test higher voltages with AC fields, a different and more stable coating of the silicon wafer is required.

All tests in this part were conducted with a DNA concentration of 2.5μg/mL and with a soaking time of 60 seconds followed by retraction at 2mm/s.

Figure 1.10 shows that with the increasing strength of the pulsed field, the densities of adsorbed DNA molecules increase steadily while for the AC fields the increase is more unstable. However, even in the case AC fields, with the overall increase in the strength of the field, a general increase in adsorbed DNA density suggests that it is possible to control the density of the DNA molecules with varying AC fields as well. Compared with the DC field, the AC and pulsed field are less effective in increasing the adsorbed DNA density as the field strength gets larger. It is possibly because the 0.5 second of reverse field/without field pushes back/stops the DNA molecules from getting onto the PMMA surface. To reach the highest possible adsorbed DNA density, it is preferable to use a DC field.

1.3.8 Average Length of Adsorbed DNA Molecules

A primary concern of applying external electric field during molecular combing is that DNA molecules might be damaged in the process. To address this concern, the average lengths of adsorbed DNAs under different types of electric field were measured and the results are shown at Figure 1.11. Without an electric field, the adsorbed DNA density is low and because of that, the variation and the error of the statistical analysis is relatively large. However, as the fields become stronger, most of the average lengths of the adsorbed molecules are within the optimal combed length of lambda phage DNA: 15-20μm. Furthermore, as shown in Figures 1.3, 1.5 and 1.7, the length distribution of adsorbed DNAs does not change significantly as the field strength is increased. Under all the electric field conditions, the fraction of DNA molecules that are shorter than 10μm remains very low compared with the total. At the highest field strengths, such as 10.64V/cm, the number of DNA molecules that appear to be longer than 25μm increases. However, we believe they are not single DNA molecules but rather multiple strands connected to each other as the density increases. In conclusion, among the experimental conditions that have been tested, no excessive short DNA fragments were observed and

the external electric field is not observed to introduce noticeable changes in the average length or length distribution of the adsorbed DNA molecules.

1.4 Conclusion

Electric field assisted molecular combing has been demonstrated as a successful method to deposit and stretch DNA molecules onto polymer surface with significant efficiency improvement and extra flexibility of density control. The DNA concentration required in the solution for molecular combing has been decreased as much as 20 times with the adsorption density increase being about 7 times. A large area of immobilized and stretched DNA molecules with high density can be produced with very low density of DNA in solution. Unlike other approaches that have tried to deal with extremely low DNA concentration molecular combing, often resulting in very small combing areas, our methods are capable of a large area deposition and are easy to duplicate. It has been shown that the strength of field, DNA concentration, type of field and incubation time all have interesting effects on the interaction of the DNA with the polymer surface. The extra capability of controlling the adsorbed DNA density introduced using the electric field makes it much easy to find the optimal molecular combing conditions. It is worthwhile to point out the adsorbed DNA density is repeatable for the same experimental condition in one set of experiment, i.e. all the buffer and DNA solutions plus the PMMA coated silicon surface were prepared at the same day. However, those values can be varying day to day from different sets of experiments. It has been confirmed that within the experimental conditions that we tested above, there is no significant change in the pH of the DNA solution regardless the time or the strength of the electric field that we applied on (Figure 1.12). So we believe that the variability of the PMMA surface properties and the slightly pH change of the buffer solution, mainly due to the temperature and humidity change of the lab, contribute most to this variation of adsorbed DNA density. On the other hand, the ability of using electric field to control the adsorbed DNA density remains effective among all the experiments. Useful values for

the different parameters for the adsorption with electric field have been provided to achieve ‘good’ combing. The technique is well suited for many applications.

References

1 Wang, M. D., Yin, H., Landick, R., Gelles, J. & Block, S. M. Stretching DNA with optical tweezers. *Biophysical journal* **72**, 1335 (1997).

2 Bennink, M. L. *et al.* Single-molecule manipulation of double-stranded DNA using optical tweezers: interaction studies of DNA with RecA and YOYO-1. *Cytometry* **36**, 200-208 (1999).

3 Neuman, K. C. & Nagy, A. Single-molecule force spectroscopy: optical tweezers, magnetic tweezers and atomic force microscopy. *Nature methods* **5**, 491 (2008).

4 Haber, C. & Wirtz, D. Magnetic tweezers for DNA micromanipulation. *Review of Scientific instruments* **71**, 4561-4570 (2000).

5 Zlatanova, J. & Leuba, S. H. Magnetic tweezers: a sensitive tool to study DNA and chromatin at the single-molecule level. *Biochemistry and cell biology* **81**, 151-159 (2003).

6 Smith, S. B., Finzi, L. & Bustamante, C. Direct mechanical measurements of the elasticity of single DNA molecules by using magnetic beads. *Science* **258**, 1122-1126 (1992).

7 Cluzel, P. *et al.* DNA: an extensible molecule. *Science-new york then washington-*, 792-794 (1996).

8 Leger, J.-F., Robert, J., Bourdieu, L., Chatenay, D. & Marko, J. F. RecA binding to a single double-stranded DNA molecule: a possible role of DNA conformational fluctuations. *Proceedings of the National Academy of Sciences* **95**, 12295-12299 (1998).

9 Bensimon, A. *et al.* Alignment and sensitive detection of DNA by a moving interface. *Science* **265**, 2096-2098 (1994).

10 Bensimon, D., Simon, A., Croquette, V. & Bensimon, A. Stretching DNA with a Receding Meniscus: Experiments and Models. *Physical Review Letters* **74**, 4754-4757, doi:10.1103/PhysRevLett.74.4754 (1995).

11 Herrick, J. & Bensimon, A. Invited Review. Imaging of Single DNA Molecule: Applications to High-Resolution Genomic Studies. *Chromosome Research* **7**, 409-423 (1999).

12 Bustamante, C., Bryant, Z. & Smith, S. B. Ten years of tension: single-molecule DNA mechanics. *Nature* **421**, 423-427 (2003).

13 Yuying, L., Pengye, W. & Shuoxing, D. Single-molecule studies of DNA by molecular combing. *Progress in Natural Science* **17**, 493-499 (2007).

14 Stoltenberg, R. M. & Woolley, A. T. DNA-templated nanowire fabrication. *Biomedical microdevices* **6**, 105-111 (2004).

15 Gu, Q. *et al.* DNA nanowire fabrication. *Nanotechnology* **17**, R14 (2005).

16 Allemand, J. F., Bensimon, D., Jullien, L., Bensimon, A. & Croquette, V. pH-dependent specific binding and combing of DNA. *Biophysical journal* **73**, 2064-2070 (1997).

17 Herrick, J. & Bensimon, A. Single molecule analysis of DNA replication. *Biochimie* **81**, 859-871 (1999).

18 Benke, A., Mertig, M. & Pompe, W. pH- and salt-dependent molecular combing of DNA: experiments and phenomenological model. *Nanotechnology* **22**, 035304, doi:10.1088/0957-4484/22/3/035304 (2011).

19 Esmail Nazari, Z. & Gurevich, L. Molecular Combing of DNA: Methods and Applications. *Journal of Self-Assembly and Molecular Electronics* **1**, 125-148, doi:10.13052/same2245-4551.116 (2013).

20 Strick, T., Allemand, J.-F., Croquette, V. & Bensimon, D. Twisting and stretching single DNA molecules. *Progress in biophysics and molecular biology* **74**, 115-140 (2000).

21 Bustamante, C., Smith, S. B., Liphardt, J. & Smith, D. Single-molecule studies of DNA mechanics. *Current opinion in structural biology* **10**, 279-285 (2000).

22 Kim, J. H., Shi, W.-X. & Larson, R. G. Methods of stretching DNA molecules using flow fields. *Langmuir : the ACS journal of surfaces and colloids* **23**, 755-764 (2007).
23 Kudo, H., Suga, K. & Fujihira, M. Fabrication of substrates with various wettabilities for DNA molecular combing. *Colloids and Surfaces A: Physicochemical and Engineering Aspects* **313-314**, 651-654, doi:10.1016/j.colsurfa.2007.04.126 (2008).
24 Deng, Z. & Mao, C. DNA-templated fabrication of 1D parallel and 2D crossed metallic nanowire arrays. *Nano Letters* **3**, 1545-1548 (2003).
25 Yokota, H., Sunwoo, J., Sarikaya, M., van den Engh, G. & Aebersold, R. Spin-stretching of DNA and protein molecules for detection by fluorescence and atomic force microscopy. *Analytical chemistry* **71**, 4418-4422 (1999).
26 Yokota, H. *et al.* A new method for straightening DNA molecules for optical restriction mapping. *Nucleic acids research* **25**, 1064-1070 (1997).
27 Zhang, J., Ma, Y., Stachura, S. & He, H. Assembly of highly aligned DNA strands onto Si chips. *Langmuir : the ACS journal of surfaces and colloids* **21**, 4180-4184 (2005).
28 Michalet, X. Dynamic Molecular Combing: Stretching the Whole Human Genome for High-Resolution Studies. *Science* **277**, 1518-1523, doi:10.1126/science.277.5331.1518 (1997).
29 Kwak, K., Yoda, S. & Fujihira, M. Observation of stretched single DNA molecules by Kelvin probe force microscopy. *Applied Surface Science* **210**, 73-78 (2003).
30 Labit, H. *et al.* A simple and optimized method of producing silanized surfaces for FISH and replication mapping on combed DNA fibers. *BioTechniques* **45**, 649-658, doi:10.2144/000113002 (2008).
31 Klein, D. C. G. *et al.* Ordered stretching of single molecules of deoxyribose nucleic acid between microfabricated polystyrene lines. *Applied Physics Letters* **78**, 2396, doi:10.1063/1.1365099 (2001).
32 Nyamjav, D. & Ivanisevic, A. Alignment of Long DNA Molecules on Templates Generated via Dip-Pen Nanolithography. *Advanced Materials* **15**, 1805-1809 (2003).
33 Guan, J. & Lee, L. J. Generating highly ordered DNA nanostrand arrays. *Proceedings of the National Academy of Sciences of the United States of America* **102**, 18321-18325 (2005).
34 Nakao, H., Gad, M., Sugiyama, S., Otobe, K. & Ohtani, T. Transfer-printing of highly aligned DNA nanowires. *Journal of the American Chemical Society* **125**, 7162-7163 (2003).
35 Nazari, Z. E. & Gurevich, L. Controlled deposition and combing of DNA across lithographically defined patterns on silicon. *Beilstein journal of nanotechnology* **4**, 72-76 (2013).
36 Gad, M., Sugiyama, S. & Ohtani, T. Method for patterning stretched DNA molecules on mica surfaces by soft lithography. *J Biomol Struct Dyn* **21**, 387-393, doi:10.1080/07391102.2003.10506934 (2003).
37 Pasero, P., Bensimon, A. & Schwob, E. Single-molecule analysis reveals clustering and epigenetic regulation of replication origins at the yeast rDNA locus. *Genes & development* **16**, 2479-2484 (2002).
38 Lebofsky, R. & Bensimon, A. Single DNA molecule analysis: applications of molecular combing. *Briefings in functional genomics & proteomics* **1**, 385-396 (2003).
39 Norio, P. & Schildkraut, C. L. Visualization of DNA replication on individual Epstein-Barr virus episomes. *Science* **294**, 2361-2364 (2001).
40 Herrick, J. & Bensimon, A. Introduction to molecular combing: genomics, DNA replication, and cancer. *DNA Replication: Methods and Protocols*, 71-101 (2009).
41 Gad, S. *et al.* Bar code screening on combed DNA for large rearrangements of the BRCA1 and BRCA2 genes in French breast cancer families. *Journal of medical genetics* **39**, 817-821 (2002).
42 Gueroui, Z., Place, C., Freyssingeas, E. & Berge, B. Observation by fluorescence microscopy of transcription on single combed DNA. *Proceedings of the National Academy of Sciences* **99**, 6005-6010 (2002).
43 Taylor, J. R., Fang, M. M. & Nie, S. Probing specific sequences on single DNA molecules with bioconjugated fluorescent nanoparticles. *Analytical Chemistry* **72**, 1979-1986 (2000).
44 Liu, Y. *et al.* Study of the interaction of DNA and histones by spin-stretching and droplet evaporation. *Chinese Science Bulletin* **56**, 1234-1240 (2011).
45 Nickels, P., Dittmer, W. U., Beyer, S., Kotthaus, J. P. & Simmel, F. C. Polyaniline nanowire synthesis templated by DNA. *Nanotechnology* **15**, 1524 (2004).

46 Nyamjav, D. & Ivanisevic, A. Templates for DNA-templated Fe 3 O 4 nanoparticles. *Biomaterials* **26**, 2749-2757 (2005).
47 Keren, K. *et al.* Sequence-specific molecular lithography on single DNA molecules. *Science* **297**, 72-75 (2002).
48 Liu, Y. Y. *et al.* Ionic effect on combing of single DNA molecules and observation of their force-induced melting by fluorescence microscopy. *J Chem Phys* **121**, 4302-4309, doi:10.1063/1.1777220 (2004).
49 van Mameren, J., Peterman, E. J. & Wuite, G. J. See me, feel me: methods to concurrently visualize and manipulate single DNA molecules and associated proteins. *Nucleic acids research* **36**, 4381-4389 (2008).
50 Marie, R. *et al.* Integrated view of genome structure and sequence of a single DNA molecule in a nanofluidic device. *Proceedings of the National Academy of Sciences* **110**, 4893-4898 (2013).
51 Wang, X. *et al.* Microfluidic extraction and stretching of chromosomal DNA from single cell nuclei for DNA fluorescence in situ hybridization. *Biomedical microdevices* **14**, 443-451 (2012).
52 Yu, M., Stott, S., Toner, M., Maheswaran, S. & Haber, D. A. Circulating tumor cells: approaches to isolation and characterization. *The Journal of cell biology* **192**, 373-382 (2011).
53 Wieacker, P. & Steinhard, J. The prenatal diagnosis of genetic diseases. *Deutsches Aerzteblatt International* **107**, 857 (2010).
54 Deen, J. *et al.* Combing of genomic DNA from droplets containing picograms of material. *ACS nano* **9**, 809-816 (2015).

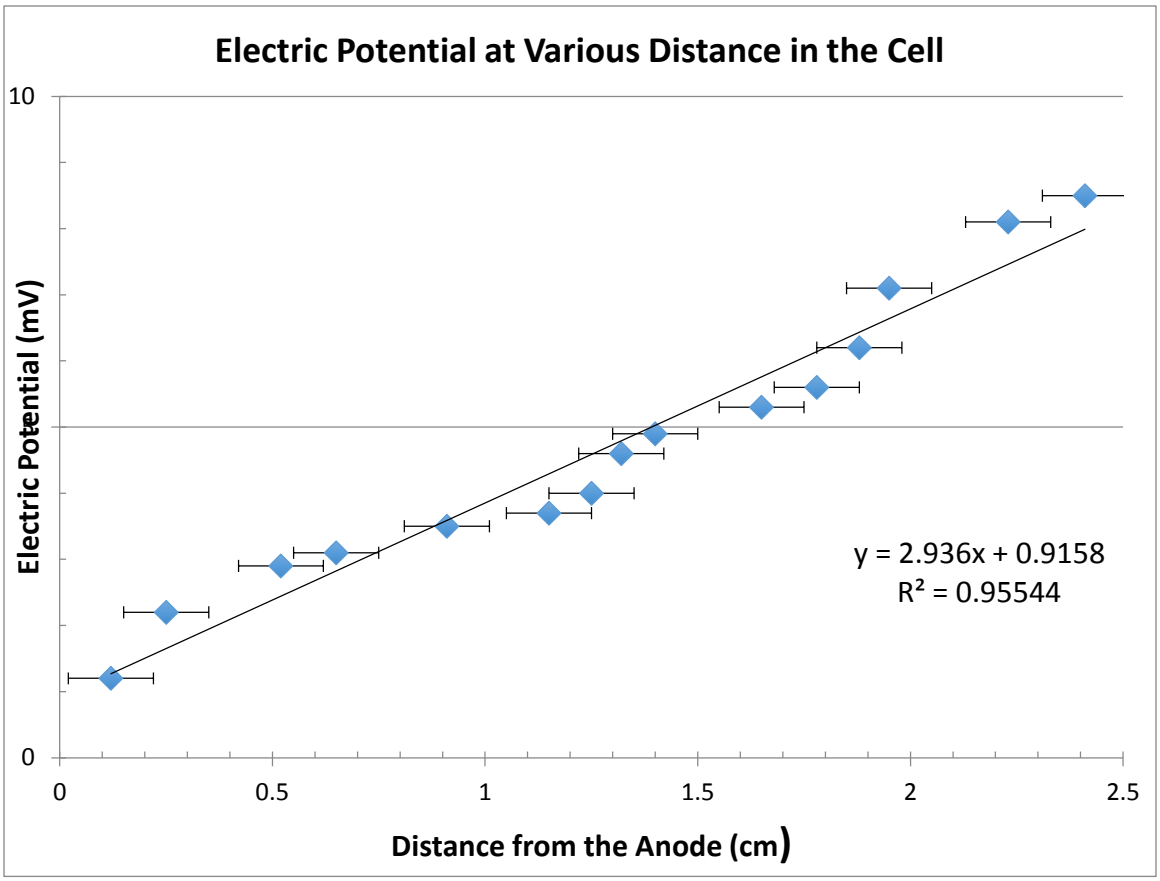

Figure 1.1: Graph of electric potential vs. the distance from the cathode at inter-electrode voltage = 10V, measured current = 3.48 mA, resistance of the cell = 2730 Ω, distance between two electrodes = 0.0268m.

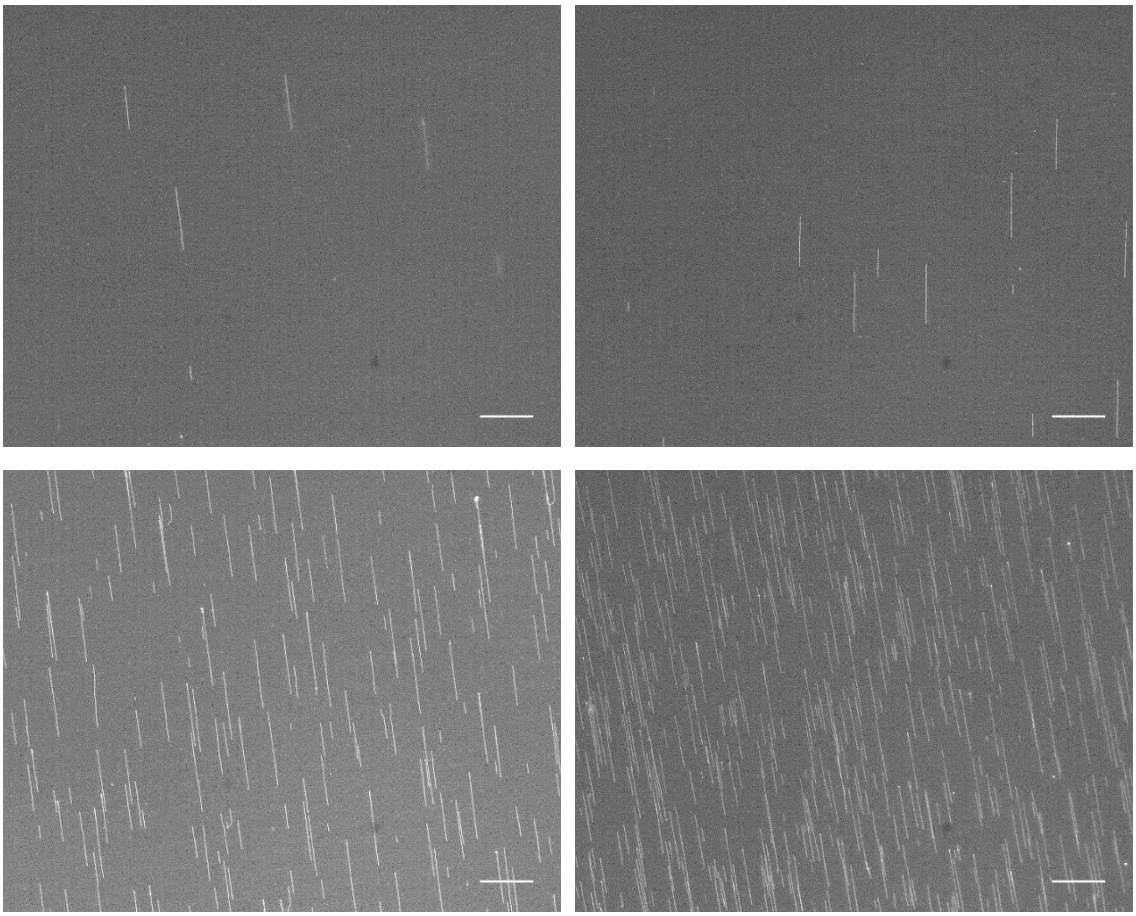

Figure 1.2: Variations of the density of adsorbed DNA with strength of applied electric field. The electric field strength are: 0V/cm (upper left), 3.54V/cm (upper right), 7.09V/cm (lower left), and 10.64V/cm (lower right). Scale bar is 20 microns in length. DNA concentration of the dipping solution is 500ng/mL.

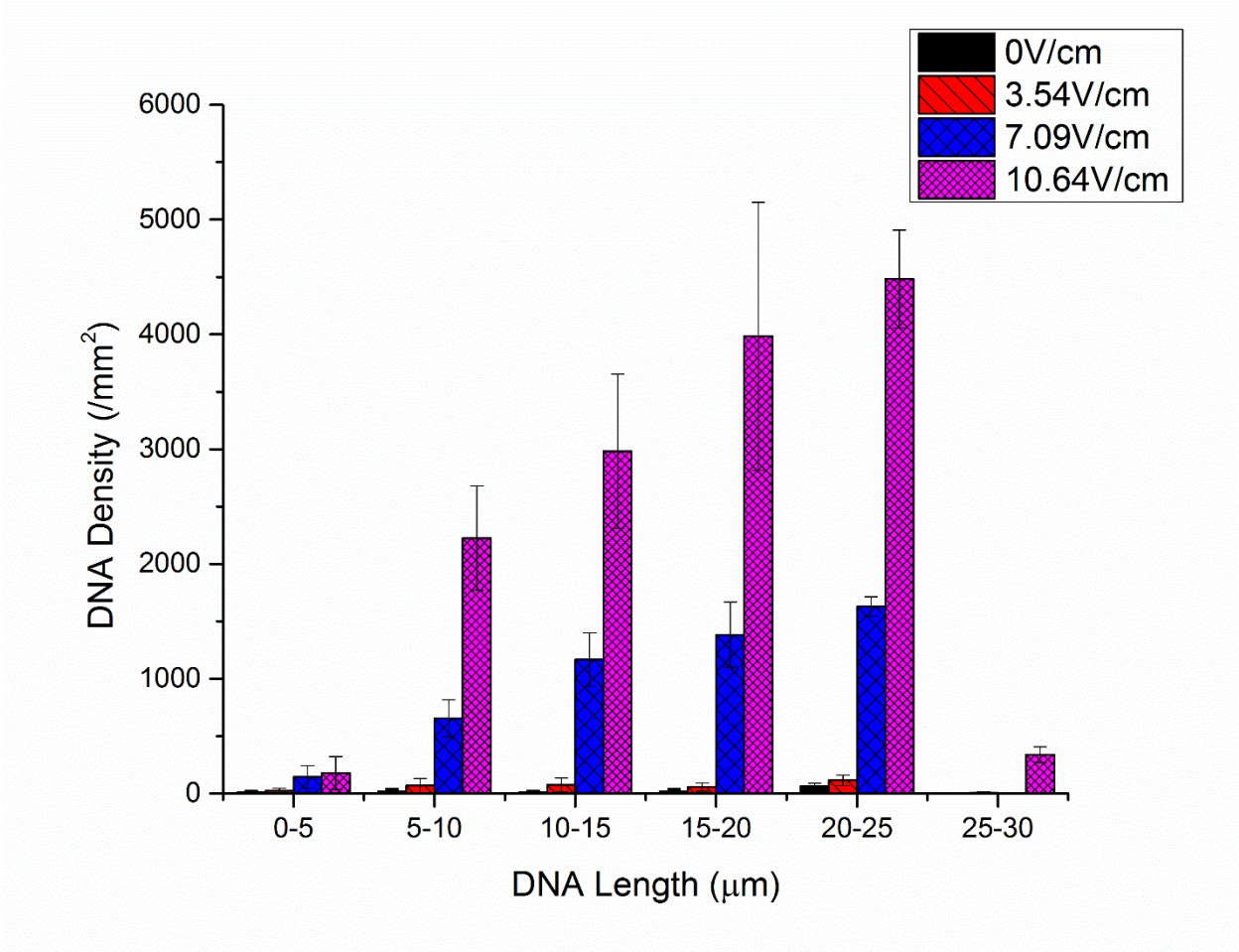

Figure 1.3: Histograms of adsorbed DNA density vs. DNA molecular length for different electric field strengths. DNA concentration of the dipping solution is 500ng/mL.

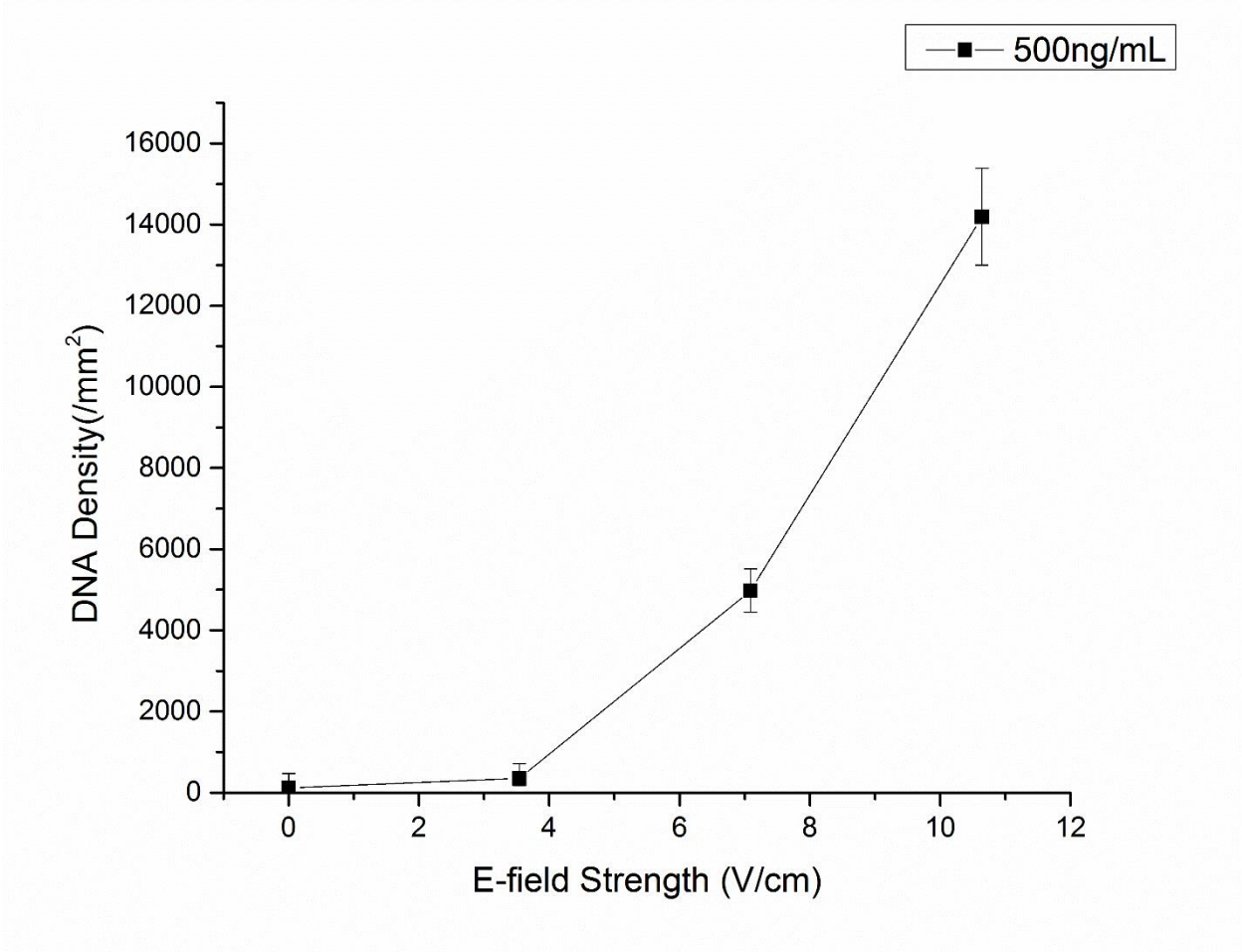

Figure 1.4: Adsorbed DNA density vs. electric field strength for DNA concentration of the dipping solution of 500ng/mL.

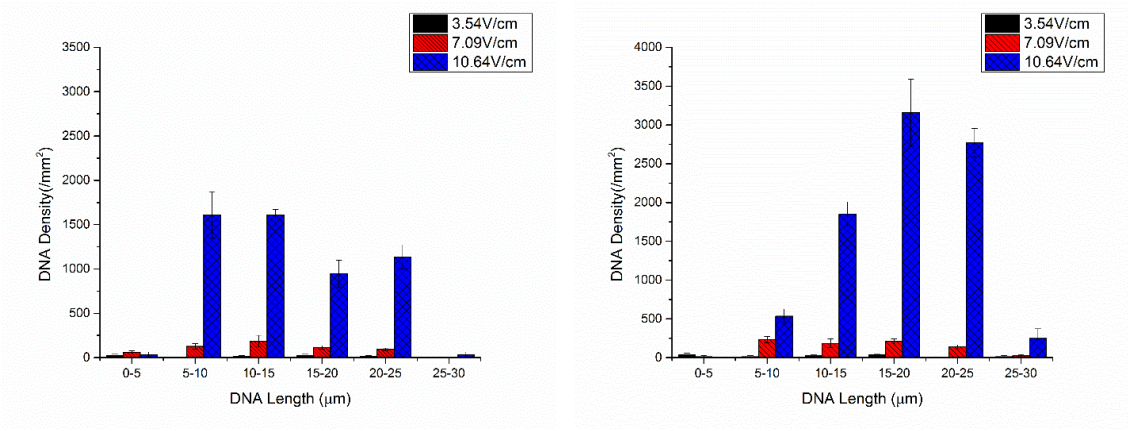

Figure 1.5: Histograms of lengths of adsorbed DNA Density for different electric field strengths. Left: DNA concentration of dipping solution is 125ng/mL. Right: DNA concentration of dipping solution is 250ng/mL.

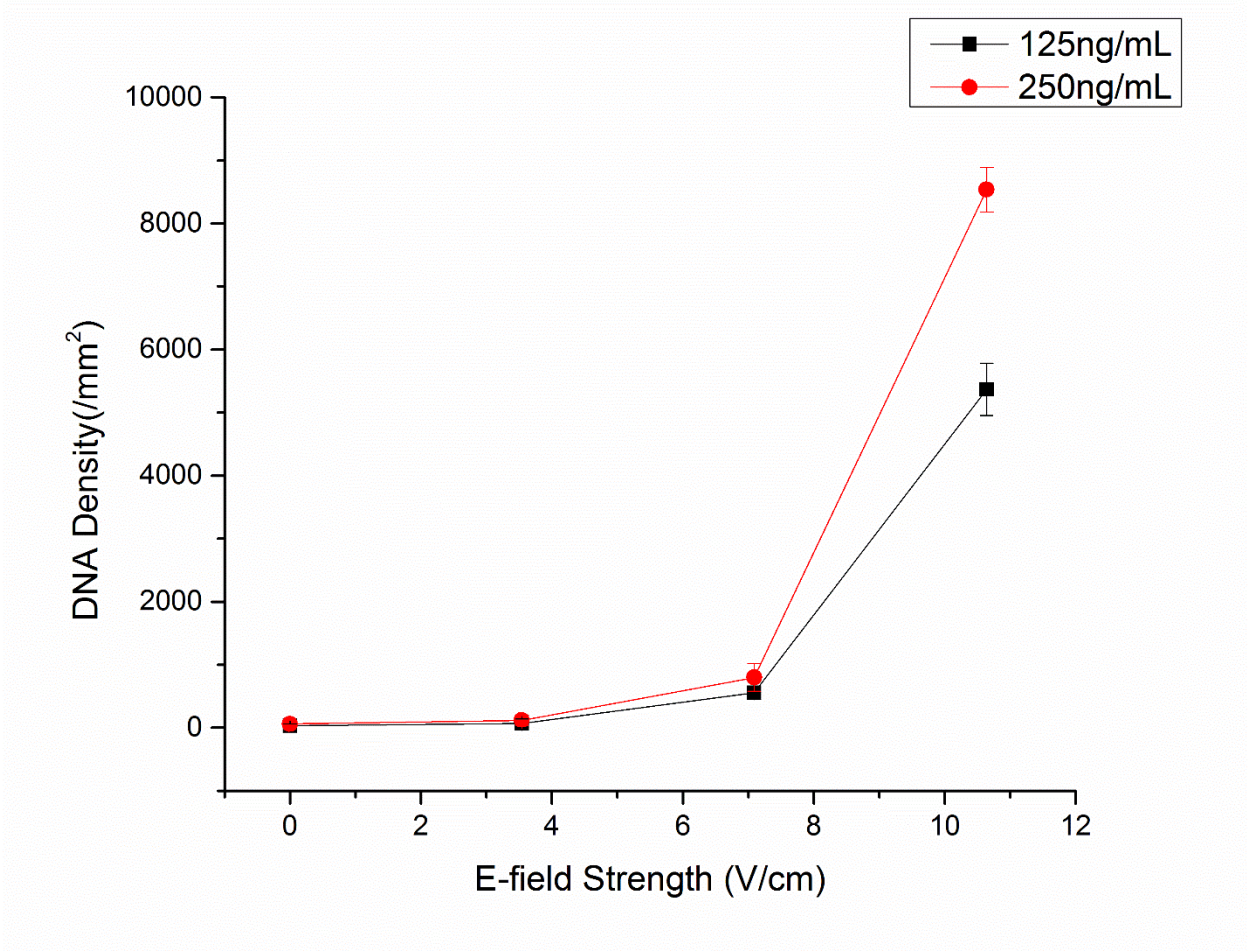

Figure 1.6: Adsorbed DNA density vs. electric field strengths for different DNA concentration of the dipping solution of 125ng/mL and 250ng/mL.

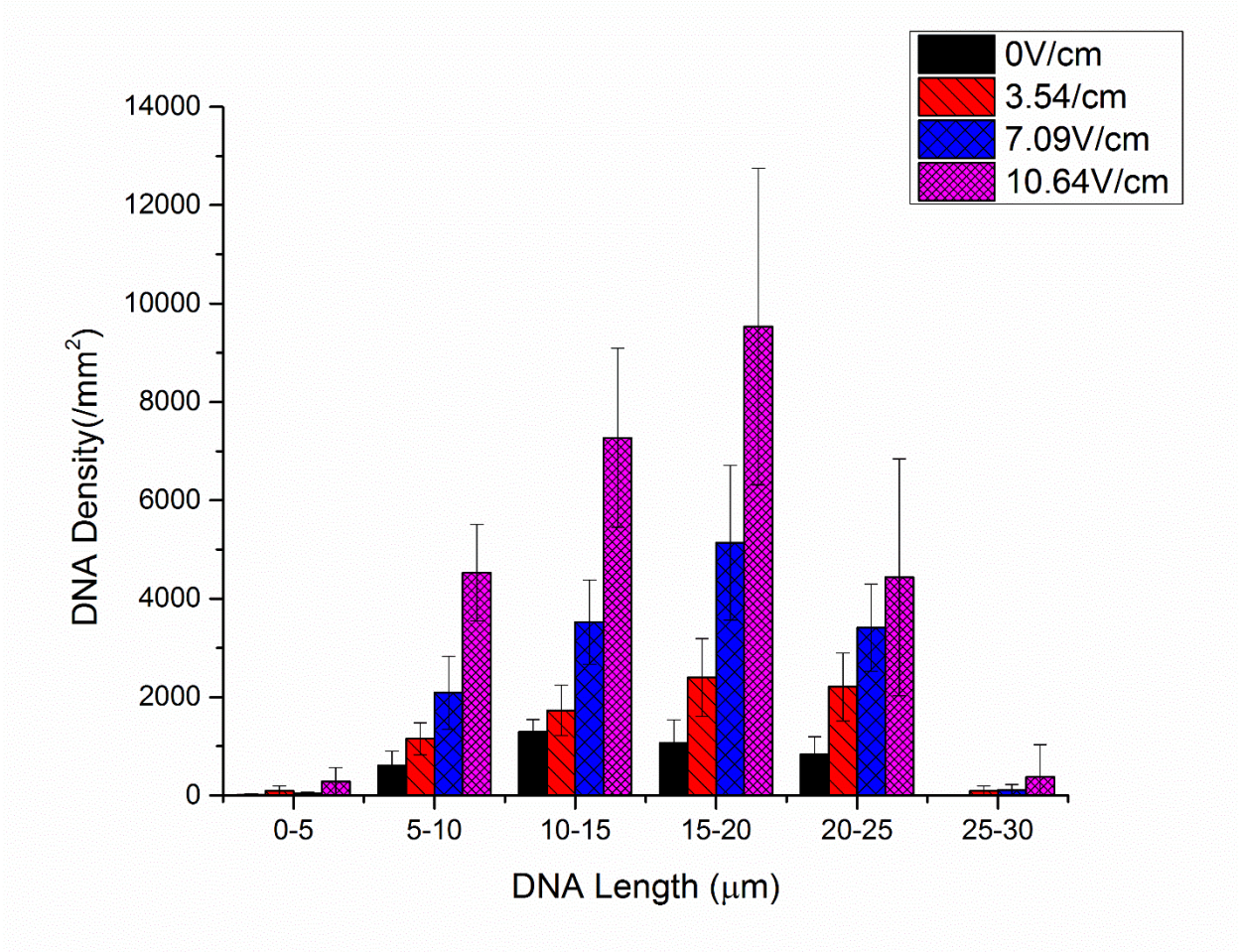

Figure 1.7: Histograms of lengths of adsorbed DNA density for different electric field strengths. DNA concentration of the dipping solution is 1.25μg/mL.

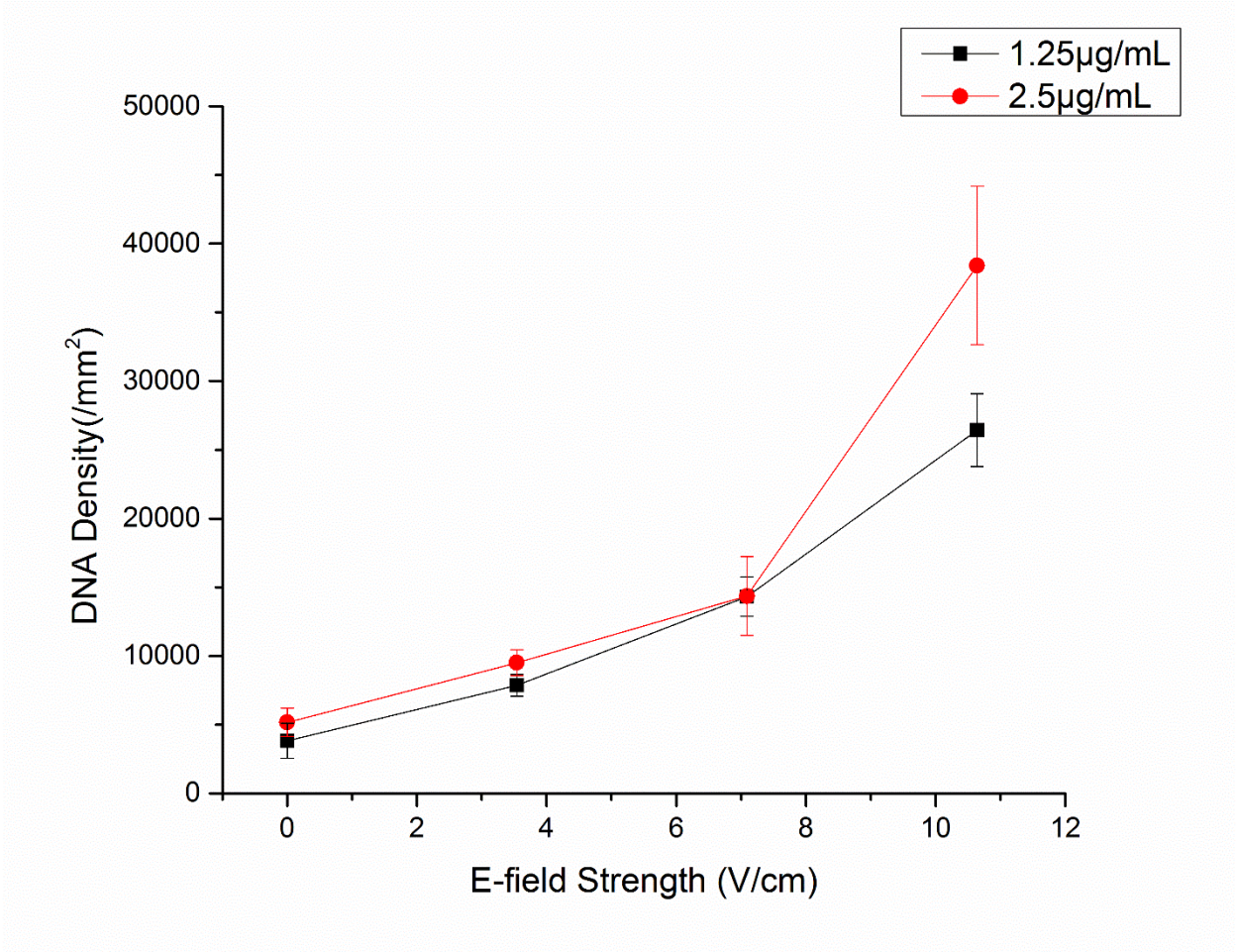

Figure 1.8: Adsorbed DNA density vs. electric field strengths for different DNA concentration of the dipping solution of 1.25µg/mL and 2.5µg/mL.

Table 1.1: Modified DNA adsorption efficiency

DNA Concentration in solution	**Electric Field Strength**			
	0V/cm	**3.54V/cm**	**7.09V/cm**	**10.64V/cm**
0.125ng/mm^3		5.55×10^2	4.62×10^3	4.29×10^4
0.25ng/mm^3		4.70×10^2	3.19×10^3	3.41×10^4
0.5ng/mm^3	2.43×10^2	6.93×10^2	9.96×10^3	3.10×10^4
1.25ng/mm^3	3.06×10^3	6.29×10^3	1.15×10^4	2.11×10^4
2.5ng/mm^3	2.07×10^3	3.4×10^3	5.74×10^3	1.54×10^4

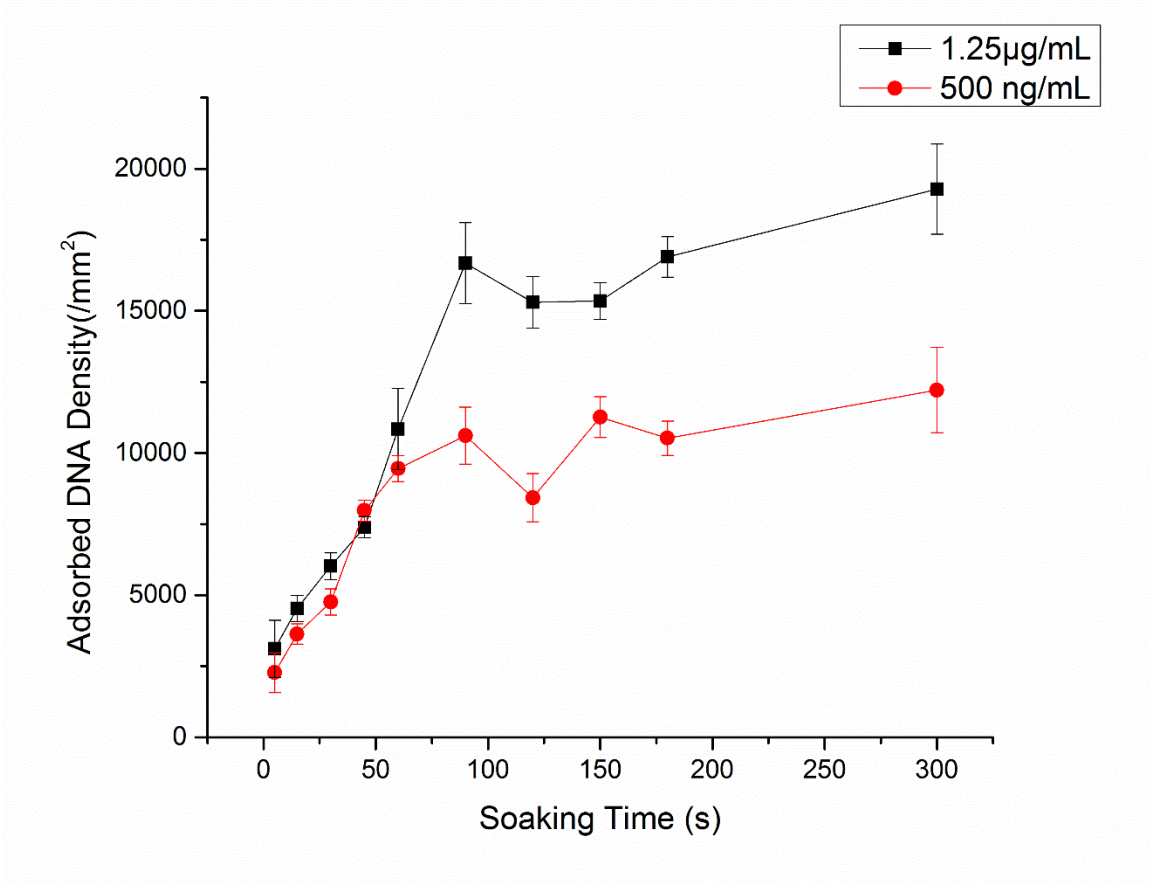

Figure 1.9: Adsorbed DNA density vs. soaking time for different DNA concentration of dipping solution of 500ng/mL and 1.25µg/mL.

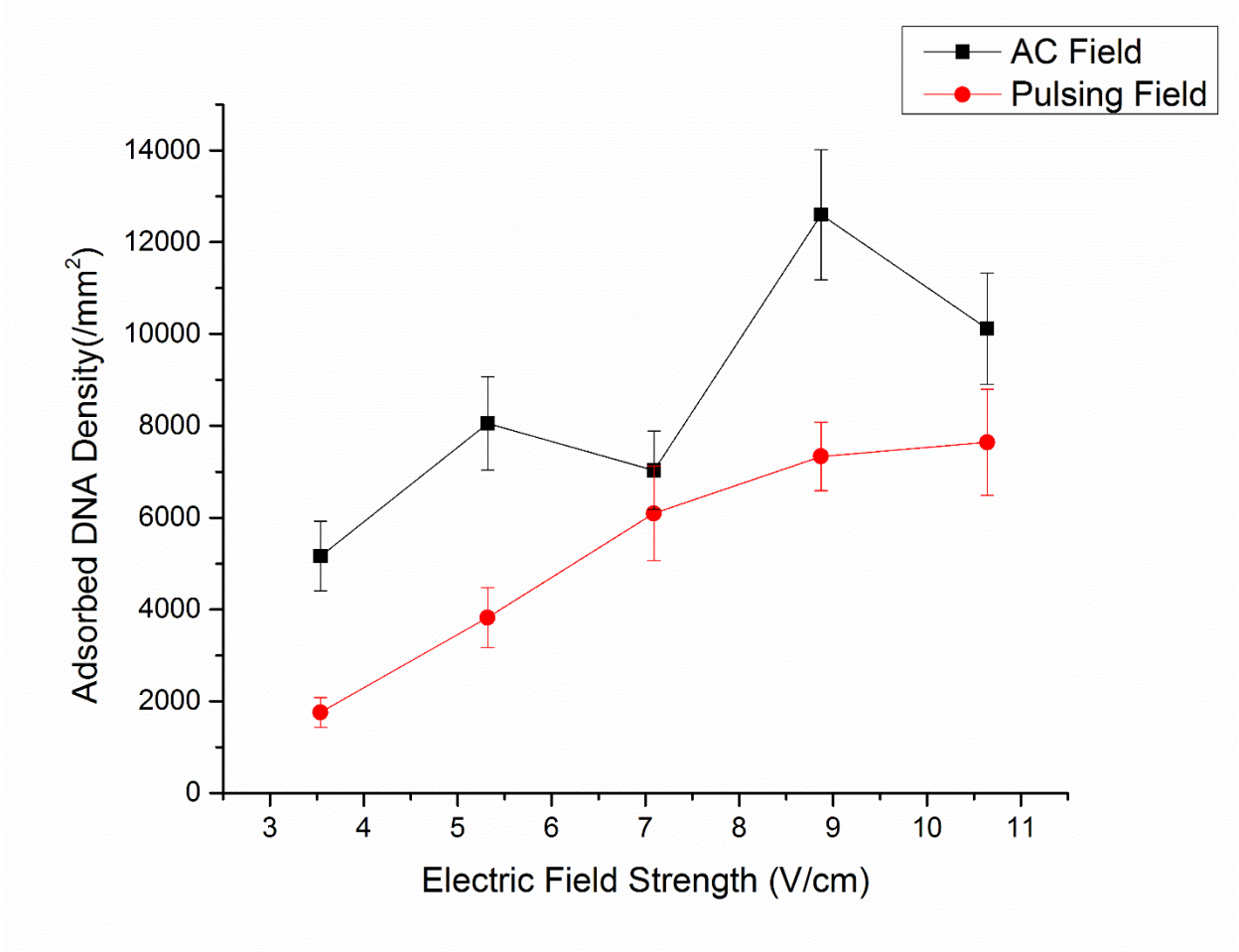

Figure 1.10: Adsorbed DNA density vs. electric field Strength for different types of electric field.

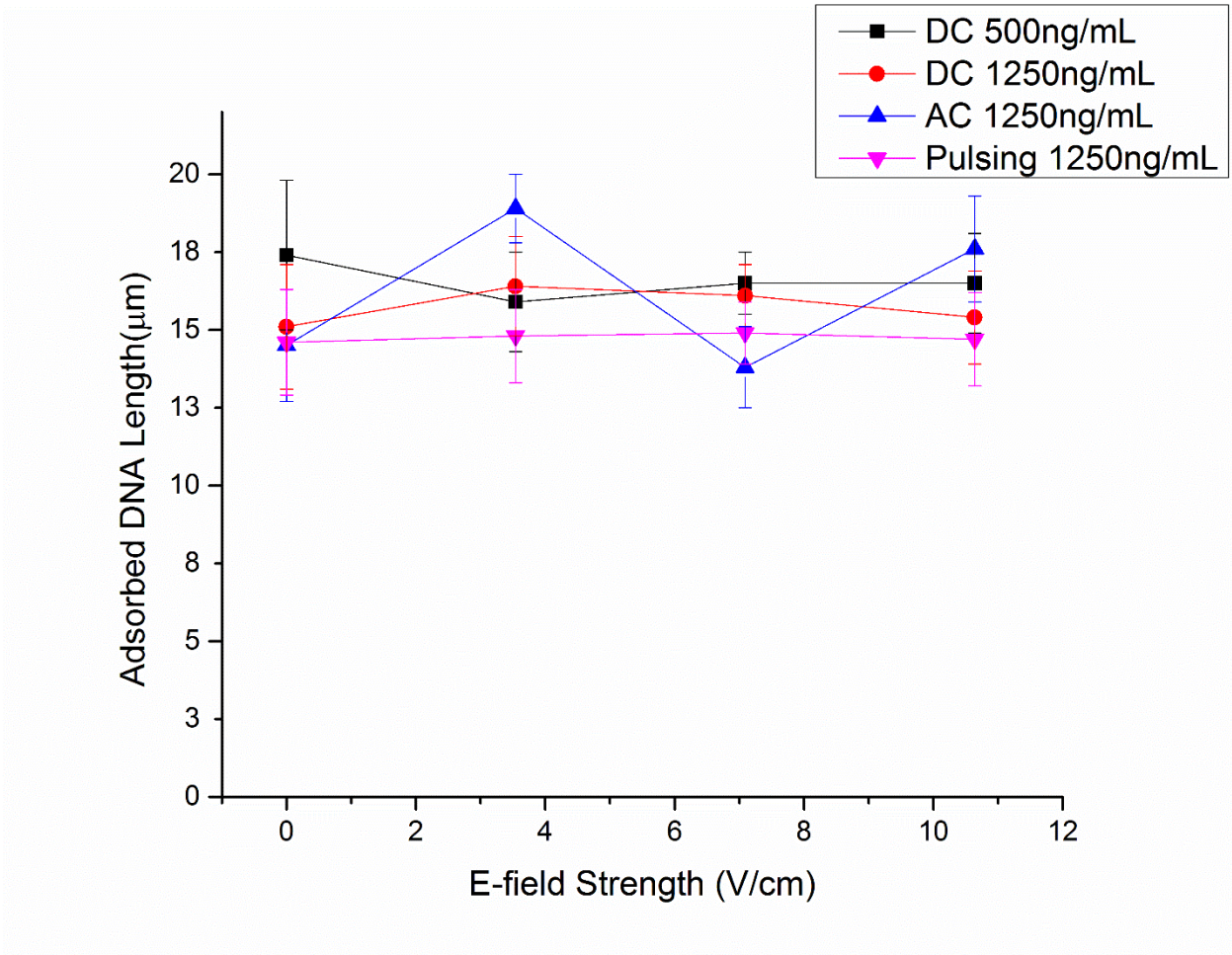

Figure 1.11: Adsorbed DNA length vs. electric field Strength for different types of electric field.

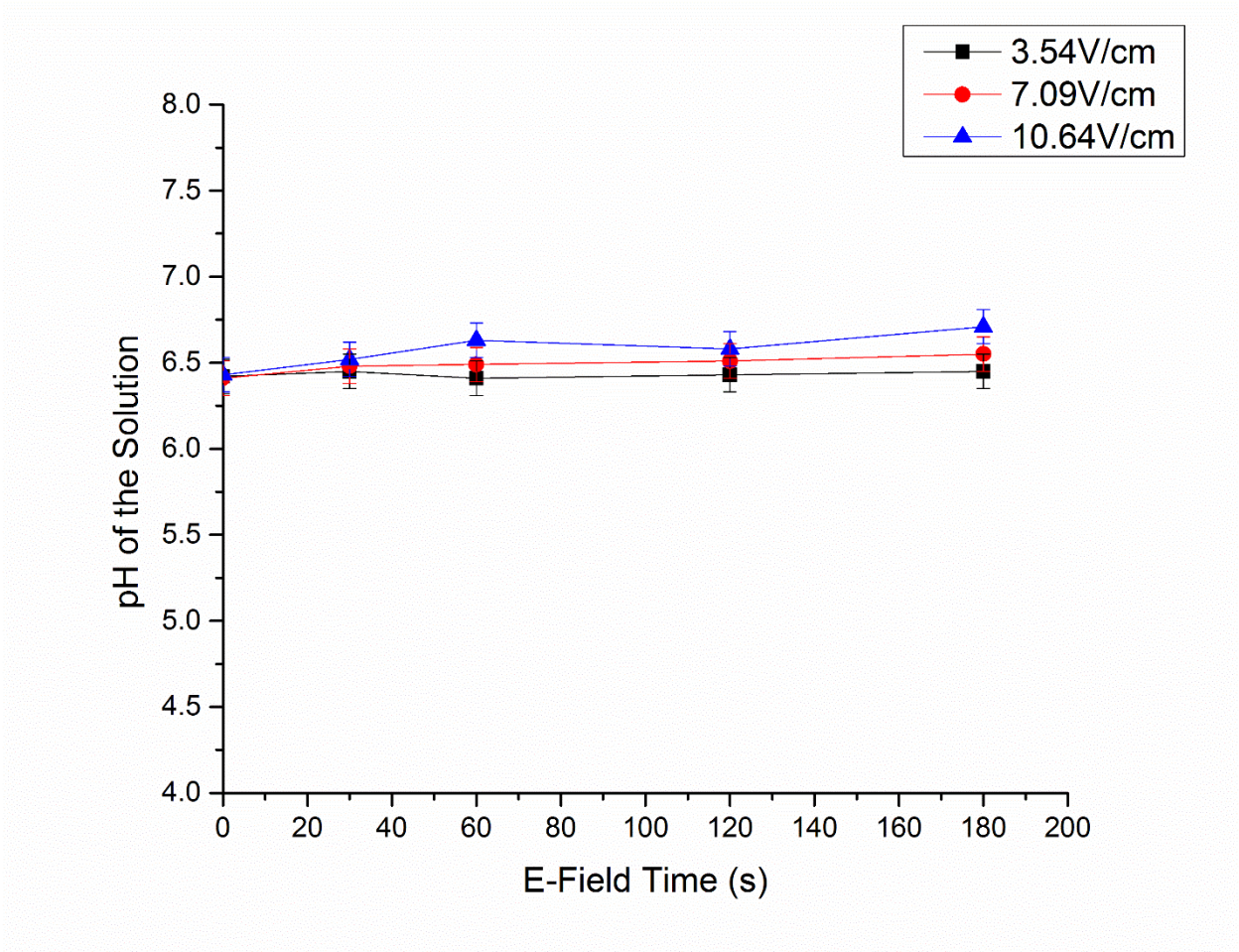

Figure 1.12: pH of the DNA solution vs. the electric field applying time of different electric field strengths. The e-field time here means how long the electric field was on before we measure the pH of the DNA solution. A slight incense was observed at 10.64V/cm, but it is less than 5% (from 0 to 180 seconds).

Chapter 2: Patterned Cutting of Surface-Adsorbed DNA Molecules

2.1 Introduction

DNA sequencing has a long history dating back to more than 30 years ago when F. Sanger and his co-workers proposed their famous DNA sequencing method[1]. A decade later, with the advent of 'first generation' automated sequencing instruments that were based on capillary electrophoresis, the Human Genome Projects became possible[2]. Because the read length of this technique is approximately 750bps or less, which is significantly shorter than the human chromosome (between 48×10^6 to 249×10^6 bps), DNA needs to be cut into small pieces to be analyzed. To date, cutting is done either completely randomly ("shotgun" method, usually by sonication) or by restriction enzymes (which cut at specific base sequences but show person-to-person variability). Both methods require complex methods and multiple, parallel experiments to string together ("assemble") the full sequence. The main improvements in the first 20 years of sequencing included more automation and a larger number of experiments done in parallel but the reconstruction process remained tedious and time-consuming. Significant errors are possible since repetitions are widespread in DNA sequences.

To speed up and lower the cost of DNA sequencing, various new DNA sequencing methods have been reported[3-8]. However, for most of these techniques, the reading lengths are shorter[3,9] than for the Sanger method: 1) the reading length of Roche GS FLX and TitanimuXL+ is about 700bps; 2) Illumina Hiseq 2000/2500 is able to read as long as 2×100bps, Miseq is 2×300bps; 3) the reading length of Ion torrent from Life Technologies is about 200-400bps; 4) RSII from Pacific Biosciences has a reading length that can be longer than 10kbps but it has not been yet widely used. Nanopore sequencing has been reported that their reading length can be up to 25 kbps or even longer but some fundamental problems have to be solved before it is put into practice[10-12]. Shorter reading length means more random cutting of DNA, massive data output and heavier work of reconstruction. A significant improvement could be made if a practical cutting method can be developed which cuts DNA segments from known locations within the genome, thus simplifying the assembly of the whole genome sequence.

In recent years, several research groups have tried to fragment and/or manipulate DNA with atomic force microscopy. For example, Xu and Ikai[13] reported that plasmid DNA can be picked up from a mica surface using an AFM tip. Hartman et al.[14] proposed a special method that combined AFM fragmentation with molecular combing to form complex nanopatterns of DNA molecules on solid substrates. Hu et al.[15] reported positioning isolation of DNA molecules that are stretched on substrates using AFM and they performed single molecular PCR to confirm that cut DNA molecules can be picked up by an AFM tip. Later on, their group reported another experiment using the same concept to demonstrate that DNA fragments produced by AFM ordered cutting can be sequenced and the sequence data was successfully pasted together from each fragments[16]. Furthermore, Washizu and his group have reported a series of experiments that aimed to connect controlled DNA fragmentation to next-generation DNA sequencing[17-19]: First, a pair of aluminum electrodes was patterned onto a substrate. When a 1MV/m 1MHz electric field was applied, DNA molecules were stretched and moved towards the edge of the electrode by dielectrophoresis, and one end of the molecules was firmly anchored onto an electrode. After that, the electric field is removed and a coverslip is put onto the chip. By slowly removing the coverslip in the direction that parallel to the DNA strands, the DNA molecules will be immobilized and stretched onto the substrates. Finally, DNA molecules, as well as the soft substrate layer, are cut together by an AFM tip. After releasing the DNA from the sublayer, DNA fragments cut from a specific position can be isolated. The group also explored other possibilities of cutting DNA molecules from a known position by AFM, such as using a cutting enzyme[20].

Here we propose a method based on cutting DNA molecules with a soft lithography technique. Our method can cut large numbers of DNA in parallel, promising proportionate improvements in efficiency and sensitivity. Also, since the spacing of the patterns may be varied easily, cuts of widely varying sizes may be readily produced.

Soft lithography

Soft lithography was invented as an alternative to photolithography and e-beam lithography[21,22]. Usually there are four major steps in the process of soft lithography[23]: 1) pattern design, 2) fabricating mask and master, 3) creating the soft stamp, 4) making micro or nanostructures on different surfaces or in different materials with the soft stamp by different application methods including printing, molding and embossing[24].

The molding material: Polydimethylsiloxane

Soft lithography refers to the fabrication of patterned copies using an elastomer stamp, and in most cases, is made of polydimethylsiloxane (PDMS). PDMS is a silicone elastomer with a very low melting point (about -50°C) and glass transition temperature (about -120°C)[25]. To fabricate a PDMS stamp or templates with micro or nanostructures, PDMS is usually prepared by a mix of a PDMS pre-polymer with a cross-linker. Then the mixture is poured onto a master to produce a faithful reproduction of the master pattern after curing.

PDMS offers a number of advantages including 1) it is elastomeric with a shear modulus of 0.25MPa and Young's Modulus of 0.5MPa[25], so the PDMS stamp deforms macroscopically to conform to surfaces with molecular-level contact over large area; 2) It is fairly easy to separate the PDMS from the master because of its flexibility and low surface energy. Binding fluorinated silanes onto the master surface can further enhance the ease of peeling off; 3) It is hydrophobic but can be modified by exposure to an oxygen plasma or Ozone treatment to become hydrophilic[26,27]; 4) It is non-toxic and non-reactive to most chemicals that are commonly used in biology and chemistry labs; 5) It is optically transparent.

Pattern Design

A pattern is usually designed by computer-aided design software programs and then sent to a manufacturer of the photomask. The pattern is then transferred to a thin layer of metal (usually chromium) that is coated on a glass slide using a laser or e-beam mask writer.

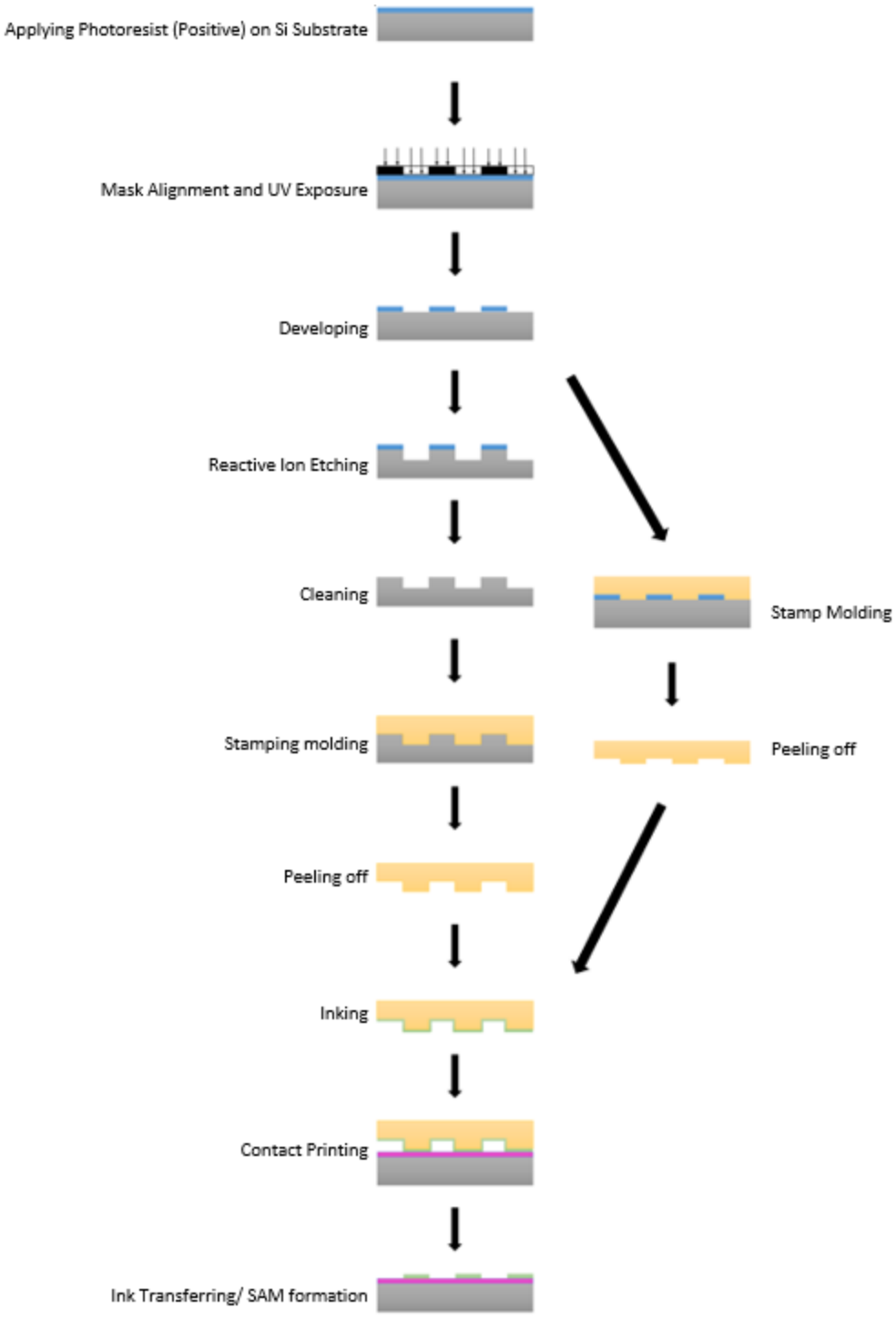

Figure I: Schematic diagram to show the process of making silicon master, PDMS stamp and micro-contact printing (on the left).

Master fabrication

The master used in the molding of PDMS stamp is fabricated in a clean room. UV photolithography is the most commonly used technique for this process: First, a thin layer of photoresist was spun onto a silicon wafer, the thickness of the photoresist film can be controlled by changing the concentration of the photoresist solution, the spin cast speed and duration time. After baking on a hot plate, the photoresist coating is exposed to the UV light through a mask. The mask allows light to pass through in certain areas and is blocked where Cr is present so that the designed pattern can be transferred into the photoresist film. The photoresist coated silicon wafer is then immersed into a developer, which is designed to wash off the soluble part of the photoresist. For the positive photoresist, the soluble part would be the area that was irradiated by the UV light, causing polymer chain scission, while for the negative photoresist, on the contrary, would be the area free from the irradiation of the UV light (the UV light causing crosslinking of polymer chains).

After cleaning, what is left on the silicon surface is a protective cross-linked photoresist layer with the desired pattern, and this can be used directly as a master for stamp molding (not shown in the schematic). The height of the pattern in the stamp is then controlled by the thickness of the photoresist layer. On the hand, one can perform reactive ion etching on it, the bare silicon area would be etched and once the photoresist is completely washed off, the pattern would be transferred into the silicon wafer. In this case, the height of the pattern in the stamp is determined by the etching process, including the etching time, gas composition and mix radio. The resolution can be affected by the etching process as well, due to the lateral etching. Usually, the resolution of UV photolithography is about 1 to 2μm, which is limited by the diffraction of the light at the edge of the opaque areas of the mask and the thickness of the photoresist film.[28] A primary master can be fabricated by e-beam lithography as well. The advantage of e-beam lithography over photolithography is that it can generate structures with much higher resolution, typically 20 to 30nm in lateral dimensions. However, the processing time of e-beam lithography is much longer and it is much harder to gain access to an e-

beam lithography facility so that the whole soft lithography process can be less efficient or convenient.

Fabrication of the PDMS stamp

In soft lithography, the product that is produced from the master is usually referred as a stamp, which is the core component and is usually made with PDMS as we described previously. The mixture of PDMS pre-polymer and cross-linker, usually at the mass ratio of 10:1, is cast against a master whose surface has been patterned. Then the master with the mixture is put onto a 65°C hot plate to cure for more than 2 hours. The mechanical properties of the PDMS stamp are very important for both transferring a pattern with high accuracy and downstream applications. Finally, after peeling off from the master, the PDMS stamp with pattern is ready for use. By repeating this casting and embossing step, multiple replicas can be produced from the same master rapidly, which is another useful feature of soft lithography.

Micro-contact Printing

The most common application of soft lithography is micro-contact printing[29-31]. In μCP, the surface of the patterned PDMS stamp is loaded with a certain material that is often referred as "ink". The stamp is made to fully contact the substrate, causing the ink molecules to bind to the new surface. Thus the pattern is transferred from the PDMS stamp to the new surface.

For the process of μCP, the surface chemistry of the stamp surface and printing surface are very important in determining the efficiency of transferring ink molecules. For a successful μCP, the ink molecules must be transferred onto the new substrate from the patterned stamp surface, thus the ink molecules binding to the new surface must be more energetically favorable than remaining on the stamp. Also, due to the nature of PDMS, the stamp surface is hydrophobic, which is well suited for inks like alkyl thiols. However, if the ink contains more polar molecules, such as proteins or DNA, these water-soluble inks will not wet the stamp surface, resulting in poor pattern transfer. The most common way to increase the hydrophilicity of PDMS stamp surface is oxidation by

UV/Ozone[32] or oxygen plasma[33,34] treatment. The water contact angle can drop from 110° to less than 40° (some reports claim less than 10°) after oxidation[23].

The mechanism behind PDMS oxidation is not fully understood. It is known that when a PDMS surface is exposed to oxidation, the content of atomic oxygen increases, while the silicon content is unchanged[32]. It is also known that the binding energy of Si shifts to the values corresponding to SiO_2 as confirmed by X-ray photoelectron spectroscopy, suggesting the formation of a silica-like layer (SiO_x) on top of the PDMS surface[33,35]. In practice, an oxidation time of up to 30 minutes is sufficient to obtain a laterally homogeneous hydrophilic PDMS surface.

The polarity of the oxidized PDMS surface decreases with time after oxidation, a phenomenon known as "hydrophobic recovery" and can be explained as follows: free low molar mass PDMS chains migrate to the surface through the defects of the silica-like layer. As the tendency at equilibrium is to minimize the surface energy, these low molar mass molecules will finally cover the surface, resulting in the polarity of the PDMS surface decreasing. Another reason for hydrophobic recovery is that polar groups reorientate from the surface to the bulk or the nonpolar groups reorient from the bulk to the surface. Under mild oxidation conditions, the second mechanism contributes more to the hydrophobic recovery[32]. To reduce this effect, the oxidized PDMS stamp may be stored in water[27].

One large advantage of using PDMS stamps is the capability to attain atomic level contact on a non-flat surface during stamping because they are flexible and deformable. However, this also limits the resolution and aspect ratio of the patterns imprinted on the PDMS stamps. Usually, with the common PDMS material (Sylard 184 from Dow Corning) and processing methods, the feature size on the stamp can be as low as 500nm[24]. With a special modified hybrid stamp containing two PDMS layers, a 30-40μm thick h-PDMS stiff layer supported by a 3 to 5mm thick regular flexible PDMS layer, the resolution can be improved to 50 -100nm[36].

Typical deformations due to the flexibility of PDMS stamp include roof collapse (sagging), lateral collapse and rounding by surface tension. If the height (*h*) is much less than the distance between each feature (*d*) (typically the aspect ratio, *h*/*d* is less than 0.3), the roof of the pattern can collapse, leading to excessive undesired contact areas between the stamp and the substrate[23,37]. However, if the height (*h*) is much greater than the width of the feature (*h*/*l* is larger than 5), lateral collapse or pairing is likely to occur[23,37]. Another type of deformation that can occur to PDMS stamps during pattern transfer or μCP is the rounding of the shape due to surface tension. Calculations suggest that the lower limit to the radius of curvature of corners in 184 PDMS is on the order of 50 nm[37].

a)

b)

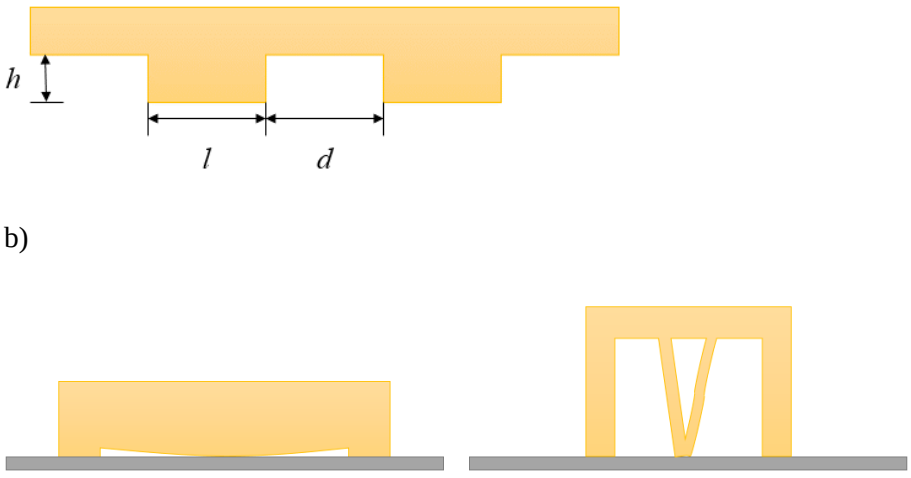

Figure II: a) A schematic diagram to show the feature height (*h*), width (*l*) and the distance between each feature (*d*) of a PDMS stamp; b) Common deformations of a PDMS stamp: sagging or roof collapse (left), pairing or lateral collapse (right).

Applications of Micro-contact Printing

In its original form, μCP was used to pattern organic thiols onto gold surfaces[21], and since then it has been widely used in printing and patterning on Ag[38], Cu[39], Pd[40] and glass surfaces. In addition to molecules that form self-assembled monolayers[41], various types of "inks", including DNA molecules[42-44], proteins[45-47] and cells[47,48] have been used

in the μCP process. Controlling DNA molecules so that they can attach to a solid substrate in an array fashion has application to gene expression profiling[49-51], gene mutation detection[52] and sequencing[53]. Depositing small droplets of DNA solution sequentially onto a solid substrate using needles or ink jet nozzles has become a standard way to fabricate DNA arrays[51]. A major drawback of these techniques is the inhomogeneity caused by the drying process of the DNA droplet. For example, different shapes of rims around different individual spots may form after the evaporation. Another drawback is that each DNA array is written as an original and has to be fabricated one after another. When combined with μCP, the processing speed can be improved significantly because of the capability of printing multiple arrays from a single loaded stamp. Also, once the DNA molecules are loaded onto the stamp surface, the following transferring step does not require water or any other solution, so the dots are much more homogeneous.

Micro-contact printing has been incorporated with molecular combing to fabricate well-defined arrays with stretched DNA molecules. Nakao et al. [54]deposited a DNA solution droplet onto a flat unmodified PDMS stamp. After removal of the droplet, DNA molecules were successfully absorbed and stretched onto the stamp surface. Next, the DNA molecules were transferred onto an unmodified glass coverslip or mica surface using μCP. The transfer rate of DNA was reported to be nearly 100%. Gad et al.[55] stretched and patterned DNA molecules on a mica surface using dynamic molecular combing and μCP. A line-patterned PDMS stamp, which was pre-silanized with highly diluted aminopropyl trimethoxysilane, was used as a solid surface to adsorb DNA by dynamic molecular combing. It was dipped into the DNA solution in such a way that the line patterns were parallel to the liquid surface and therefore the combed DNA strands would be perpendicular to those line patterns. Then the stamp was printed onto the mica surface. A high density of stretched DNA molecules was obtained and if the length of the dipped DNA molecules is the same as the width of the line pattern, selectivity of adsorption can be achieved. Both of the experiments showed that DNA molecules that were combed on patterned/flat PDMS stamp surfaces can be transferred onto other solid surfaces.

In another experiment by Guan et al.[56], a PDMS stamp patterned with microwell arrays was pressed against a glass coverslip that was preloaded with a DNA solution. Different methods were then used to peel off the glass coverslip. In the method of peeling off the stamp at a low speed, the combed DNA strands were likely to follow the shape of the microwell while at high speed, the DNAs were likely to bridge over the microwell and be connected with another combed DNA molecule to form a much longer strand compared with its contour length. For the former case, stretched DNA strands broke at the edges of the microwells during contact printing, resulting in portions of DNA that in the well had not been transferred. The length of transferred DNA strands was determined by the distance between each microwell. For the latter one, the part of DNA strands that was suspended over the microwell would be transferred with the part that was on the top of the stamp surface as well, resulting in long, stretched and unbroken DNA strands on the solid surface. Furthermore, by rotating the stamp 90° and re-stamping, arrays of DNA strands 'crosses' could be fabricated for both long and short methods. This work showed that DNA molecules that were combed on patterned PDMS stamp surfaces can be transferred onto other flat solid surfaces but DNA strands can be broken at the edge of the PDMS stamp pattern during the contact printing. The work also demonstrated that by careful design of stamp patterns and performing multiple contact printings with different alignments, various stretched DNA arrays with well-defined arrangements can be fabricated.

Instead of depositing and stretching DNA strands on a PDMS stamp surface, Bjork et al.[57] proposed another way to fabricate arrays of stretched DNA. Hydrophobic patterns can be fabricated by applying a patterned PDMS stamp onto the desired surface. During the contact time, low-molecular weight species from the PDMS stamp would transfer onto the new surface and then form a thin hydrophobic layer. Because DNA combing only takes place at the hydrophobic area of the surface, the stretched DNA array can be created by simply performing molecular combing with this surface-energy patterned substrate. In another set of experiments, conjugated polyelectrolyte-decorated DNA molecules were combed onto PMMA-coated flat PDMS stamps, as they had previously demonstrated that PMMA-coated stamps would result in a more well-defined stretching length of the DNA compared to the results with a bare PDMS stamp. After

that, the stamp was printed to an energy-patterned glass coverslip (since the DNA molecules would only transfer at the hydrophilic area), stretched DNA arrays can be fabricated on specific regions. This work offers other ways for localization of stretched DNA arrays on solid substrates and demonstrated the potential of applying μCP and molecular combing to nanotechnology. It also confirmed that hydrophobic substrates are suitable for molecular combing while hydrophilic substrates are better for transfer printing of DNA.

The method we propose here utilizes molecular combing, soft lithography and micro-contact printing to fragment DNA molecules on surfaces with high efficiency. We believe that this method not only has the potential to enhance the speed and accuracy of DNA sequencing when combined with NGS platforms, but also can make a contribution to construction of future nanodevices.

2.2 Materials and Methods

The process of this experiment includes 3 parts: silicon mold and PDMS stamp nanofabrication, dynamic molecular combing and cutting of adsorbed DNA molecules on a PMMA surface using microcontact printing.

2.2.1 Silicon mold fabrication

Silicon molds were fabricated at Brookhaven National Lab: 1) 4-inch clean silicon wafers were rinsed with acetone and then DI water, 2) incubated at 110°C on a hotplate for 10 minutes, 3) spin coating of HMDS (hexamethyldisilazane) onto silicon wafer at 3000rpm for 30 seconds to enhance the adhesion of photoresist and silicon surface, 4) spin coating of photoresist onto surface at 3000rpm for 30 seconds, 5) incubation at 100°C on a hotplate for 90 seconds, 6) exposure to UV light on a MA-6 mask aligner with a photomask (made by aBeam Technologies), 7) developed in the corresponding developer for sufficient time, usually 30s to 2minutes depending on the type of photoresist 8) etching by a plasma that contains SF_6 and CHF_3(Oxford-F) for 30 to 180 seconds, 9) O_2 plasma cleaning for 5 minutes to remove photoresist (an optional step that is mainly used for negative tone photoresist), 10) immersion into solution to

clean the photoresist left on the surface. Atomic Force Microscopy (Bruker) was performed to measure the depth of the resulting pattern features.

2.2.2 PDMS Stamp fabrication

Usually the silicon mold surfaces were cleaned as follows: 1) boiling in 1:1:4 solution of ammonium hydroxide: hydrogen peroxide: DI water for 10 minutes then rinsing with DI water, 2) soaking at room temperature for 15 minutes in 1:1:3 solution of sulfuric acid: hydrogen peroxide: DI water, 3) DI water rinse. Then 1.5mg/mL PMMA (Mw=70k) solution was spun cast onto the mold surface at the speed of 2500 rpm for 30 seconds.

A mixture of 10 ± 0.01g of PDMS with 1 ± 0.01g of silicone elastomer curing agent was mixed with a Teflon "policeman" in a petri dish. The petri dish was then placed in a vacuum for at least 15 minutes to remove bubbles. After that, the PDMS curing agent mixture was carefully cast onto a silicon mold, making sure that the whole mold surface was covered. Lastly, the mold was placed onto a 65°C hot plate for another 24 hours before removing the PDMS layer.

2.2.3 Molecular combing

The molecular combing process follows the same procedure as we described in the previous chapter except that higher concentrations of DNA solution (from 25μg/mL to 50μg/mL) were used in order to increase the adsorbed DNA density on the surface. Also, larger 2cm by 5cm PMMA coated silicon wafers were used in some of the experiments instead of 1cm by 1cm samples.

2.2.4 Stamping procedure

The stamp was placed in an Ultraviolet Thermal Ozone Modifier for 15 minutes immediately before the stamping process in order to make the stamp hydrophilic and improve the adhesion of the DNase I enzyme to the stamp. During the experiment, the stamp was placed back in the UV Thermal Ozone Modifier every hour because of "hydrophobic recovery". The DNase I enzyme solution was prepared by mixing 180μL

of deionized water, 20µL of 1X DNase I buffer, and 10µL of DNase I enzyme in a 1.5mL test tube. The enzyme was then incubated at 36°C for 10 minutes.

Several stamping methods have been explored during the experiments and the best one is described as follows: 60µL of enzyme solution was loaded onto a 5cm by 5cm rectangle of sterile Technicloth. The PDMS stamp that was pretreated with the Ultraviolet Ozone step was placed pattern side down on the Technicloth stamping pad for thirty seconds. The stamp was removed from the Technicloth and then the stamp was picked up and the patterned surface was gently tapped with another dry Technicloth to remove excessive enzyme solution. The stamp was placed onto the silicon wafer using tweezers to ensure that the surfaces made full contact. A foam pad, a thin aluminum plate and a metal weight of about 600g were added on top of the PDMS stamp to ensure the conformal contact over the entire stamping area. The set up was then placed on a 40°C hot plate to optimize the DNase I activity. After 15 minutes the stamp was removed and the sample was imaged by fluorescence microscopy and AFM.

2.2.5 DNA Desorption Method

A Phenol Chloroform Isoamyl Extraction Procedure is an effective method to remove the DNA from the surface into the solution. The procedure is as follows: 1) about 20 to 50 2cm by 5cm samples were immersed two at a time in the phenol chloroform isoamyl (25:24:1) solution and immediately pulled out, then the solution was transferred equally into two 1.5ml Eppendorf tubes. 2) 500µL of TE buffer were added to each Eppendorf tube. Each test tube was shaken 20 times and then centrifuged for 5 minutes at 14000rpm. The top part of each test tube was extracted and transferred into new Eppendorf tubes. 3) The extracted TE buffer and DNA solution were mixed with 180µL of 7.5M ammonium acetate, 1µL of glycogen, and 600µL of 100% ethanol. The solution was left at room temperature for 20 minutes and then centrifuged for 30 minutes at 14000rpm. 4) After that, a DNA pellet can be seen by eye and the liquid is discarded as much as possible without disturbing the pellet. 5) 600µL of 95% percent ethanol were added to the precipitate and the solution was centrifuged for 10 minutes at 14000rpm. The supernatant was discarded. 6) Repeat step 5 with 600µL of 80% percent ethanol. 7)

The precipitate was left at room temperature and placed beside a fan for 5 minutes to dry out any remaining liquid. 8) Add sufficient buffer solution into the test tube.

2.3 Results

2.3.1 Optimize the conditions for PDMS stamp microfabrication

The choice of photoresist

The silicon mold fabrication was done by photolithography in the Center for Functional Nanomaterials at Brookhaven National Laboratory. Three kinds of photoresist were tested during our experiments: negative photoresist MaN-1410 and positive photoresists S1811 and S1805. Because the smallest feature size of our pattern is 1.5μm, which requires relatively high resolution, thicker photoresists such as MaN-1410 (film thickness is 1.0μm) and S1811 (film thickness is 1.1μm) often result in insufficient exposure, leading to pattern features missing in the silicon mold as well as the PDMS stamp (Figure 2.1c). On the other hand, when using S1805 (film thickness is 0.5μm), the pattern can be etched into the silicon wafer with high fidelity (Figure 2.1a and b).

Pattern depth in the silicon mold

The pattern depth in the silicon mold is controlled by the plasma etching time. Etching times longer than 150 seconds were not acceptable since the plasma would penetrate the photoresist layer. If the depth of the patterns on the silicon mold is too small, then the PDMS stamp made from it would collapse when printing onto the surface. On the other hand, if the etching depth is too deep, then it would be harder to peel off the PDMS stamp from the mold since some part of the stamp would be broken and remain inside the etched part of the silicon mold. In addition, the etched line will become wider with the increasing of the etching time due to the horizontal etching by the plasma. Considering all the conditions above, a range of 300-500nm of depth, corresponding to 60-120 seconds of etching time, is an optimized range for our experiment.

Distance between each cutting line

The distance between each etching line corresponds to the length of DNA

molecules that remain on the surface after cutting. In the experiments, the mask we designed has increasing line distances ranging from 1.5μm to 40μm. A PDMS stamp was then made using the silicon mold. After that, 5000X diluted (from stock) Sybr Gold dye solution was applied onto the patterned PDMS stamp surface which allows us to check the pattern quality on the PMMA surface after contact printing. As we expected, once the distance extended over 10μm (h/l is about 0.05), the pattern quality is reduced and extra, undesired, contact areas appear, suggesting that roof collapse of the PDMS stamp occurs during the contact printing process (Figure 2.1, c and d). In conclusion, for the pattern depth that we choose, the distance between each etching line should be smaller than 10μm to get consistent faithful pattern transfer.

Surface treatment of the silicon mold

The positive photoresist is much easier to clean compared to the negative photoresist, which usually requires an O_2 plasma cleaning process and specialized remover. For our experiment, acetone is sufficient to clean the left-over S1805 photoresist on the silicon surface. In addition, each time before pouring on PDMS, the silicon mold was cleaned by ammonium hydroxide with hydrogen peroxide followed by a solution of sulfuric acid and hydrogen peroxide. However, due to the adhesion force between the PDMS and the Si/Si oxide surface, it is almost impossible to peel off the stamp cleanly, without disrupting the pattern's features. Usually, to reduce the adhesion, the silicon mold surface has been pre-silanized before casting PDMS onto it to eliminate this effect[58]. Here a much simpler method is used to address this issue: a highly-diluted PMMA solution (3mg/mL) is spun cast onto the silicon mold surface, resulting in a sub-100Å thick PMMA film. This PMMA film acts as a release layer that separates the PDMS from the mold surface and makes it very easy to peel off the PDMS stamp. Although this layer may introduce some distortion to our pattern, we believe that the variation is small (10nm/500nm, or about 2%) and so far no significant degradation of the patterns have been noticed in our experiments.

2.3.2 Stamping Methods

DNA molecules that are adsorbed onto solid surfaces can be fragmented by micro-contact printing. Figure III shows the concept of this method. First, DNase I is applied onto the pattern surface of the PDMS stamp. DNase I is a non-specific enzyme that attacks the phosphate backbone of the DNA molecule. Then the stamp is brought into contact with the surface that contains adsorbed DNA molecules. By carefully adjusting the parameters like the pressure applied to the stamp and the amount of DNase I, the only contact areas between the stamp and the DNA molecules are the designed cutting areas, so that the DNA molecules can be fragmented at the desired positions.

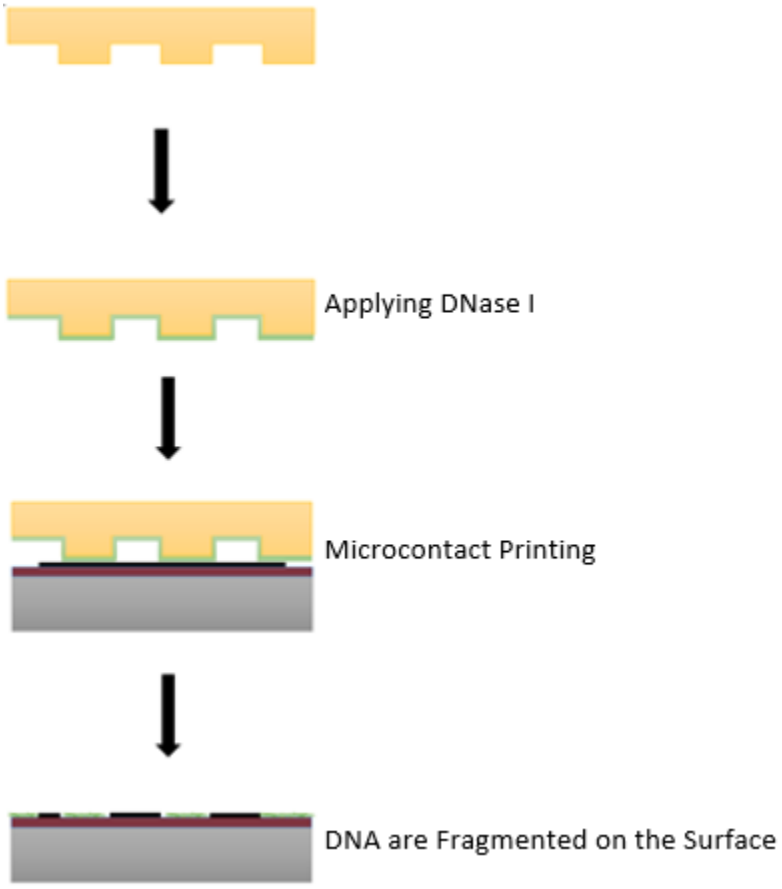

Figure III: Schematic diagram to show the designed cutting process: 1) applied the enzyme onto the patterned PDMS stamp surface; 2) cut adsorbed DNA molecules on surface by micro contact printing.

In the following series of experiments, the stamps we used were about 1cm by 1cm, with a symmetric grating pattern, meaning both the width of the cutting line and the distance between each cutting line is the same. After confirmation of the presence of surface-adsorbed DNA, the sample was stamped. Different enzyme "inking" methods were tried in an effort to optimize conditions: 1) Micropipette method: a large droplet of diluted DNase 1 (50-100μL) was applied onto the stamp to completely cover the patterned surface by a micropipette and incubated for 1-5 minutes, followed by wiping away excess solution with a cotton-tipped applicator. To obtain more consistent results, variations were made on the procedure, including drying the DNase 1 with Technicloth cleanroom wipes. 2) Swab method: DNase I was applied by using a swab to spread the solution across the stamp surface, then using another dry swab to remove the remaining excess liquid. 3) Dipping method: immerse the stamp into the enzyme solution and then pull it out at a constant speed. 4) Stamp pad method: the PDMS stamp was placed in contact with a Technicloth wetted with the DNase 1 solution, thereby adsorbing a minimal amount of the solution, then the stamp was picked up and the patterned surface was gently tapped with another dry Technicloth to remove excess enzyme solution. 5) Exposing the stamp to an ozone plasma for 20 minutes and try all the methods we described above again. For the stamping step, tweezers are used to place the PDMS stamp onto the surface until a color change is observed, which indicates proper contact between the surfaces. If a colorful diffraction pattern is observed, that usually means there are air bubbles and dust inside and the contact is poor between the stamp and the surface with adsorbed DNA. Different weights up to 800g were tested to apply different pressures on the PDMS stamp.

Results from the different methods are shown on Figure 2.2. To summarize the results, the ozone plasma is an absolutely necessary step since it makes the stamp surface hydrophilic. Without this step, the enzyme solution would form small droplets on the PDMS surface after the inking process rather than spread out evenly and form a thin enzyme layer, which is the desired situation. If the stamp is directly printed with the enzyme droplets on it, the surface often ended up with too much enzyme solution and most DNA molecules on the surface were "wiped out". On the other hand, if those enzyme droplets were removed from the stamp surface as we described in steps 1 or 2

above, there will be too little enzyme left on the stamp surface and it is insufficient to cut the DNA molecules. Furthermore, even with the ozone step, the Stamp Pad Method produces much better results compared with the rest in both cutting uniformity and in process repeatability, especially when dealing with large cutting stamps as discussed below. As for the stamping process, too little weight often causes non-uniformed cutting, as there is not enough pressure to push down the stamp. As the weight ranged from 600g to 800g, a good conformal contact between the stamp and the surface with adsorbed DNA molecules was reached while the PDMS stamp itself is still rigid enough to hold its conformation.

2.3.3 Cutting DNA with asymmetric PDMS stamp

PDMS stamps have been reported to transfer printed DNA onto a new surface after adsorbing DNA molecules onto the stamp surface, including both modified and unmodified stamps. However, use of a PDMS stamp to cut DNA that is adsorbed on surfaces has not been previously reported. Here we present is a new method for ordered cutting DNA into desired lengths. In many applications, especially in next-generation DNA sequencing, there are requirements on the length of the target DNA molecules. As for this method, the length requirements can be satisfied by adjusting the distance between each cutting line. In addition, in order to preserve as much DNA as possible after the cutting process, the cutting area should be designed as small as possible. In the following experiments, the PDMS stamps are made using a photo mask with an asymmetric grating pattern. The distance between each cutting line is 3.5μm, corresponding to 10kbps of DNA molecules left over on the surface after cutting. This length is compatible to some NGS techniques such as Pacific biosciences platform. The width of the cutting line is 2.5μm, which is the finest resolution the mask company (a-beam) reports that they could maintain pattern quality over a large pattern area (2cm by 5cm).

As shown in Figure 2.3, lambda DNA molecules that were adsorbed on a PMMA-coated silicon surface were successfully fragmented over a fairly large area. The edges of the cutting lines are well defined and can be seen clearly. The average length of 20

fragmented DNA strands was measured and the result was $3.40 \pm 0.18\,\mu m$. The average gap distance of 20 different positions is $2.40 \pm 0.13\,\mu m$. Three reasons are possiblly responsible for the small: the etching on the silicon mold may not be perfectly vertical, the deformation of the stamp during contact printing and the angle between the adsorbed DNA strand and the stamp gratings. However, the results are still very close to our design.

One issue that has to be considered is the migration of the low molar mass PDMS chains. During contact printing, the low molar mass PDMS chains are able to migrate from the PDMS stamp onto the PMMA surface. There is thus a possibility that the dark portion of DNA stands under the fluorescence microscope are not because of cutting but due to the low molar PDMS chains blocking the fluorescence signal.

To address this issue, we modified our experimental procedure: instead of staining the DNA molecules with YOYO prior to molecular combing, the whole process, including combing and cutting, was carried out blindly. No fluorescence dye was added until the DNA was stamped by the PDMS stamp. After that, the sample was immersed into a 6:50 (0.1M NaOH: 0.02M MES) buffer solution that contains diluted fluorescence dye. Since the staining process for YOYO requires heating at elevated temperature and incubation for a longer time, 5000X diluted Sybr Gold was used instead. As the results show in Figure 2.4, the same pattern is observed. DNA strands are rarely observed within the designed cutting area. The length of fragmented DNA molecules and the length of the cutting gap are also the same as the result from the original method.

Atomic force microscopy imaging was also carried out to further prove our conclusion (Figure 2.5a). Although the PMMA surface is not perfectly flat, the contrast between the surface and the DNA molecules is high enough for the DNA to be visualized and the height range of DNA strands on the surface varied from 0.46nm to 3.72nm. The reported height of stretched isolated DNA molecules that on mica surfaces is $\leq$0.4nm, suggesting that some of the DNA strands on our PMMA surfaces consist of multiple DNA molecules bundled together due to the high concentration of the dipping solution. Figure 2.5b shows an image after the cutting. Figure 2.5c is an image from the area where

the cutting lines are offset. In Figure 2.5d, which is the processed image of 2.5c, the green and yellow lines represent the DNA strands while the red lines correspond to the edge of the cutting area. As can be seen clearly, once the DNA strands are intersected (i.e. contacted) by the cutting lines (green lines), the molecules are fragmented. However, in the area away from stamp contact, the DNA strands (yellow lines) remain complete even after the cutting process. Most of the cutting areas are as flat as other PMMA areas, suggesting there is no presence of DNA molecules (inside the red line).

2.3.4 The cutting efficiency

The cutting efficiency has two parts. The first part is how much of the area of adsorbed DNA molecules has actually been cut as fraction of the whole stamping area. The second part is the portion of DNA molecules that have been cut into the desired length. For the first part, multiple areas on six samples were viewed under a fluorescence microscope and the efficiency was estimated by measuring the area of the actual cutting versus the entire field of view (using ImageJ software). The results are shown on Table 2.1. To estimate the percentages of DNA molecules that have the same length as designed, the length of DNA fragments after cutting were measured from 5 AFM images and the average portion of numbers of DNA fragments were 10kbps in length versus the total number of DNA fragments is $68.4 \pm 5\%$. This value is in accordance with the design of the pattern and the length of the adsorbed DNA molecule. For our design, this number can be improved if we use longer DNA molecules. Taking these two values together, the cutting efficiency would be $55 \pm 14\%$. Based on the counting result of fluorescence imaging, the number of DNA molecules adsorbed onto a 2cm by 5cm area is estimated to be 3.8×10^6, about 0.2ng, and there will be $2.1 \times 10^6 \pm 0.6 \times 10^6$ DNA strands with the length of 10kbps after cutting for each chip.

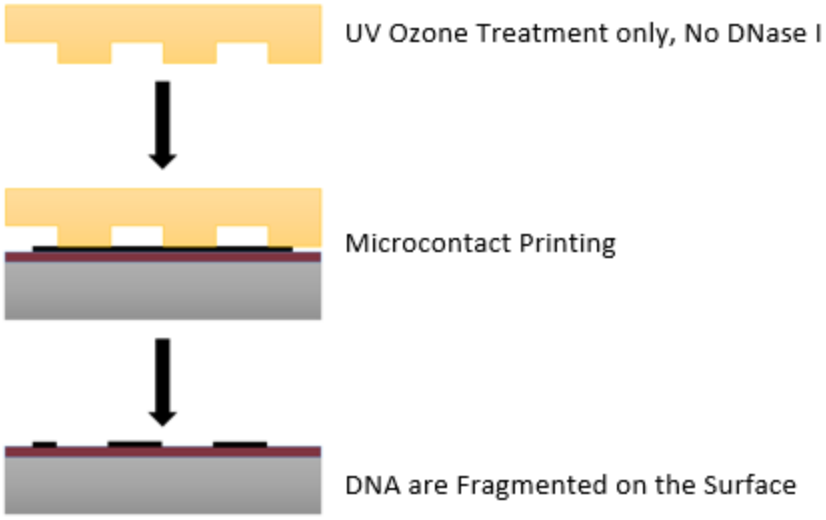

Figure IV: Schematic diagram of the stamping process with the PDMS stamp that only treated with UV ozone.

2.3.5 The Stamp Cutting mechanism

Although the DNase I is the intended mechanism for cutting the DNA molecules in the system, it appears that there is a competing mechanism. The first clue was found when the stamp from the control group sometimes can cause cutting of DNA molecules as well. In Figure 2.6, the left one is the result from a bare patterned PDMS stamp, the middle one was a PDMS stamp with enzyme reaction buffer (both of them had no DNase I enzyme applied on their surfaces). However, the DNA stands were cut as they came across the cutting areas. Figure IV is the schematic diagram of the stamping process with the PDMS stamp that was only treated with UV ozone. Figure 2.7 is a fluorescence image to show that a large area of DNA molecules was fragmented with this method.

The DNA fragmentation without enzyme can be explained as follows: after the ozone treatment, the PDMS stamp surface is covered by a silica-like layer (SiO_x) and becomes hydrophilic, so the adhesion force between the stamp and the DNA molecules is strong due to the phosphate backbone of the DNA molecule being hydrophilic. The DNA molecules are also bound to the PMMA surface during the molecular combing process,

however the force between them is weaker compared with the force between the DNA and stamp. The PMMA is more hydrophobic (water contact angle on PMMA surface are reported in the range of 60° to 80° while for the UV Ozone treated PDMS is less than 40°), yet the force is stronger than the force that is required to break the DNA double strands. When the PDMS stamp is peeled off from the PMMA surface, the part of the DNA strand that was in contact with the stamp will break off from the original DNA molecule and be transferred onto the stamp surface.

To test this picture, the first step is to verify if the DNA can be picked up from the PMMA. Previously, DNA molecules were adsorbed onto PDMS surfaces and transferred to other surfaces such as glass or mica successfully but here is the reverse process that transfers DNA from PMMA surface to PDMS surface. In the experiment, a flat PDMS stamp treated with ozone for 15minutes was then stamped onto a PMMA surface with adsorbed DNA molecules, then a weight of 800g was applied for 2 minutes. Finally, the PDMS stamp is peeled off and the result is shown in Figure 2.8b: the lower side is where the flat stamp made contact. As one may see, relatively few DNA molecules were left over after the stamp was removed and a large number of fragmented DNA strands can be observed at the intersection area. Figure 2.8c shows the DNA molecules that had been transferred onto the PDMS stamp surface.

The next step is to try to observe the DNA fragments from the stamp surface after cutting. Figure 2.9a is the PMMA surface after cutting and Figure 2.9b is the corresponding stamp surface after cutting. As one can clearly see, there are DNA fragments on the cutting area of the PDMS stamp. Furthermore, the average width of the cutting area on the PMMA surface is 2.02 ± 0.13 μm and the average length of the DNA fragments on the PDMS stamp surface is 1.95 ± 0.14 μm. The results are consistent within the experimental error range. AFM imaging is also carried out to verify the presence of DNA fragments on the PDMS stamp surface after cutting. As shown in Figure 2.10, DNA strands are observed and the average length of the DNA strands that throughout the whole width of the cutting area is 1.93 ± 0.09 μm, which is in the same range of the previous results from the fluorescence images. Notice that due to the roughness of the stamp surface, the flexibility of the stamp and the strong adhesion force

between the AFM tip and the PDMS surface, the AFM image has low contrast and the individual molecules are difficult to see. All these three values are smaller than our design width of is 2.5μm. The reason for this is likely the underexposure or insufficient developing time during the fabrication process of this particular silicon mold. However, since they are almost identical to each other within the error range, it is possible for us to draw the conclusion that the DNA is fragmented because part of the strands are transferred from the PMMA surface onto the PDMS stamp surface during the micro contact printing.

2.4 Discussion

The data has confirmed that adsorbed DNA strands on the surface can be fragmented by microcontact printing. Compared with other techniques that cut DNA on surfaces, the novelty of our methods is the high efficiency: AFM cutting methods, for example, work on 1 to 10 DNA molecules per run while our method produces about 100 picograms of DNA molecules (about $2.1\times10^6 \pm 0.6\times10^6$ DNA strands with the length of 10Kbps) per stamp, which is a large step towards producing sufficient quantities for DNA amplification and sequencing. What's more, because of the advantage of soft lithography, multiple identical stamps can be rapidly fabricated from one single silicon mold, which makes it possible to run multiple samples in parallel using our methods. Furthermore, by changing the design of the mask, it is possible to adjust the cutting length, cutting shape and cutting position, which means more flexibility in fabricating different kinds of stretched DNA nanoarrays.

Adsorbed DNA density on the PMMA surface plays an important role in the process. A high density of DNA molecules makes it easier to verify the cutting results. What's more, higher concentration increases the final amount of fragmented DNA, which is important for further application. In the high-density regime, the DNA strands show different brightnesses in the fluorescence microscopy image and different heights in the AFM image, suggesting that they have formed bundles that contain different amounts of DNA molecules. Most of them can still be cut by our method with the exception of extremely large and thick ones. Sometimes, in order to form complex stretched DNA

nanoarrays, multiple dipping has to be done (such as to create DNA "cross"[56]), and our method is fully capable of working in this situation. The stamp can cut the DNA strands that lie in the direction that is parallel to the cutting line as well. Thus, more complex stretched DNA nanoarrays can be fabricated through our method.

The nanofabrication conditions of the silicon mold and the PDMS stamp have a great impact on the quality of the cutting result. Up till now, the best combination is found to be as follows: the etching depth of the lithographic pattern is 300nm to 500nm, the width of cutting area is 2.5μm with the distance of each cutting line being not greater than 10μm.

The fragmentation mechanism includes both enzyme cutting and the cutting due to the hydrophobicity difference of surfaces. Ozone treatment of PDMS stamp surface is necessary because it helps the enzyme solution spread evenly on the surface while the treatment itself can cause DNA fragmentation after the micro contact printing. Reports have been confirmed that DNA strands can be transferred from one surface to another by contact printing[54,55,57] and stretched DNA molecules can be broken at the edge of the pattern features[56], resulting in DNA being partially transferred. As the result of our experiment, DNA molecules were successfully fragmented without applying any enzyme and the "been cut part" of DNA strands from the stamp after cutting were observed. It is important to point out that the external weight of 600g that was applied onto the stamp is crucial to the process because it ensures the conformal contact between the stamp surface and the DNA molecules. The observed result also confirms that DNA molecules on the surface have been fragmented by our method. However, both of effects can incur possible DNA end damage of the fragments that are cut, which is less favorable in further applications such as DNA ligation or DNA amplification.

In order to be able to serve as an input system for current NGS technologies, the DNA fragments should be either on the specially designed surface of the NGS platform or desorbed into solution. The advantage of maintaining DNA on the surface is that the order can be preserved. Although now the DNA molecules are randomly adsorbed onto the PMMA surface in our method, several ways have been reported to control the deposit

position of DNA molecules so that ends are lined up on the surface[59,60]. If those methods can be adapted into our experiment, ordered cutting of DNA molecules on surface can be achieved. A current obstacle to this approach is that most of the chip surfaces are commercial and the detailed formulation is not publicly available.

An alternative way is to desorb the DNA molecules into a buffer solution, with or without maintaining the order. Up till now, several buffer solutions, including heated pure DI water, ethanol, formamide/SSC buffer, commercial NEB buffers and so on (data not shown), have been tried and the best result we can get so far is by the PCI method. The basic idea here is to use chloroform to dissolve the PMMA layer so that the DNA molecules will be dissolved into solution as well. Later, they can be separated by phase separation. The disadvantage of PCI method is the efficiency: although the sample that we stamped is fairly large ($10\,cm^2$), 20-50 samples are needed to be prepared so that the PCI process can yield enough DNA for sequencing. However, lambda DNA and E.coli DNA have been successfully sequenced using this method. Another downside of dissolving is that the order of the DNA fragments could be lost but this can be solved by using a progressively graded pattern: lined up DNA molecules adsorbed on surfaces are fragmented by the graded pattern, then the DNA molecules will be desorbed from the surfaces into solution and separated by length with gel electrophoresis. Based on the length, the order of DNA fragments can be easily retrieved. Desorbing DNA into solution also simplifies DNA end repair and DNA amplification since most of these techniques work best in the solution. However, due to the low yield, an optimized amplification method is needed.

Another main issue that needs to be addressed now is the resolution of our pattern. Most of the NGS techniques now work with the DNA strands less than 1Kbp, corresponding to DNA lengths less than 350nm on the surface after molecular combing. Although the best resolution of soft lithography stamps has been reported down to sub 100nm level, our stamp is currently restricted to 1.5μm due to the experimental limitations (the resolution is determined mainly by the UV wavelength used). To get finer resolution, e-beam lithography is a standard choice but it is not ideal to us since a long writing time for a 2cm by 5cm area is needed and the facility accessibility is limited.

On the other hand, laser interference lithography[61,62] should work well. This technique is able to rapidly fabricate symmetric grating patterns with resolution down to 0.2-0.4 μm feature size. We are planning to increase our resolution by using this technique. The cutting efficiency can be improved as well if the length of the fragmented DNA is shorter.

2.5 Conclusion

A novel DNA cutting method based on molecular combing and soft lithography has been established. Various experimental conditions have been explored to optimize the cutting results. Well-defined arrays of stretched and fragmented DNA strands can be produced over a centimeter-scale area. The cutting length and position can be easily adjusted through this method. During the micro contact printing, the part of DNA strands that is in contact with the stamp can be transferred from the PMMA surface onto the PDMS surface due to the different hydrophilicity of these two surfaces and this is at least part of the reason for the DNA fragmentation. This technique can serve as a new input method for next-generation sequencing technologies that can potentially improve both efficiency and accuracy of DNA sequencing. Further extension of this technique can lead to fabrication of DNA-based 2-D nanostructures.

References

1 Sanger, F., Nicklen, S. & Coulson, A. R. DNA sequencing with chain-terminating inhibitors. *Proceedings of the National Academy of Sciences* **74**, 5463-5467 (1977).

2 Collins, F. S., Morgan, M. & Patrinos, A. The Human Genome Project: lessons from large-scale biology. *Science* **300**, 286-290 (2003).

3 Buermans, H. & Den Dunnen, J. Next generation sequencing technology: advances and applications. *Biochimica et Biophysica Acta (BBA)-Molecular Basis of Disease* **1842**, 1932-1941 (2014).

4 Hutchison, C. A., 3rd. DNA sequencing: bench to bedside and beyond. *Nucleic acids research* **35**, 6227-6237, doi:10.1093/nar/gkm688 (2007).

5 Mardis, E. R. Next-generation sequencing platforms. *Annu Rev Anal Chem (Palo Alto Calif)* **6**, 287-303, doi:10.1146/annurev-anchem-062012-092628 (2013).

6 Metzker, M. L. Sequencing technologies - the next generation. *Nat Rev Genet* **11**, 31-46, doi:10.1038/nrg2626 (2010).

7 Niedringhaus, T. P., Milanova, D., Kerby, M. B., Snyder, M. P. & Barron, A. E. Landscape of next-generation sequencing technologies. *Anal Chem* **83**, 4327-4341, doi:10.1021/ac2010857 (2011).

8 Zhou, X. *et al.* The next-generation sequencing technology and application. *Protein Cell* **1**, 520-536, doi:10.1007/s13238-010-0065-3 (2010).

9 Goodwin, S., McPherson, J. D. & McCombie, W. R. Coming of age: ten years of next-generation sequencing technologies. *Nature Reviews Genetics* **17**, 333-351 (2016).

10 Wang, Y., Yang, Q. & Wang, Z. The evolution of nanopore sequencing. *Frontiers in genetics* **5**, 449-449 (2013).

11 Branton, D. *et al.* The potential and challenges of nanopore sequencing. *Nature biotechnology* **26**, 1146-1153 (2008).

12 Carson, S. & Wanunu, M. Challenges in DNA motion control and sequence readout using nanopore devices. *Nanotechnology* **26**, 074004 (2015).

13 Xu, X.-M. & Ikai, A. Recovery and amplification of plasmid DNA with atomic force microscopy and the polymerase chain reaction. *Analytica chimica acta* **361**, 1-7 (1998).

14 Hu, J., Zhang, Y., Gao, H., Li, M. & Hartmann, U. Artificial DNA patterns by mechanical nanomanipulation. *Nano Letters* **2**, 55-57 (2002).

15 Lü, J.-h. *et al.* Positioning isolation and biochemical analysis of single DNA molecules based on nanomanipulation and single-molecule PCR. *Journal of the American Chemical Society* **126**, 11136-11137 (2004).

16 An, H. *et al.* Single-base resolution and long-coverage sequencing based on single-molecule nanomanipulation. *Nanotechnology* **18**, 225101 (2007).

17 Washizu, M. in *Microtechnologies in Medicine & Biology 2nd Annual International IEEE-EMB Special Topic Conference on.* 1-3-6 (IEEE).

18 Washizu, M. Biological applications of electrostatic surface field effects. *Journal of Electrostatics* **63**, 795-802, doi:10.1016/j.elstat.2005.03.074 (2005).

19 Kurosawa, O. & Washizu, M. Dissection, acquisition and amplification of targeted position of electrostatically stretched DNA. *Journal of Electrostatics* **65**, 423-430, doi:10.1016/j.elstat.2005.03.094 (2007).

20 Yamamoto, T., Kurosawa, O., Kabata, H., Shimamoto, N. & Washizu, M. Molecular surgery of DNA based on electrostatic micromanipulation. *Industry Applications, IEEE Transactions on* **36**, 1010-1017 (2000).

21 Kumar, A. & Whitesides, G. M. Features of gold having micrometer to centimeter dimensions can be formed through a combination of stamping with an elastomeric stamp and an alkanethiol ‘‘ink’’followed by chemical etching. *Applied Physics Letters* **63**, 2002-2004 (1993).

22 Xia, Y. & Whitesides, G. M. Soft lithography. *Annual review of materials science* **28**, 153-184 (1998).

23 Qin, D., Xia, Y. & Whitesides, G. M. Soft lithography for micro-and nanoscale patterning. *Nature protocols* **5**, 491-502 (2010).

24 Weibel, D. B., Diluzio, W. R. & Whitesides, G. M. Microfabrication meets microbiology. *Nature reviews. Microbiology* **5**, 209-218, doi:10.1038/nrmicro1616 (2007).
25 Chojnowski, J., Clarson, S. & Semlyen, J. Siloxane polymers. *Englewood Cliffs, New Jersey: Prentice-Hall*, 1-62 (1993).
26 Sadhu, V. B. *et al.* Surface modification of elastomeric stamps for microcontact printing of polar inks. *Langmuir : the ACS journal of surfaces and colloids* **23**, 6850-6855 (2007).
27 Kaufmann, T. & Ravoo, B. J. Stamps, inks and substrates: polymers in microcontact printing. *Polymer Chemistry* **1**, 371-387 (2010).
28 Madou, M. J. *Fundamentals of microfabrication: the science of miniaturization*. (CRC press, 2002).
29 Quist, A. P., Pavlovic, E. & Oscarsson, S. Recent advances in microcontact printing. *Analytical and bioanalytical chemistry* **381**, 591-600 (2005).
30 Ruiz, S. A. & Chen, C. S. Microcontact printing: a tool to pattern. *Soft Matter* **3**, 168-177 (2007).
31 Perl, A., Reinhoudt, D. N. & Huskens, J. Microcontact printing: limitations and achievements. *Advanced Materials* **21**, 2257-2268 (2009).
32 Hillborg, H., Tomczak, N., Olàh, A., Schönherr, H. & Vancso, G. J. Nanoscale hydrophobic recovery: A chemical force microscopy study of UV/ozone-treated cross-linked poly (dimethylsiloxane). *Langmuir : the ACS journal of surfaces and colloids* **20**, 785-794 (2004).
33 Olander, B., Wirsen, A. & Albertsson, A. C. Oxygen microwave plasma treatment of silicone elastomer: Kinetic behavior and surface composition. *Journal of applied polymer science* **91**, 4098-4104 (2004).
34 Sriram, K., Chang, C.-L., Kumar, U. R. & Chou, C.-F. DNA combing on low-pressure oxygen plasma modified polysilsesquioxane substrates for single-molecule studies. *Biomicrofluidics* **8**, 052102 (2014).
35 Graubner, V.-M. *et al.* Photochemical modification of cross-linked poly (dimethylsiloxane) by irradiation at 172 nm. *Macromolecules* **37**, 5936-5943 (2004).
36 Odom, T. W., Love, J. C., Wolfe, D. B., Paul, K. E. & Whitesides, G. M. Improved pattern transfer in soft lithography using composite stamps. *Langmuir : the ACS journal of surfaces and colloids* **18**, 5314-5320 (2002).
37 Hui, C., Jagota, A., Lin, Y. & Kramer, E. Constraints on microcontact printing imposed by stamp deformation. *Langmuir : the ACS journal of surfaces and colloids* **18**, 1394-1407 (2002).
38 Xia, Y., Kim, E. & Whitesides, G. M. Microcontact printing of alkanethiols on silver and its application in microfabrication. *Journal of The Electrochemical Society* **143**, 1070-1079 (1996).
39 Xia, Y., Kim, E., Mrksich, M. & Whitesides, G. M. Microcontact printing of alkanethiols on copper and its application in microfabrication. *Chemistry of materials* **8**, 601-603 (1996).
40 Carvalho, A., Geissler, M., Schmid, H., Michel, B. & Delamarche, E. Self-assembled monolayers of eicosanethiol on palladium and their use in microcontact printing. *Langmuir : the ACS journal of surfaces and colloids* **18**, 2406-2412 (2002).
41 Love, J. C., Estroff, L. A., Kriebel, J. K., Nuzzo, R. G. & Whitesides, G. M. Self-assembled monolayers of thiolates on metals as a form of nanotechnology. *Chemical reviews* **105**, 1103-1170 (2005).
42 Xu, C., Taylor, P., Ersoz, M., Fletcher, P. D. & Paunov, V. N. Microcontact printing of DNA-surfactant arrays on solid substrates. *Journal of Materials Chemistry* **13**, 3044-3048 (2003).
43 Lange, S. A., Benes, V., Kern, D. P., Hörber, J. H. & Bernard, A. Microcontact printing of DNA molecules. *Analytical Chemistry* **76**, 1641-1647 (2004).
44 Cerf, A., Dollat, X., Chalmeau, J., Coutable, A. & Vieu, C. A versatile method for generating single DNA molecule patterns: Through the combination of directed capillary assembly and (micro/nano) contact printing. *Journal of Materials Research* **26**, 336-346 (2011).
45 Bernard, A. *et al.* Printing patterns of proteins. *Langmuir : the ACS journal of surfaces and colloids* **14**, 2225-2229 (1998).
46 Bernard, A., Renault, J. P., Michel, B., Bosshard, H. R. & Delamarche, E. Microcontact printing of proteins. *Advanced Materials* **12**, 1067-1070 (2000).
47 Kane, R. S., Takayama, S., Ostuni, E., Ingber, D. E. & Whitesides, G. M. Patterning proteins and cells using soft lithography. *Biomaterials* **20**, 2363-2376 (1999).
48 Weibel, D. B. *et al.* Bacterial printing press that regenerates its ink: contact-printing bacteria using hydrogel stamps. *Langmuir : the ACS journal of surfaces and colloids* **21**, 6436-6442 (2005).

49 Soares, M. B. Identification and cloning of differentially expressed genes. *Current opinion in biotechnology* **8**, 542-546 (1997).

50 Watson, A., Mazumder, A., Stewart, M. & Balasubramanian, S. Technology for microarray analysis of gene expression. *Current opinion in biotechnology* **9**, 609-614 (1998).

51 Shalon, D. Gene expression micro-arrays: a new tool for genomic research. *Pathologie et biologie* **46**, 107-109 (1998).

52 Hacia, J. G. Resequencing and mutational analysis using oligonucleotide microarrays. *Nature genetics* **21**, 42-47 (1999).

53 Drmanac, R. *et al.* DNA sequencing by hybridization with arrays of samples or probes. *DNA Arrays: Methods and Protocols*, 173-179 (2001).

54 Nakao, H., Gad, M., Sugiyama, S., Otobe, K. & Ohtani, T. Transfer-printing of highly aligned DNA nanowires. *Journal of the American Chemical Society* **125**, 7162-7163 (2003).

55 Gad, M., Sugiyama, S. & Ohtani, T. Method for patterning stretched DNA molecules on mica surfaces by soft lithography. *J Biomol Struct Dyn* **21**, 387-393, doi:10.1080/07391102.2003.10506934 (2003).

56 Guan, J. & Lee, L. J. Generating highly ordered DNA nanostrand arrays. *Proceedings of the National Academy of Sciences of the United States of America* **102**, 18321-18325 (2005).

57 Bjork, P., Holmstrom, S. & Inganas, O. Soft lithographic printing of patterns of stretched DNA and DNA/electronic polymer wires by surface-energy modification and transfer. *Small* **2**, 1068-1074, doi:10.1002/smll.200600126 (2006).

58 Minteer, S. D. *Microfluidic techniques: reviews and protocols*. Vol. 321 (Springer Science & Business Media, 2006).

59 Klein, D. C. G. *et al.* Ordered stretching of single molecules of deoxyribose nucleic acid between microfabricated polystyrene lines. *Applied Physics Letters* **78**, 2396, doi:10.1063/1.1365099 (2001).

60 Greene, E. C., Wind, S., Fazio, T., Gorman, J. & Visnapuu, M.-L. DNA curtains for high-throughput single-molecule optical imaging. *Methods in enzymology* **472**, 293-315 (2010).

61 Johnson, L., Kammlott, G. & Ingersoll, K. Generation of periodic surface corrugations. *Applied Optics* **17**, 1165-1181 (1978).

62 Wolferen, H. & Abelmann, L. Laser interference lithography. (2011).

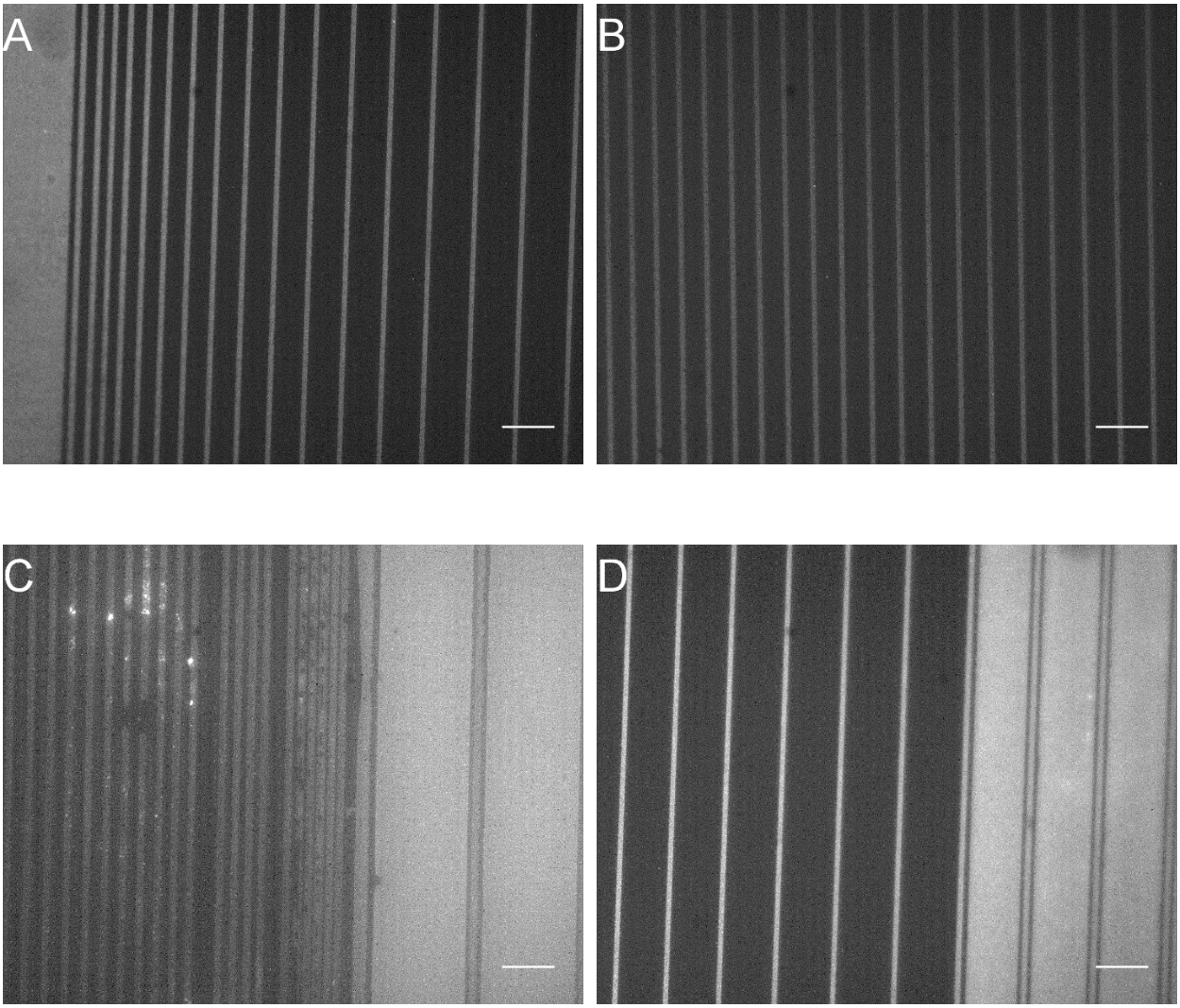

Figure 2.1: Fluorescence images of SyBr Gold stamped onto PMMA-coated silicon wafers. A SyBr Gold solution (diluted 5000X from stock) was applied to a patterned PDMS stamp and contact-imprinted onto the PMMA surface. A, B are the result using optimized microfabrication conditions. C shows missing cutting lines due to insufficient exposure pattern formation in thick photoresists. In both C and D, roof collapse of the areas with the widest spacing has occurs (bright regions between lines). [Scale bar, 20μm (A-D).]

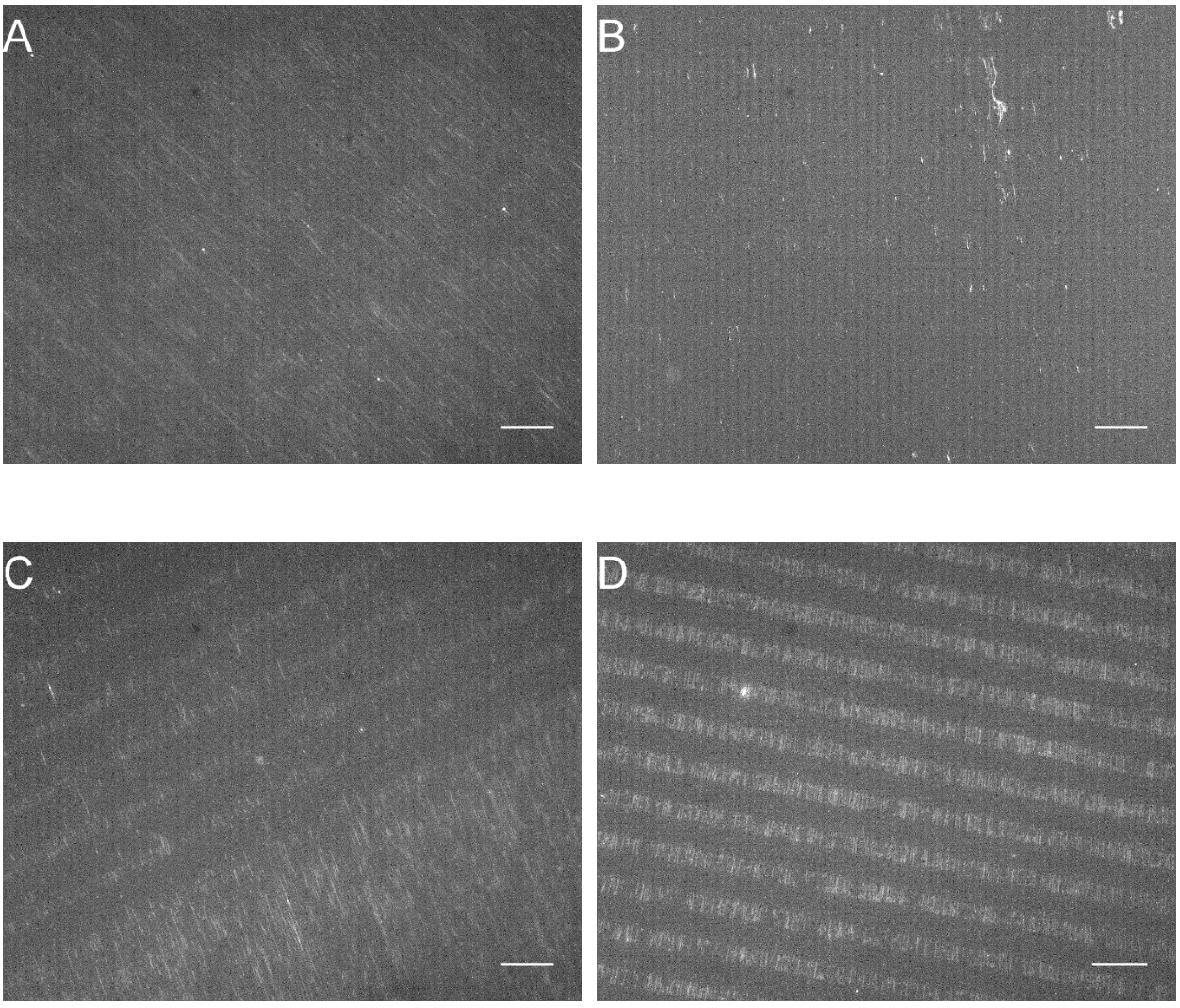

Figure 2.2: Different cutting results observed using different enzyme application methods. A: Too little enzyme was applied on the stamp surface. This is a typical result from method 1 and 2 (no UV Ozone treatment of the stamp. B: Too much cutting enzyme on the stamp that has digested almost all the DNA molecules on the surface. Such a result is usually produced by Method 3. C: Uneven cutting caused by either uneven enzyme application or uneven pressure. Since the untreated PDMS surface is hydrophobic, the enzyme solution cannot spread uniformly on the stamp surface. D: A good cutting result produced by the Stamping Pad method. [Scale bar, 20μm (A-D).]

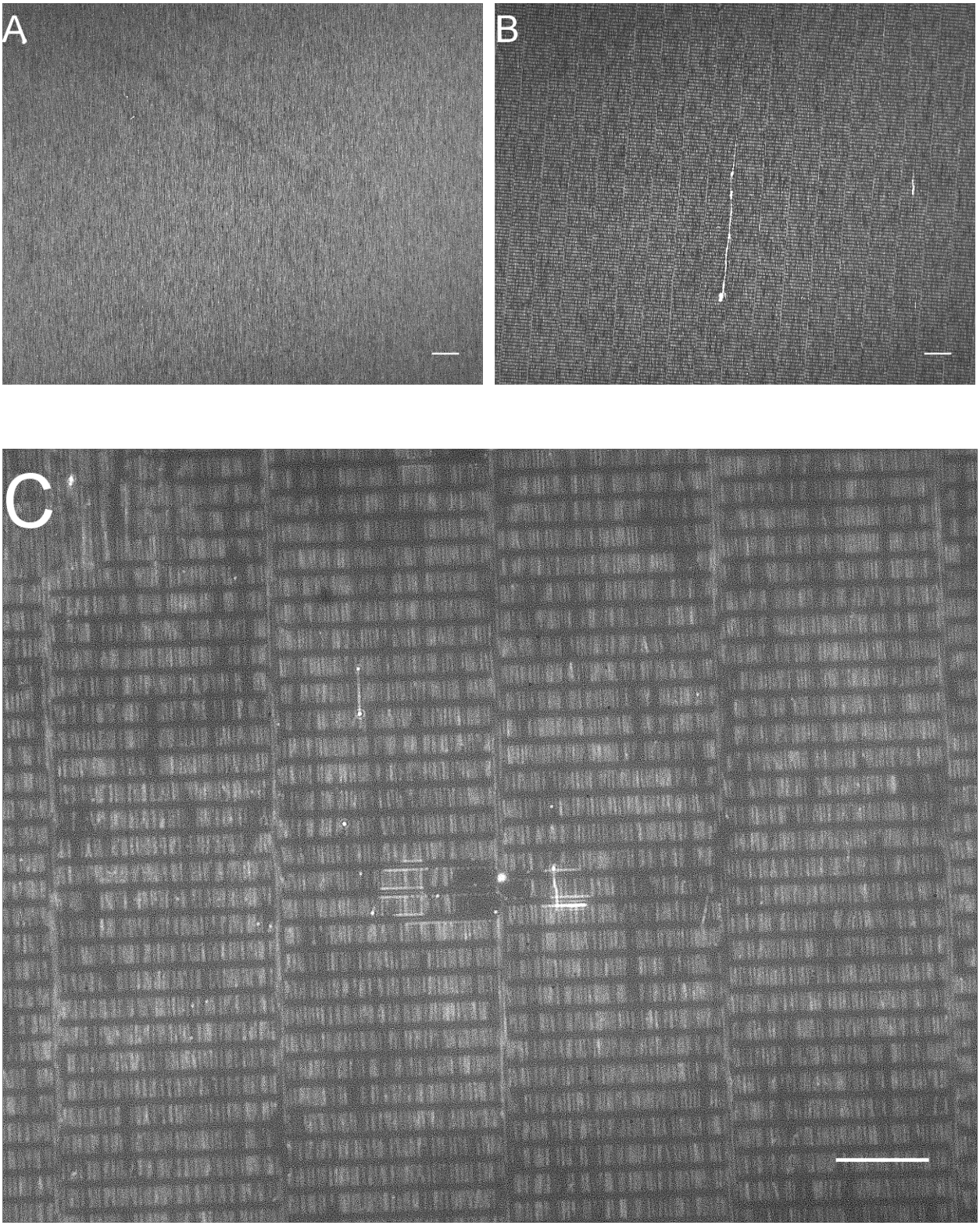

Figure 2.3: The cutting result of the asymmetric stamp, the width of the cutting lines was designed to be 2.5μm while the distance between each cutting line was designed to be 3.5μm. Upper left is the molecular combing result, i.e., before cutting. Upper right is the cutting result obseved using a 10X dry lens. C is the cutting result observed with a 40X oil lens. A sampling 20 DNA strands' lengths were measured and

resultant average was 3.40 ± 0.18 μm. The average gap distance of 20 different positions was 2.40 ± 0.13 μm. Both values are within the experimental error range of the designed values. [Scale bar, 50μm (A-B), 20μm (C).]

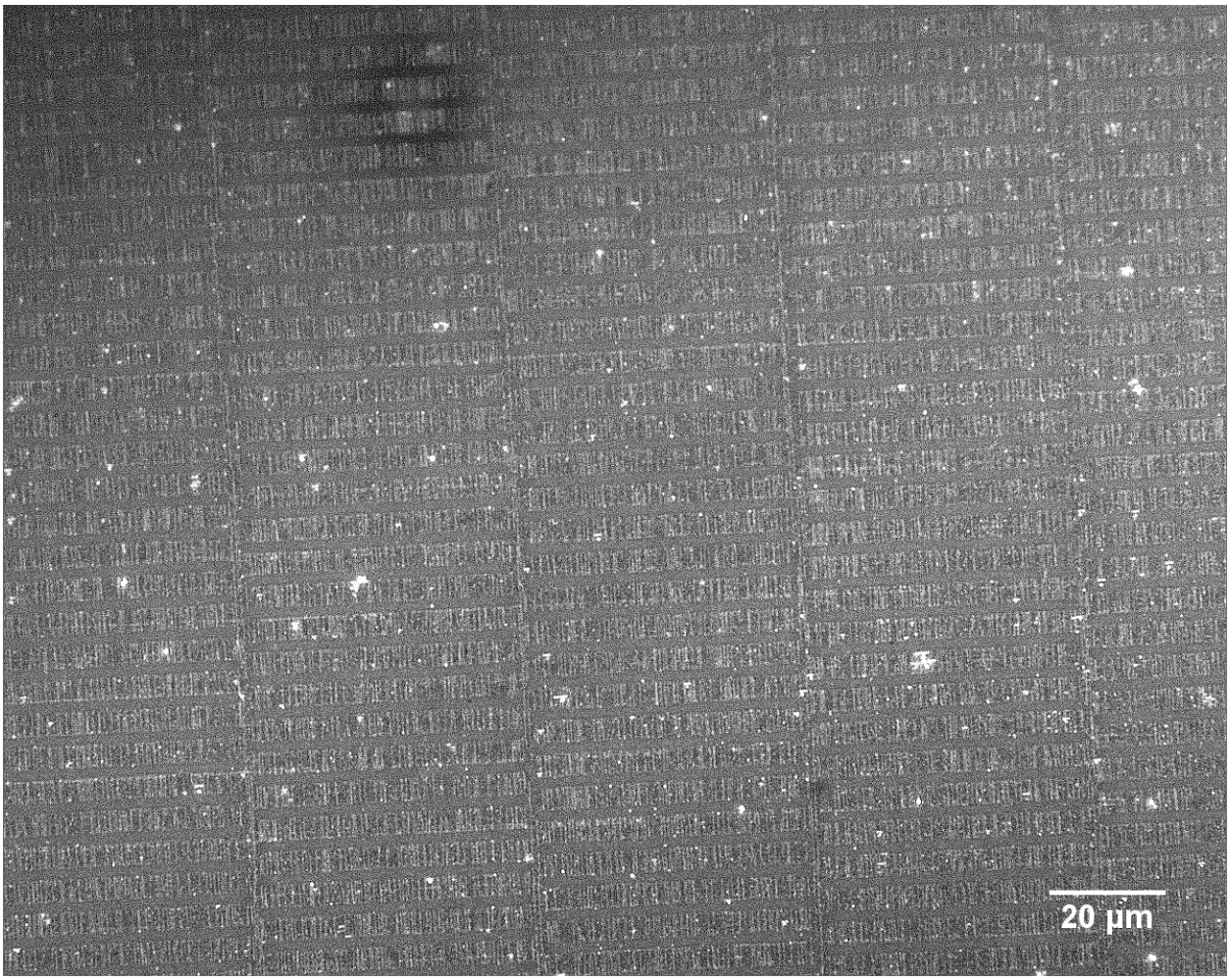

Figure 2.4: The fluoresence microscope image of fragmented DNA molecules on PMMA surface that were stained by 5000X diluted Sybr Gold after cutting. Although the image is not as clear as the image with the regular pre-staining method, it is still possible to see that vert low DNA strands are found inside the cutting area.

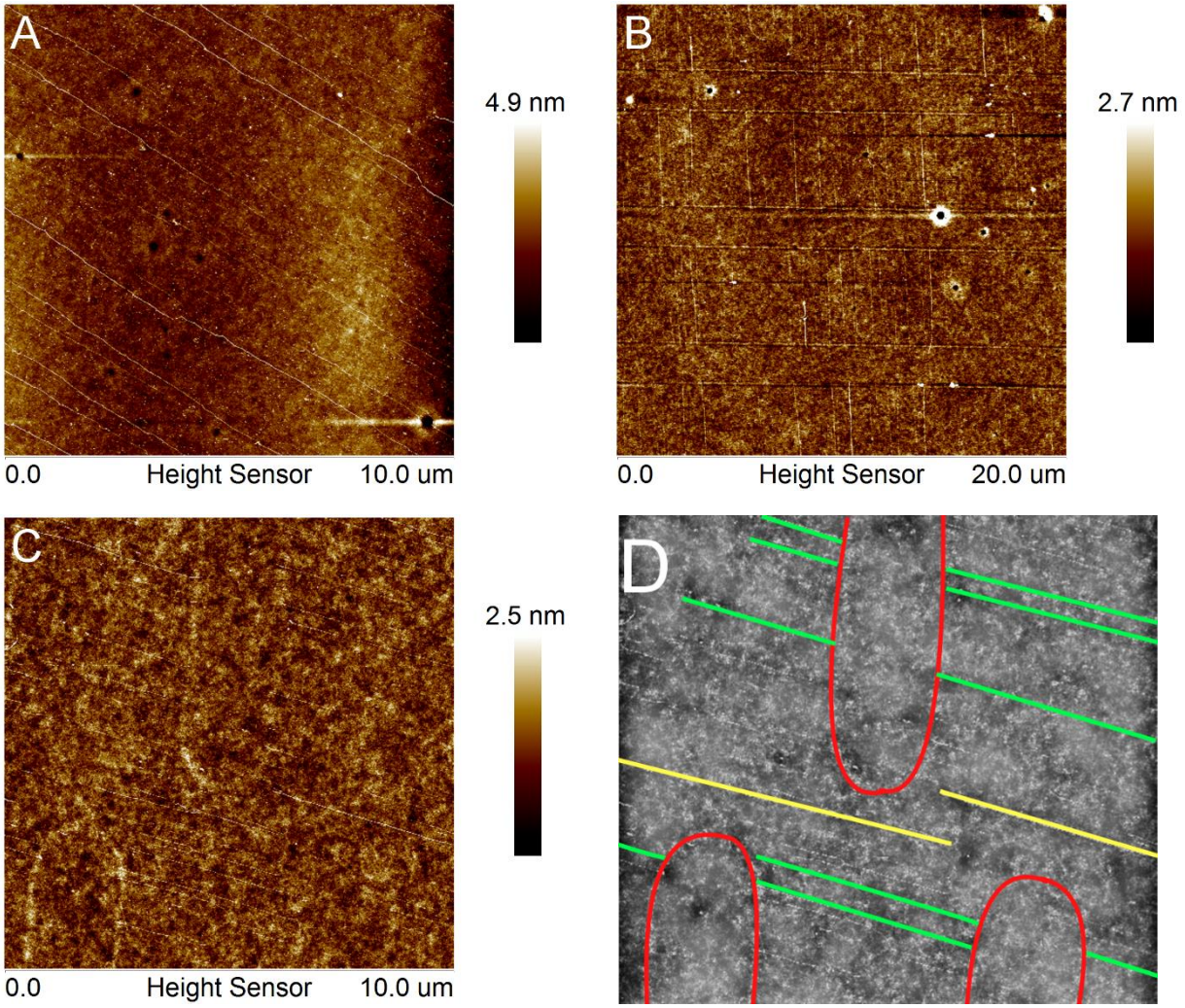

Figure 2.5: A is the dipping result showing uncut DNAs on the surface. The height difference of the DNA strands on the surfaces indicates that some of those are bundles containing multiple DNA strands. B is the cutting result. As can be seen, the cutting lines are well defind and most of the DNA strands are broken along the cutting lines. C is the area where the cutting lines are offset. D (lower right) is a schematic diagram of C. The green lines are DNA molecules which were fragmented by the cutting area (red line), while the yellow lines are molecules which did not encount intersect cutting area.

Table 2.1: Percentages of surface areas that cut successfully

Trial 1	**Trial 2**	**Trial 3**	**Trial 4**	**Trial 5**	**Average**	**STDEV.**
70%	80%	70%	90%	90%	80%	9%

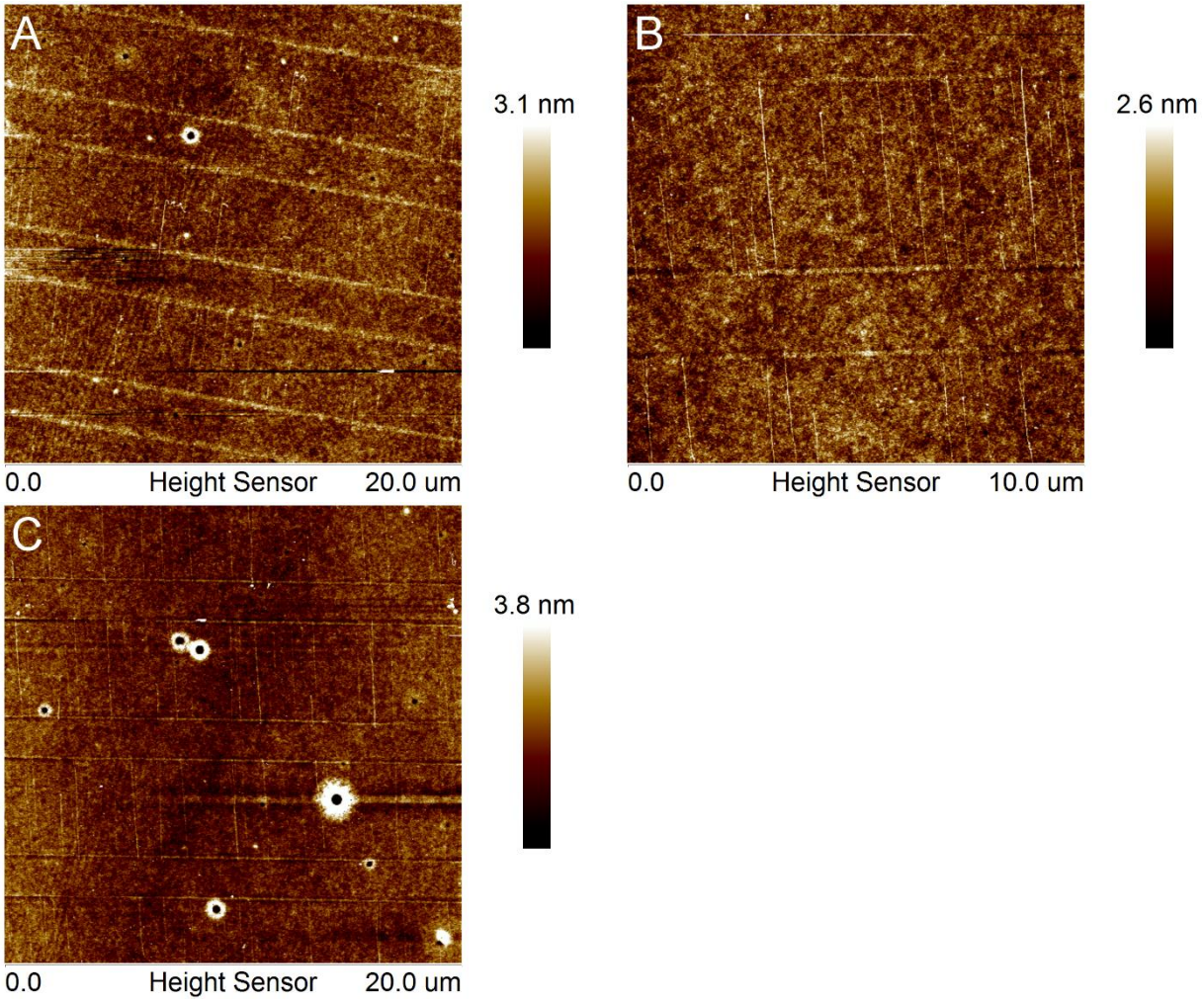

Figure 2.6: A: Stamping with a bare PDMS stamp. The stamp was pre-treated with UV Ozone; B: Stamping with enzyme buffer only; C: Stamping with buffer and DNase I. All of them show some degree of cutting.

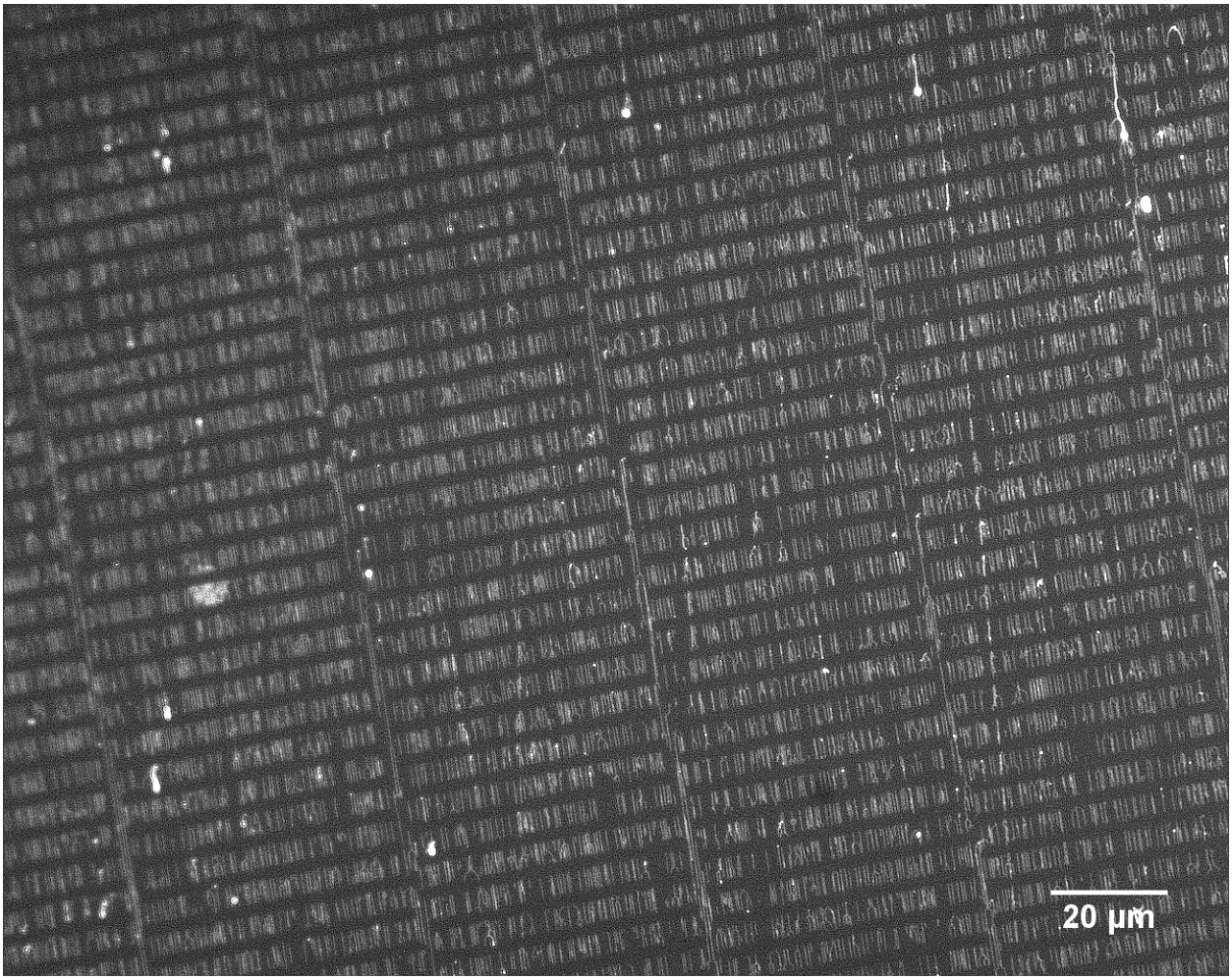

Figure 2.7: A large area of DNA molecules on the PMMA surface which were fragmented by the UV Ozone treated PDMS stamp without adding any DNase I.

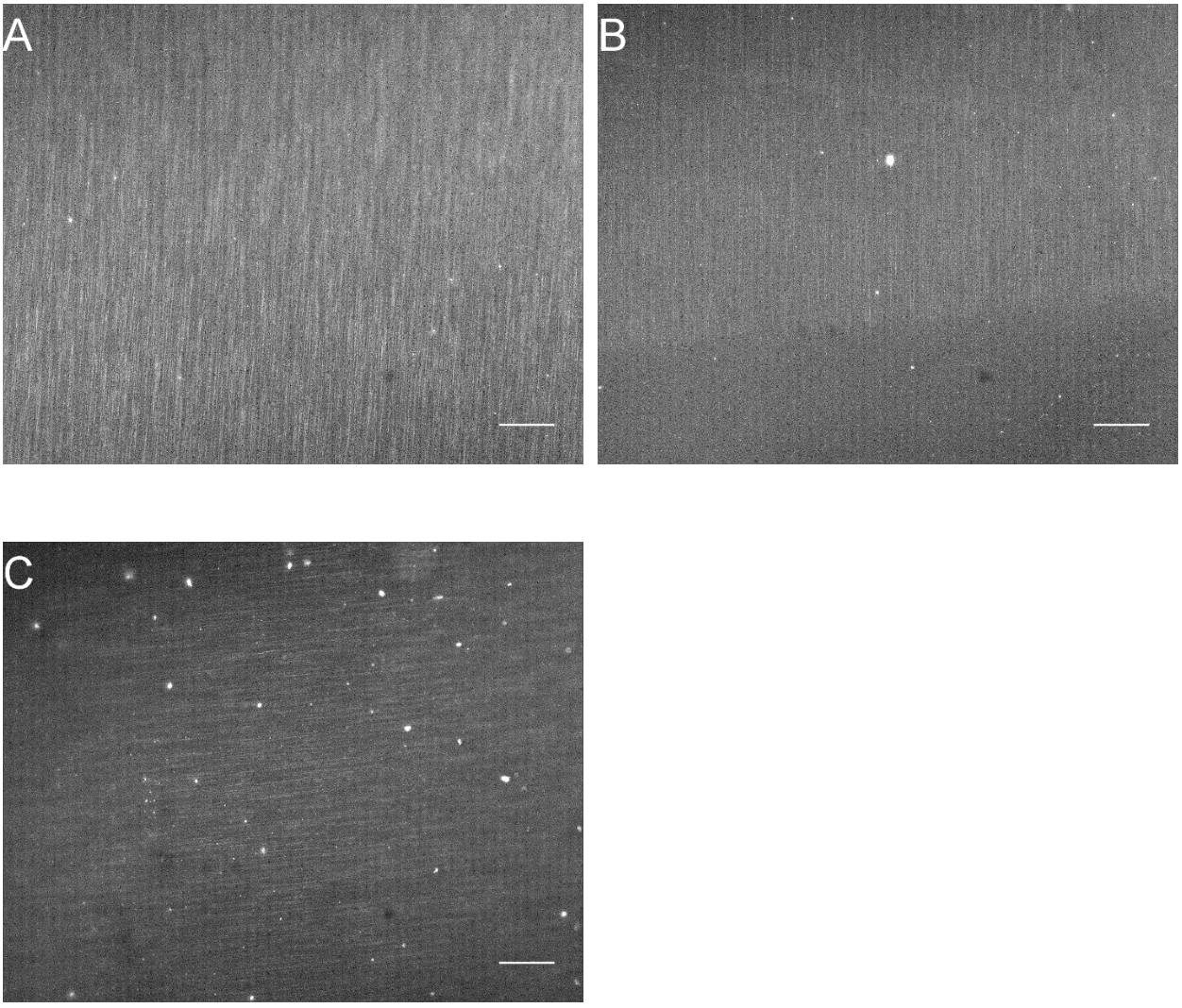

Figure 2.8: Images showing that DNA molecules have transferred from PMMA surface to PDMS surface by microcontact printing. A: DNA molecules adsorbed on PMMA surface; B: The lower part of the image is where the PDMS stamp contacted with the PMMA surface, very few DNA molecules were observed to remain after stamping; C (lower left), DNA molecules were transferred onto the stamp surface. [Scale bar, 20μm (A-C).]

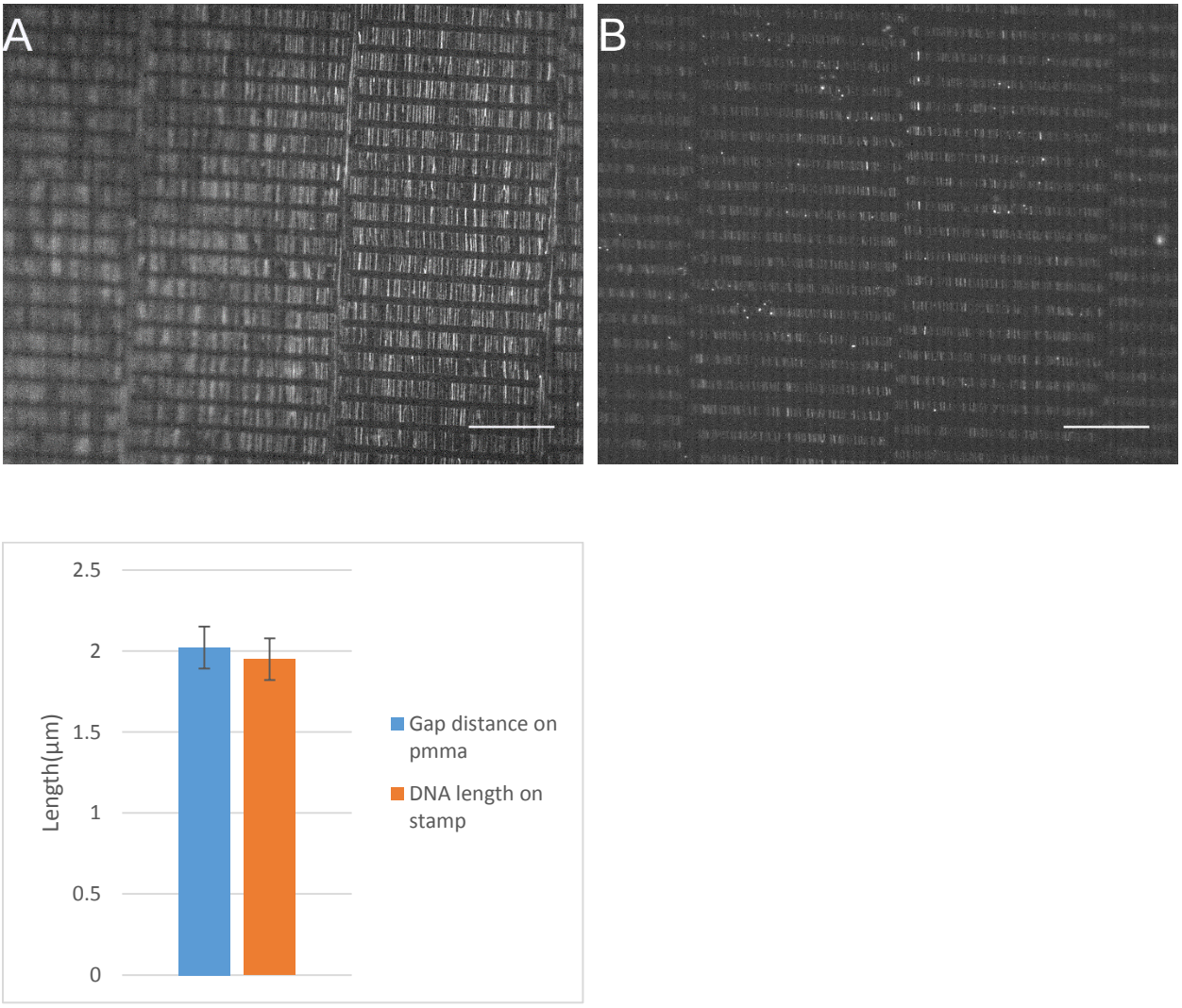

Figure 2.9: A: DNA molecules on the PMMA surface after cutting; B: Sections of DNA strands have been transferred onto the PDMS stamp surface. Both of the images were taken with a fluorescence microscope using a 63X water lens. The scale bars are 10µm. C (lower) is the comparison of the gap distances on PMMA and the transferred DNA lengths on the stamp surface. Within the experimental error range, they are the same. [Scale bar, 20µm (A and B).]

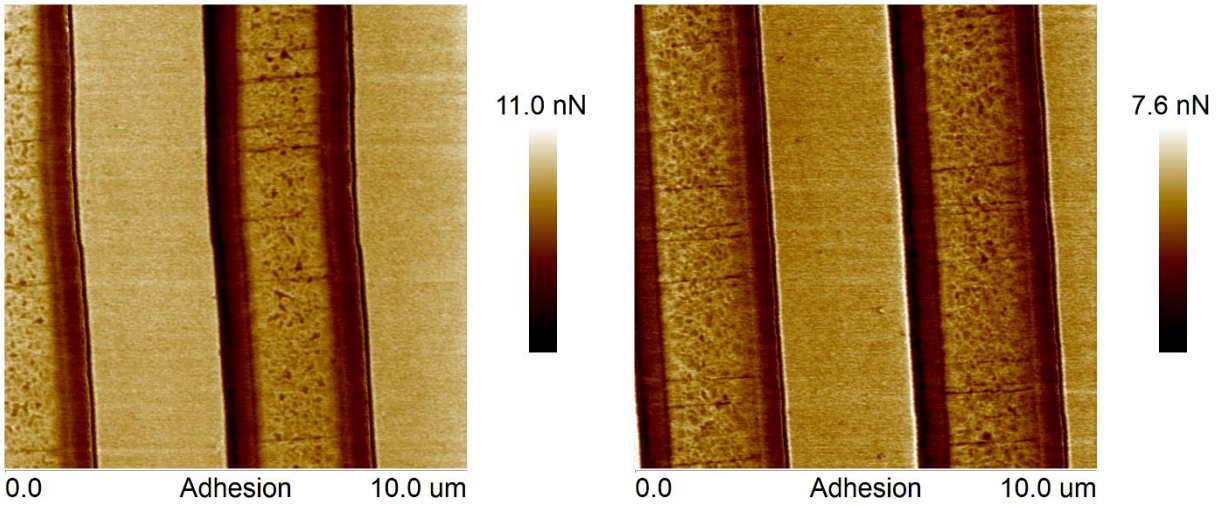

Figure 2.10: AFM images to show the sections of DNA stands that have been transferred onto the PDMS stamp surface. Because of the surface roughness, the flexibility of the PDMS and the strong adhesion force between the surface and the AFM tip, it is very difficult to observe DNA molecules from the height sensor. The images above were observed with the adhesion force sensor.

Chapter 3: Stretching DNA Molecules on a Flexible Substrate, a Polarization-Dependent Fluorescence Study

3.1 Introduction

The physical properties of DNA molecules are unique compared to other natural or synthetic polymers. For example, the bending rigidity of a double stranded DNA molecule is about 50 times higher than polyethylene, polystyrene, etc[1]. In addition, DNA is one of the longest natural molecules: a human chromosome is a few centimeters long when uncoiled. However, by highly bending and wrapping around histones, such long and stiff molecules can be squeezed into a micron-sized nucleus. Thus, it is important for us to study the DNA's behavior under stress and torsion. Such a study can also help us to understand the interaction between the DNA and the proteins involved in DNA copying, transcribing and packaging.

Up until now, stretching and breaking of DNA molecules have been carried out using various techniques. In 1992, Bustamante et. al.[2] performed an experiment to directly measure the elasticity of single DNA molecules. A lambda DNA molecule was chemically attached to a glass surface by one end and by the other end to a magnetic bead. The setup was then placed into a flow field together with movable magnets on both sides. The forces that were applied to the DNA molecules were a combination of magnetic and hydrodynamic forces. What they found was that the classical free joined chain model had failed to describe the behavior of single DNA molecules under stress. Later on, instead of using magnetic beads, optical tweezers[3] were used to measure the elastic response of single DNA molecules. Both ends of a DNA molecule were attached to separate microscopic latex bead. One bead was trapped by a dual-beam laser while the one was held by a micropipette tip. The DNA molecules were extended by moving the pipette tip. An experiment with a similar concept was performed by Cluzel et. al.[4], in which the DNA molecules are attached to an optical fiber by one end and stretched by a micropipette at the other end. Both of them confirmed that below a force of 50pN, the DNA molecules show an elastic response. However above 65pN, the length of the molecules increases dramatically with just a slight increase of stress, suggesting a structural change. In between, there is a plateau where the DNA molecules stretch at almost constant force. Such behavior of dsDNA molecules under stress has been confirmed by other stretching methods such as magnetic tweezers[5] and AFM[6]. People also notice that such a response of DNA molecules under tension is dependent on

how the molecules are connected to the bead or the hard surface. The results above are all for torsionally unconstrained molecules, which means only the 3' or 5' ends are attached to the bead or the hard surface. For the torsionally constrained DNA molecules where both 3' and 5' ends are attached, the suspected structural transition point increases to 110pN[6,7].

The DNA structure that was first discovered by Watson and Crick[8] is often referred as B-DNA: the double helix is right-hand twisted with an atomic diameter of about 24Å and a helical pitch of 10.4 bps per turn. B-DNA is the canonical structure that predominates in cells and in nature generally. Other than that, DNA molecules can undergo different structural transitions based on the external environment[1,9]. For example, under low humidity and low dendity of cations, DNA molecules can transition into a more compact structure called A-DNA. A-DNA has the same handedness as the B-DNA but larger molecular diameter and larger base pair spacing. There is also a left-handed DNA structure called Z-DNA. The molecular diameter of Z-DNA is about 1.8nm and the helical pitch is about 12bps per turn. This structure is found to be stable in high salt conditions and with an alternating purine-pyrimidine sequence of the DNA molecule. However, unlike in the elastic region, where most of the reports agree that the worm-like chain model is the best one to describe the DNA's behavior under tension, the structural transition of DNA molecules under overstretching is still under debate. Early reports suggested that at the extension of about 1.7 times to its counter length, corresponding to about 65pN, the DNA molecule would change into other forms of structures such as S-DNA[4] or P-DNA[10]. However, other reports proposed that under extreme tension, a force-induced melting would occur and the double stranded DNA would denature into two single-stranded DNA molecules[11]. Both of the hypotheses were supported by some degree of experimental evidence: for the experiments that are in favor of the nonmelting mechanism, the results showed that the force response of an overstretched double stranded DNA is different from one ssDNA or two separated ssDNA[12,13]. In addition, another structural transition that was confirmed to be a melting transition was observed at a higher force level[14,15], which suggested that the first one is unlikely to be a melting transition. On the hand, the results from another series of experiments support the force-induced melting mechanism. What they found was that the structural transition behavior is dependent on the same factors that affect DNA melting[16-19]. The force that leads to the structural transition is lower if the DNA is in melting-favored solution conditions. The experiment of the

temperature dependence of single molecule stretching also reported that the entropy and heat capacity changes were similar to a melting transition[20,21].

Recently, the multicolor single-molecule fluorescence imaging technique was introduced into the research of DNA stretching. By using the Single Strand Binding(SSB) protein that wraps around ssDNA only and a fluorescence dye that stains dsDNA only, van Mameren et. al.[22] found that for the 3'-3' end-attached DNA molecule, the structural transition is likely due to the melting transition that is caused by unpeeling of one strand from the other initiating from the open ends. Yan's group took this a step further, by combining the single-molecule calorimetry result of a series of experiments[23,24] and fluorescence microscopy results from King et. al.[25], they draw a conclusion that DNA topology is crucial for the structural transition mechanism of overstretching. For the torsionally unconstrained DNA molecules with free ends or nicks (a nick is a discontinuity in a double stranded DNA where there is no phosphodiester bond between adjacent nucleotides of one strand), the structural transition at about 65pN is a competition of S-DNA formation, strand unpeeling and localized base-pair breaking (forms two single-stranded DNAs locally). For topologically closed but still torsionally unconstrained DNA molecules, the strand unpeeling is suppressed, the structural transition contains localized base-pair breaking and the B to S transition. The pathway of the transition is highly sensitive to the DNA sequence, DNA topology and the ionic strength of the solution: the B to S transition is more favored at GC-regions while base-pair breaking is likely to occur at AT-rich regions. When more nicks and free ends are present on the DNA molecule, the localized base-pair breaking dominates. Under the low salt condition, the localized base-pair breaking is again more favored while at high salt conditions, the B to S transition is the primary structural transition mechanism. Research has been conducted on the structural transition under stretching of torsionally constrained DNA molecules as well[7,26,27]. In most reports, both theoretical predictions and experimental results agreed that the structural transition at 110pN involves 20% of B to P-DNA transition and 80% of localized base-pair breaking/ B to S transition based on the lower/ higher ionic strength condition of the solution.

Although the current methods are able to study DNA response and structural transition at the single molecule level, none of these methods result in 1) linearly stretched untwisted DNA molecules on a surface or 2) allow for the observing of DNA breaking. Point 1) is relevant for some new generation sequencing techniques (ZS Genetics[28]) and point 2) holds a key on

confirming if there is any weak spot along the DNA strand. Previous research has indicated that the mechanical properties of DNA molecules are dependent on their own sequence[14].

Here we proposed a new method that is aiming to address these issues by depositing DNA molecules on a flexible PDMS surface followed by stretching the PDMS substrate. PDMS is a widely used elastomeric polymer with high flexibility and surface hydrophobicity. With these unique properties, linearly overstretched DNA molecules can be produced by adsorbing DNA onto it by molecular combing and then stretching the flexible PDMS substrate. Furthermore, a polarization-dependent fluorescence study is carried out to try to determine the structure of the DNA molecules on the PDMS surface. Study of the polarization of fluorescence of DNA stains is an effective way to probe the binding between the DNA molecules and surfaces[29]. There are three main modes of fluorescence dye molecules binding to the DNA: 1) base intercalation, 2) minor/major groove binding and 3) side binding. In the experiment, we use YOYO-1, which is a base intercalation dye, to stain the double-stranded lambda DNA. Generally, the relationship between the emission intensity of the fluorescence dye and the incident beam can be described as:

$$I = k\vec{\mu}\cdot\vec{E} = k\mu E\cos\theta_{\mu E}$$

Where k is a constant, $\vec{\mu}$ is the dipole moment of the dye molecule and $\vec{E}$ is the electric field intensity of the incident beam. In the case of intercalation dye, the angle between the dipole moment of the dye molecule and the long axis of DNA molecule is about 90°. If the unstretched DNA molecule with an intercalating dye lies horizontally in the view, and the angle between the long axis of the molecule and the polarizer in front of the detector is θ, then the detected fluorescence emission intensity is

$$I_d = I\,\mathrm{Sin}\,\theta \quad I_d = I\,\mathrm{Sin}\,\theta$$

so a peak of detected emission signal intensity will be at θ=90° (the angle between the light polarization and the long axis of the DNA molecule), and then subsequent peaks every 180° following the first one. In our experiment, a polarizer is installed before the camera to measure the polarization dependence of the emission light. The emission intensity as a function of polarization angle was measured before and after stretching.

3.2 Materials and Methods

3.2.1 Preparation of PDMS substrate

This process shares the same PDMS preparation method as we described in Chapter 2. The PDMS pre-polymer/ crosslinking agent mixture was then poured into a petri dish. After that, the petri dish was placed on a 65°C hot plate for 24 hours before the PDMS became solid enough for the following experiment.

3.2.2 Preparation of DNA solution

This step shares the same process as described in previous chapters. The final concentration of DNA in solution was 2.5μg/ml unless stated otherwise.

Adsorption of DNA molecules onto PDMS surface

This step also shares the same methods as mentioned in Chapter 1 except that PDMS substrates (usually about 50mm by 8mm) were used in this experiment instead of PMMA coated silicon substrate. Soaking time was set at 1 minute and the retraction speed was 2mm/s.

Some of the samples in this experiment were prepared by droplet evaporation method: several 2μL droplets of DNA solution (DNA concentration is also 2.5μg/ml) were placed near the center area of the PDMS substrate, each of them was about 2mm apart. Then they were placed in the dark room for evaporation at room temperature. After the droplet is totally dry, most of the combed DNA is to be found near the droplet's round periphery, forming a ring pattern. Usually, we also put several droplets on the dipping sample to aid in focusing.

3.2.3 Stretching and imaging

PDMS samples with adsorbed DNA molecules were installed on a custom made stretching apparatus for stretching and imaging. Each end of the sample was compressed between two metal plates, and clamped down over about .5cm on either side, leaving about 4cm of length to be stretched and manipulated. The plates were attached to a split leadscrew, whereby turning the knob that controlled the screw one rotation would make the plates move a distance of

635μm apart from each other. Usually, one image was taken after rotating the screw by one turn. When approaching to the breaking point of DNA molecules, each image was taken after a half turn. More frequent imaging was not practical for the reason that each of our images takes about 3 to 5 seconds to expose and multiple long-time exposure at the same imaging area would result in severe dye bleaching.

3.2.4 Polarization

Polarization data was collected by installing a polarizer before the CCD camera (Leica DC350F) to measure the angular dependence of the emission light and a mercury light has been used as a light source.

All the stretching and imaging work for this experiment was conducted on a Leica Laser Scanning Confocal Microscope (TCS2 SP2). Finally, data analysis was done with ImageJ software (NIH).

3.3 Results and discussion

3.3.1 Stretching and elongation of DNA molecules

Figure 3.1a and 3.1c are the results from molecular combing. DNA molecules are adsorbed onto the PDMS surface by molecular combing. The brightness and contrast of these pictures were adjusted for better visibility, but the DNA molecules after stretching are still more difficult to be observed compared to unstretched ones due to the bleaching effect.

DNA molecules are elongated as the PDMS substrates are stretched (Figure 3.1). We chose 16 individual DNA molecules and measured their length before stretching and after stretching but before breaking (Figure3.2). As we explained previously, because of the bleaching effect, it is impossible to follow the stretching process in live time. So the "after stretching but before breaking" means that exceeding this length, the DNA molecules that are on the PDMS surface would be broken within half a turn of rotation on the stretcher (about 317μm). The elongation fraction of the PDMS substrate stretching is defined as $(l_{as} - l_{bs}) / l_{bs}$, where the l_{bs} is the length before stretching and l_{as} is the length after stretching. The corresponding elongation

fractions of those 16 DNA molecules are shown in Figure 3.2. The average elongation fraction is 0.48 ± 0.04. From the result we can say that the elongation fraction is a constant number that does not depend on the DNA length. Further stretching would result in DNA breaking.

Reports have claimed that DNA molecules can be stretched as much as two times of its contour length before it breaks[30]. However, here the actual elongation fraction contains two parts: the elongation fraction due to the molecular combing and the elongation fraction due to the PDMS substrate stretching, which is the one calculated above. The elongation fraction of molecular combing is believed to be a constant value that is shared by every DNA molecule on the same sample. But it does depend on the pH value of the DNA solution and the hydrophobicity of the solid surface (see Chapter 1). To determine the elongation fraction of molecular combing of our experiment, the lengths of 100 adsorbed DNA molecules after combing process were measured and their length distribution is shown in Figure 3.3. Consider that DNA molecules can be broken or attached together during molecular combing, the elongation fraction cannot be calculated by taking those values and divided by the contour length of the molecule. On the hand, if we assume that the major proportion of DNA molecules is not broken or attached to each other during the combing process, then there should be a peak in the distribution of adsorbed DNA length. In Figure 3.3, the fraction of DNA molecules that have the length between 18μm to 24μm is 74%, which suggests that those stretched ones may be from the single unbroken DNA molecules. The average length from this group is 21.2 ± 1.7 μm, so the elongation fraction from molecular combing is 0.31 ± 0.11 (the contour length of the lambda DNA is 16.2 μm), and the elongation fraction from the whole process is 0.94 ± 0.15. This value is very close to the reported elongation faction before DNA breaking, the slight difference might due to the fact that DNA molecules here are deposited on a surface, the extra binding points might restrict the flexibility and twisting of the DNA molecule.

3.3.2 DNA breaking on PDMS surface

Current techniques for stretching DNA are not able to image after breaking because the DNA molecules are only anchored at two ends. For this experiment, as shown in Figure 3.4, we observed DNA molecules' breaking in real-time. DNA breakage is approximately at constant elongation fraction of PDMS substrate stretching, which is about 50%.

Up till now, the positions of the breaking points on DNA molecules are pretty random. However, as mentioned before, due to the bleaching effect, the number of images that were taken around the critical point (the stretched length that molecules are about to break) was not high enough to catch the initial breaking. The amount of fluorescence dye used in the experiment has to be minimized since the binding ligands may change the mechanical properties of the DNA molecules[31]. A new staining method is needed to overcome this problem.

3.3.3 Polarization study on adsorbed DNA molecules

The original plan of this part of the research is to determine whether the DNA molecules would untwist or not during PDMS substrate stretching process. According to the structure of B-DNA, if the intercalation dye (YOYO-1) is bound to the DNA molecule, the projection of dye molecules perpendicular to the long axis of the DNA molecule will be much larger as compared to the projection along the long axis, resulting in the peak of relative emission light intensity at $\theta=90°$ and $\theta=270°$, etc (Figure 3.5). And if the DNA did untwist, the relative intensity of the peaks would be higher than before stretching because before stretching, parts of the light emit from different dye molecules would cancel each other due to the turn of the DNA molecule but after stretching, if DNA did straighten out, all the base pairs and intercalated dye molecules would be parallel to each other with the same angle relative to the phosphate backbone.

Interestingly, as shown in Figure 3.6, instead of observing the intensity increase, what we observed is that the actual peaks are at $\theta=0°$ and $\theta=180°$ regardless the degree of stretching. In addition, no dependence was observed of the emission peak intensity on the degree of stretching (Figure 3.6).

One possible explanation would be that the DNA molecules have already been stretched during the process of molecular combing. During the molecular combing, the stretching force applied on the DNA molecules caused by the surface tension is calculated to be in the range of 160pN[32,33], which is above the stretching force required for DNA to have a structural transition (70pN for torsionally unconstrained and 110pN for torsionally constrained DNA). Because the DNA molecules have one free end inside the solution during the stretching of molecular combing, such a structural transition should be explained by the torsionally unconstrained model. Maaloum et. al.[34] studied the structural transition caused by molecular combing using high-

resolution AFM and what they found is that the transition is a B to S transition of the DNA molecule. The author claimed that because the molecular combing is a fast dynamic process and the moving interface applies the stretching force only for a short time to a small part of the DNA molecule, the unpeeling process is unlikely to happen. Our result seems to support to their conclusion. Although the detailed structure of S-DNA is still not completely clear, most of the simulation results indicate that the base pairs in the S-DNA tilt at a large angle[35-38]. Consider the fact that the YOYO-1 is an intercalation dye, the dye molecules will also be tilted to follow the base pairs. Then the projection of dye molecules along the long axis of DNA molecules will be larger than the projection that perpendicular to it (Figure 3.7) and this would explain the 90° peak shifting in the polarization study. Konrad[35] et. al. also pointed out that the base pair tilting would occur at the tension of 77pN, which means such base tilting is likely to happen during molecular combing. On the hand, once the DNA molecules were deposited onto the PDMS surface, no emission intensity or peak position change was observed from the polarization study. One possible explanation is that once the DNA molecules are "glued" on the surface after molecular combing, the extra binding points prevent them from denaturing or unwinding.

3.4 Conclusion

Using the PDMS substrate stretching method, we observed directly DNA breaking in real-time. The DNA breakage is approximately at a constant fraction of elongation. A polarized fluorescence study shows a 90° shift compared to our expected result for unstretched and twisted DNA suggesting a large base-pair tilt angle of deposited DNA molecules. Such a result is in accordance with previously reported ones and supports the theory that molecular combing will induce a structural transition that transfers B-DNA into S-DNA. Future work will be to develop a modified staining or imaging technique to overcome the bleaching issue so that more images can be taken for the same stained DNA molecules. In this way, the initial breaking of DNA molecules on the surface can be captured.

References

1 Strick, T. *et al.* Stretching of macromolecules and proteins. *Reports on Progress in Physics* **66**, 1 (2002).
2 Smith, S. B., Finzi, L. & Bustamante, C. Direct mechanical measurements of the elasticity of single DNA molecules by using magnetic beads. *Science* **258**, 1122-1126 (1992).
3 Smith, S. B., Cui, Y. & Bustamente, C. Overstretching B-DNA: the elastic response of individual double-stranded and single-stranded DNA molecules. *Science* **271**, 795 (1996).
4 Cluzel, P. *et al.* DNA: an extensible molecule. *Science-new york then washington-*, 792-794 (1996).
5 Strick, T., Allemand, J., Bensimon, D., Bensimon, A. & Croquette, V. The elasticity of a single supercoiled DNA molecule. *Science* **271**, 1835 (1996).
6 Clausen-Schaumann, H., Rief, M., Tolksdorf, C. & Gaub, H. E. Mechanical stability of single DNA molecules. *Biophysical Journal* **78**, 1997-2007 (2000).
7 Leger, J. *et al.* Structural transitions of a twisted and stretched DNA molecule. *Physical review letters* **83**, 1066 (1999).
8 Watson, J. D. & Crick, F. H. Molecular structure of nucleic acids. *Nature* **171**, 737-738 (1953).
9 Strick, T., Allemand, J.-F., Croquette, V. & Bensimon, D. Twisting and stretching single DNA molecules. *Progress in biophysics and molecular biology* **74**, 115-140 (2000).
10 Allemand, J., Bensimon, D., Lavery, R. & Croquette, V. Stretched and overwound DNA forms a Pauling-like structure with exposed bases. *Proceedings of the National Academy of Sciences* **95**, 14152-14157 (1998).
11 Santosh, M. & Maiti, P. K. Force induced DNA melting. *Journal of Physics: Condensed Matter* **21**, 034113 (2008).
12 Cocco, S., Yan, J., Léger, J.-F., Chatenay, D. & Marko, J. Overstretching and force-driven strand separation of double-helix DNA. *Physical Review E* **70**, doi:10.1103/PhysRevE.70.011910 (2004).
13 Fu, H., Chen, H., Marko, J. F. & Yan, J. Two distinct overstretched DNA states. *Nucleic acids research*, gkq309 (2010).
14 Rief, M., Clausen-Schaumann, H. & Gaub, H. E. Sequence-dependent mechanics of single DNA molecules. *Nature Structural & Molecular Biology* **6**, 346-349 (1999).
15 Danilowicz, C. *et al.* The structure of DNA overstretched from the 5′ 5′ ends differs from the structure of DNA overstretched from the 3′ 3′ ends. *Proceedings of the National Academy of Sciences* **106**, 13196-13201 (2009).
16 Williams, M. C., Wenner, J. R., Rouzina, I. & Bloomfield, V. A. Effect of pH on the overstretching transition of double-stranded DNA: evidence of force-induced DNA melting. *Biophysical Journal* **80**, 874-881 (2001).
17 Liu, Y. Y. *et al.* Ionic effect on combing of single DNA molecules and observation of their force-induced melting by fluorescence microscopy. *J Chem Phys* **121**, 4302-4309, doi:10.1063/1.1777220 (2004).
18 Shokri, L., McCauley, M. J., Rouzina, I. & Williams, M. C. DNA overstretching in the presence of glyoxal: structural evidence of force-induced DNA melting. *Biophysical Journal* **95**, 1248-1255 (2008).
19 Rouzina, I. & Bloomfield, V. A. Force-induced melting of the DNA double helix. 2. Effect of solution conditions. *Biophysical journal* **80**, 894-900 (2001).
20 Rouzina, I. & Bloomfield, V. A. Force-induced melting of the DNA double helix 1. Thermodynamic analysis. *Biophysical journal* **80**, 882-893 (2001).
21 Williams, M. C., Wenner, J. R., Rouzina, I. & Bloomfield, V. A. Entropy and heat capacity of DNA melting from temperature dependence of single molecule stretching. *Biophysical Journal* **80**, 1932-1939 (2001).
22 van Mameren, J. *et al.* Unraveling the structure of DNA during overstretching by using multicolor, single-molecule fluorescence imaging. *Proceedings of the National Academy of Sciences of the United States of America* **106**, 18231-18236, doi:10.1073/pnas.0904322106 (2009).
23 Zhang, X., Chen, H., Fu, H., Doyle, P. S. & Yan, J. Two distinct overstretched DNA structures revealed by single-molecule thermodynamics measurements. *Proceedings of the National Academy of Sciences* **109**, 8103-8108 (2012).
24 Zhang, X. *et al.* Revealing the competition between peeled ssDNA, melting bubbles, and S-DNA during DNA overstretching by single-molecule calorimetry. *Proceedings of the National Academy of Sciences* **110**, 3865-3870 (2013).

25 King, G. A. *et al.* Revealing the competition between peeled ssDNA, melting bubbles, and S-DNA during DNA overstretching using fluorescence microscopy. *Proceedings of the National Academy of Sciences* **110**, 3859-3864 (2013).
26 Strzelecki, J., Peplowski, L., Lenartowski, R., Nowak, W. & Balter, A. Mechanical transition in a highly stretched and torsionally constrained DNA. *Physical Review E* **89**, 020701 (2014).
27 King, G. A., Peterman, E. J. & Wuite, G. J. Unravelling the structural plasticity of stretched DNA under torsional constraint. *Nature communications* **7** (2016).
28 Bell, D. C. *et al.* DNA base identification by electron microscopy. *Microscopy and Microanalysis* **18**, 1049-1053 (2012).
29 Uy, J. L., Asbury, C. L., Petersen, T. W. & van den Engh, G. The polarization of fluorescence of DNA stains depends on the incorporation density of the dye molecules. *Cytometry Part A* **61**, 18-25 (2004).
30 Noy, A., Vezenov, D. V., Kayyem, J. F., Maade, T. J. & Lieber, C. M. Stretching and breaking duplex DNA by chemical force microscopy. *Chemistry & biology* **4**, 519-527 (1997).
31 Sischka, A. *et al.* Molecular mechanisms and kinetics between DNA and DNA binding ligands. *Biophysical journal* **88**, 404-411 (2005).
32 Bensimon, A. *et al.* Alignment and sensitive detection of DNA by a moving interface. *Science* **265**, 2096-2098 (1994).
33 Bensimon, D., Simon, A., Croquette, V. & Bensimon, A. Stretching DNA with a Receding Meniscus: Experiments and Models. *Physical Review Letters* **74**, 4754-4757, doi:10.1103/PhysRevLett.74.4754 (1995).
34 Maaloum, M., Beker, A. & Muller, P. Secondary structure of double-stranded DNA under stretching: Elucidation of the stretched form. *Physical Review E* **83**, 031903 (2011).
35 Konrad, M. W. & Bolonick, J. I. Molecular dynamics simulation of DNA stretching is consistent with the tension observed for extension and strand separation and predicts a novel ladder structure. *Journal of the American Chemical Society* **118**, 10989-10994 (1996).
36 Kosikov, K. M., Gorin, A. A., Zhurkin, V. B. & Olson, W. K. DNA stretching and compression: large-scale simulations of double helical structures. *Journal of molecular biology* **289**, 1301-1326 (1999).
37 Lebrun, A. & Lavery, R. Modelling extreme stretching of DNA. *Nucleic acids research* **24**, 2260-2267 (1996).
38 Olson, W. K. & Zhurkin, V. B. Modeling DNA deformations. *Current opinion in structural biology* **10**, 286-297 (2000).

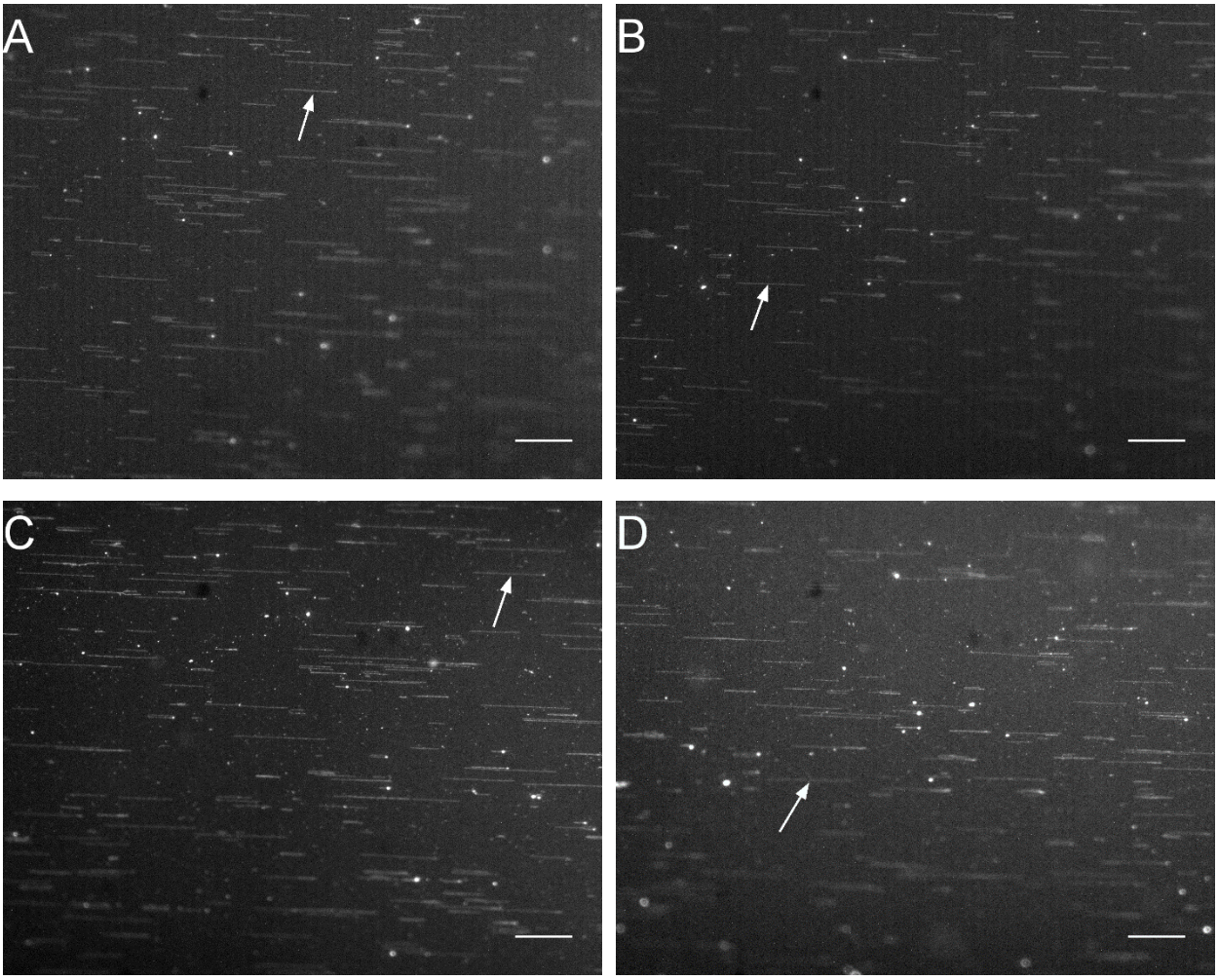

Figure 3.1: Elongation of DNA molecules by PDMS substrate stretching. A and B are before stretching, B and D are after stretching, respectively. The white arrows indicate the same molecule in A and C or B and D. [Scale bar, 20μm (A-D).]

A B

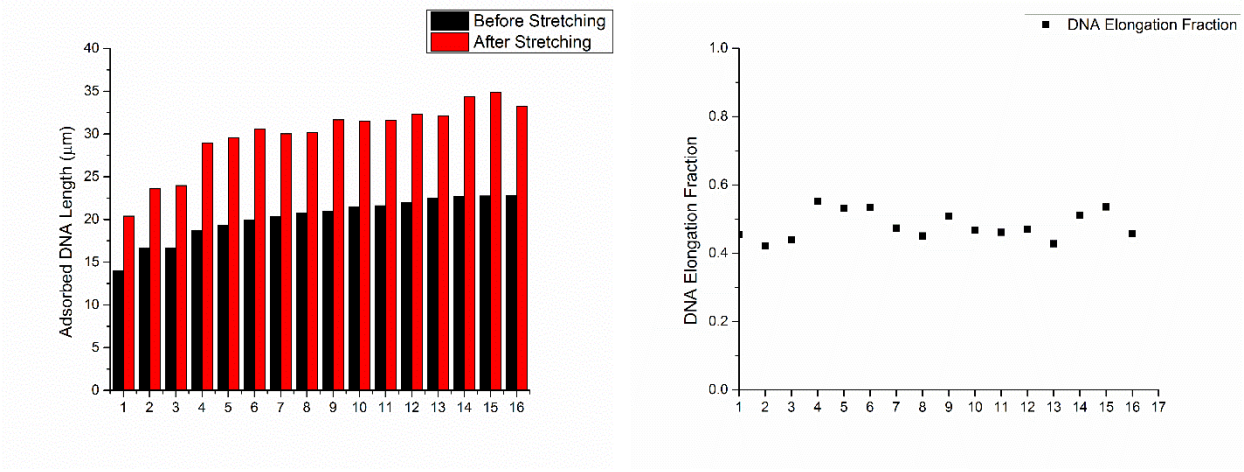

Figure 3.2: A shows the measurements on 16 adsorbed DNA molecules before and after stretching. B is their corresponding elongation fraction. The average elongation fraction is 0.48 ± 0.04.

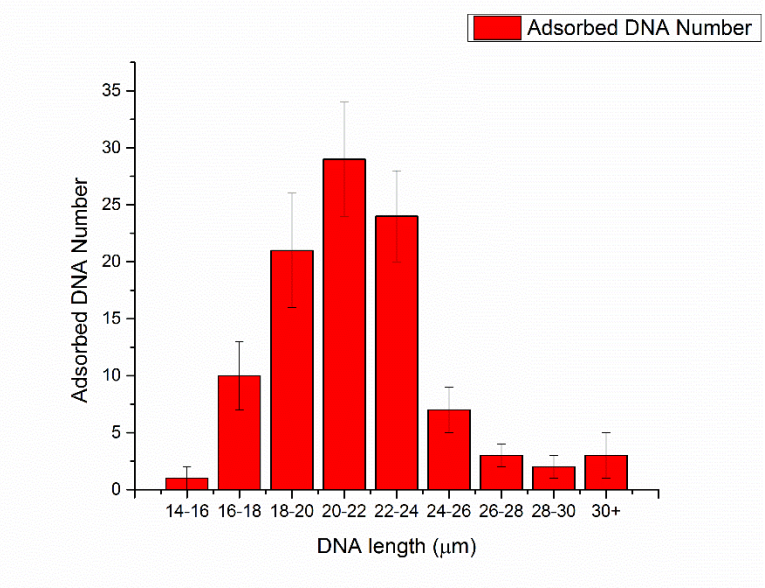

Figure 3.3: The length distribution of 100 adsorbed DNA molecules after molecular combing before PDMS substrate stretching.

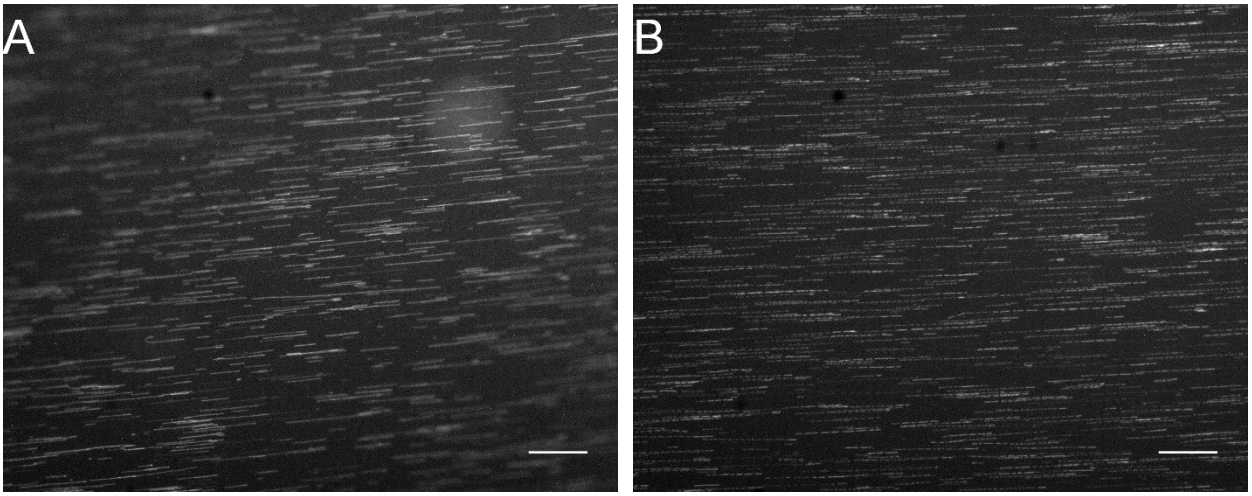

Figure 3.4: DNA breaking observed in real time. A is before stretching and B is the DNA molecules' breaking in real-time. [Scale bar, 20μm (A and B).]

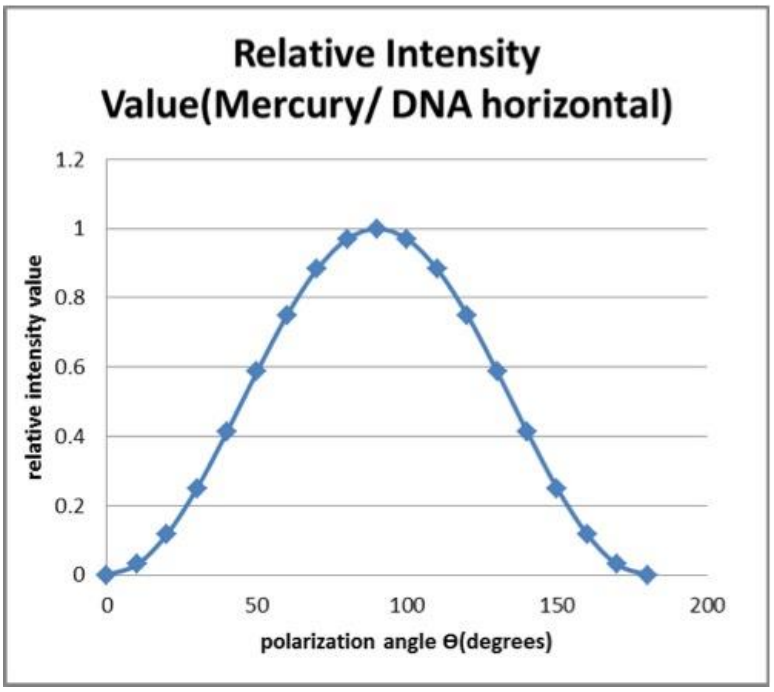

Figure 3.5: Theoretically calculated polarization dependence of emission intensity for DNA molecules lie horizontally (at θ=0°) in the view, assuming dye molecules' axis is normal to DNA long axis (for intercalation dye).

A

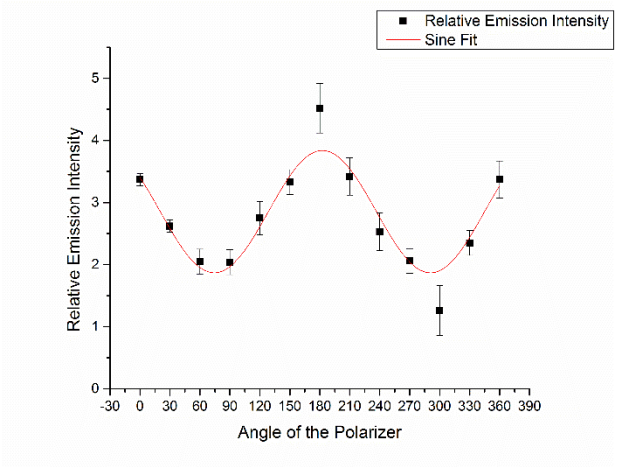

B

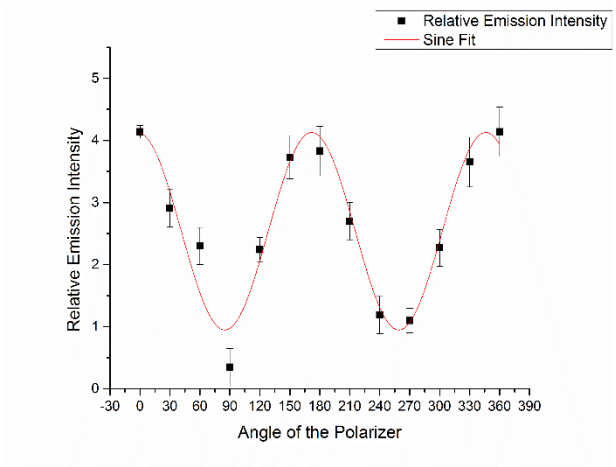

C

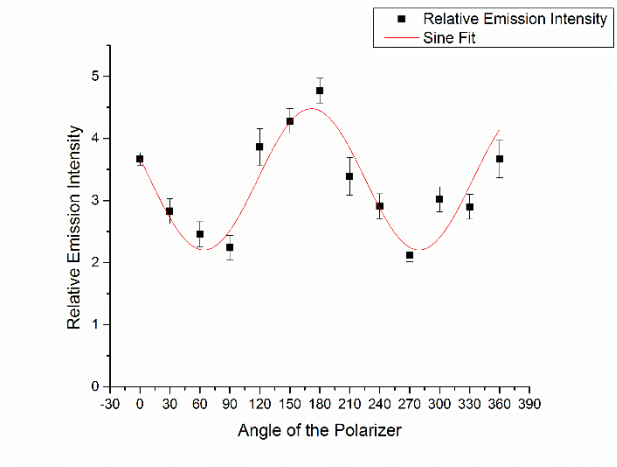

D

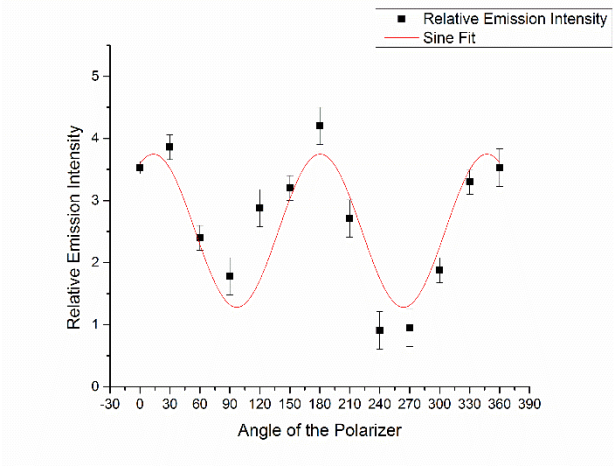

Figure 3.6: The polarization dependence of relative emission intensity for different degrees of stretching. A: before stretching; B: stretch the PDMS substrate for 1905μm; C: 3810μm; D: 7620μm. The relative emission intensity is calculated as [average brightness of the DNA molecule]-[average brightness of the background that next to the molecule].

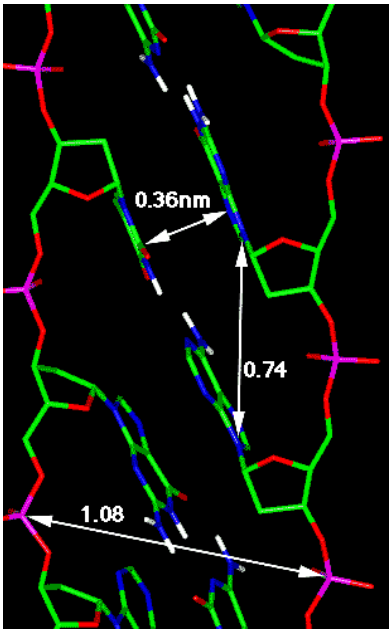

Figure 3.7: A novel ladder structure of DNA molecules with large tilt angle of base pairs under 0.4nN tension. The image is reprinted from ref. 35.